Design and Real Time Simulation of Robust Optimal Control of speed for an Induction Motor

A Thesis submitted to the Faculty of Engineering & Technology, Jadavpur University in Partial fulfilment of the requirements for the Degree of Master of Engineering in Power Engineering

Submitted by

RUPAK CHAKRABORTY

Examination Roll Number: M4POW 1610

Registration Number: 129429 of 2014-15

Under the Guidance of

Prof. Dr. Amitava Gupta

Faculty of Engineering and Technology

Department of Power Engineering

Jadavpur University

Kolkata-700098

2016

Department of Power Engineering
Faculty of Engineering & Technology
Jadavpur University
Kolkata-700098, India

Certificate of Recommendation

*We hereby recommend the thesis, entitled "**Design and Real Time Simulation of Robust Optimal Control of speed for an Induction Motor**" prepared under the guidance of **Prof. Dr. Amitava Gupta**, Department of Power Engineering, Jadavpur University, Saltlake Campus, Kolkata, by **Rupak Chakraborty** (Examination Roll Number M4POW1610 and Registration Number 129429 of 2014-2015), be accepted in partial fulfillment of the requirement of the Degree of Master of Engineering in Power Engineering of Jadavpur University.*

Prof. Dr. Amitava Gupta

Department of Power Engineering,

Jadavpur University

Counter signed by:

Head	*Dean*
Department of Power Engineering,	*Faculty of Engineering & Technology*
Jadavpur University	*Jadavpur University*

Department of Power Engineering
Faculty of Engineering & Technology
Jadavpur University
Kolkata-700098, India

<u>*Certificate of Approval*</u>

*The foregoing thesis, entitled as "**Design and Real Time Simulation of Robust Optimal Control of speed for an Induction Motor**" is hereby approved by the committee of final examination for evaluation of thesis as a creditable study of an engineering subject carried out and presented by **Rupak Chakraborty** (Examination Roll Number M4POW1610 and Registration Number 129429 of 2014-2015 in a manner satisfactory to warrant its acceptance as a prerequisite to the Degree of Master of Engineering in Power Engineering. It is understood that by this approval, the undersigned do not necessarily endorse or approve any statement made, opinion expressed or conclusion drawn therein, but approve the thesis only of the purpose for which it is submitted.*

Committee of final examination for evaluation of thesis:

                                      _____

                                      _____

                                      _____

Department of Power Engineering
Faculty of Engineering & Technology
Jadavpur University
Kolkata-700098, India

<u>*Declaration of Originality and Compliance of Academic Ethics*</u>

I hereby declare that this thesis contains Literature Survey and original research work carried out by myself, as part of my Degree of Master of Engineering in Power Engineering.

All information in this document has been obtained and presented in accordance with academic rules and ethical conduct.

I also declare that, as required by these rules and conduct, I have fully cited and referenced all material and results that are not original to this work.

Name: RUPAK CHAKRABORTY

Exam Roll Number: M4POW 1610

Thesis Title: **Design and Real Time Simulation of Robust Optimal Control of speed for an Induction Motor**

Signature with Date:

Acknowledgement

Foremost I would like to express my sincere gratitude to my thesis guide **Prof. Dr. Amitava Gupta,** *Professor***,** *Department of Power Engineering, Jadavpur University for the continuous support during the entire period of my study. During the course of my thesis work, his constant motivation, enthusiasm, immense knowledge and sustained patience with me helped me materialize the present work.*

I also wish to thank our Head of the Power Engineering Department, **Prof. Amitava Datta** *for his excellent guidance and support throughout the period of my study.*

I wish to offer my gratitude to all the faculty members of Power Engineering Department for their encouragement and active support.

Help, support, and love by Mr. Debayan Bose, Mr. Kaushik Halder, Mr. Shohan Banerjee and Mr. Soumya Dasgupta, scholars at Power engineering Department need special mention as without their brotherly love and support, this work would not have seen the light of the day.

I wish to extend my thanks to all the authorities of Jadavpur University for providing me with world class infrastructure that ensured this work was completed in time. The staff of Jadavpur University and the Library staff need special mention for the love and help throughout my study.

Finally I would like to convey my thanks to my friends and family, my parents and my brother for being there for me throughout my life, for showering their blessings and love on me.

I would also extend my gratitude to everyone who directly or indirectly offered their support for this work. Last but not the least, to God, I place my utmost regard for providing me with faith, ability and courage.

Rupak Chakraborty

Abstract

Induction motors have found wide application in industry due to its excellent robustness and low maintenance. A recent application area of Induction motors is the rapidly emerging Electric vehicle industry. This dissertation has been prepared with a view to develop a Robust control strategy for an induction motor that can drive a tractive load such as a single wheel of a 4 wheel driven electric vehicle driven by battery. Vector Control of Induction motors are prone to parameter variations that depend on operating conditions. Such variation poses challenges in the control mechanism as parametric variation directly affects system performance. This problem needs to be addressed if a tractive load is to be driven. This work presents Indirect Field Oriented Control as a powerful Control technique and identifies it as a cascaded system with two loops. The outer speed control loop has a PI controller that processes the error signal between a reference speed and the actual speed. This PI controller has been tuned in order to provide efficient and effective tracking of reference speed. For this purpose Field Oriented Control structure has been presented as a block diagram and subjected to block diagram techniques and subsequent Model Order Reduction Techniques to obtain a first order system. To this First order system, Linear Quadratic Regulator based Optimal Controller is designed. In order that the motor provides desirable response in spite of parametric variations, bounded parametric uncertainties are presented as an interval system and then a Robust Controller is designed for the interval system. Finally the entire study is analyzed through credible Real Time simulation using Opal RT OP 4500.

Keywords: Induction Motor, Vector Control, Optimal Control, Robust Control, Linear Quadratic Regulator (LQR), Opal RT OP 4500.

Contents

Chapter 1: Introduction

Chapter 2: Enabling Concepts and Modeling

Chapter 3: Field Oriented Control

Contents

Chapter 4: Optimal Controller design

Contents

Contents

Nomenclature

$d - q$	Direct and Quadrature axis
$d^s - q^s$	Direct and Quadrature axis of Stationary reference frame
$d^e - q^e$	Direct and Quadrature axis of Synchronously rotating reference frame.
$d^r - q^r$	Direct and Quadrature axis of Rotor reference frame.
$V_a - V_b - V_c$	Three phase voltages.
$V_d^s - V_q^s$	Voltages across direct and quadrature axis of Stationary reference frame.
$V_d^e - V_q^e$	Voltages across direct and quadrature axis of Synchronously rotating reference frame
$V_{ds}^s - V_{qs}^s$	Stator voltages across direct and quadrature axis of stationary reference frame
$V_{dr}^s - V_{qr}^s$	Rotor voltages across direct and quadrature axis of stationary reference frame
$V_{ds}^e - V_{qs}^e$	Stator voltages across direct and quadrature axis of synchronously rotating reference frame
$V_{dr}^e - V_{qr}^e$	Rotor voltages across direct and quadrature axis of synchronously rotating reference frame
$i_{ds}^s - i_{qs}^s$	Stator currents across direct and quadrature axis of stationary reference frame
$i_{dr}^s - i_{qr}^s$	Rotor currents across direct and quadrature axis of stationary reference frame
$i_{ds}^e - i_{qs}^e$	Stator currents across direct and quadrature axis of synchronously rotating reference frame
$i_{dr}^e - i_{qr}^e$	Rotor currents across direct and quadrature axis of synchronously rotating reference frame
$Œ_{ds}^s - Œ_{qs}^s$	d-q axis stator flux in stationary reference frame
$Œ_{dr}^s - Œ_{qr}^s$	d-q axis rotor flux in stationary reference frame

Nomenclature

Symbol	Description
$\psi_{ds}^{e} - \psi_{qs}^{e}$	d-q axis stator flux in synchronously rotating reference frame
$\psi_{dr}^{e} - \psi_{qr}^{e}$	d-q axis rotor flux in synchronously rotating reference frame
$\psi_{dm} - \psi_{qm}$	d-q axis air gap magnetising flux
ψ_{m}	Air gap magnetising flux
ψ_{r}	Total Rotor flux
R_s	Stator resistance per phase
R_r	Rotor resistance per phase referred to primary
L_s	Total stator inductance per phase
L_r	Total rotor inductance per phase
L_m	Magnetizing inductance
L_{ls}	Stator leakage inductance
L_{lr}	Rotor leakage inductance
L_{ms}	Air gap magnetising leakage inductance
ω_e	Electrical synchronous speed
ω_r	Electrical rotor speed
ω_{sl}	Slip speed
$p = \dfrac{d}{dt}$	Differentiator
s	Laplace Transform of a differentiator
T_e	Electromagnetic Torque
T_l	Load Torque

Nomenclature

J	Moment of inertia
B	Coefficient of friction
T_s	Sampling torque
θ_{sl}	Slip angle
θ_r	Rotor angle
θ_e	Angle between synchronous frame and stationary axis
‡	Rotor time constant
*	Reference quantities
P	Number of poles
m	Modulation index
V_c	Triangular carrier waveform used in PWM
V_r	Reference waveform used in PWM
†	Leakage Coefficient
i_T	Torque component of current
K_t	Torque Constant
K_{in}	Inverter gain
T_{in}	Inverter time constant
K_p	Proportional Gain
K_i	Integral Gain
x	System state vector
u	System input vector
y	System output vector

Nomenclature

Z	Aggravated state vector
w	Aggravated output vector
Q	Weighted matrix
$P(\text{s})$	Transfer Function of the IFOC plant
PI	Proportional –Integral
$\underline{x}$	Minimum value or infimum value
$\overline{x}$	Maximum value or Supremum value
$'$	Desired Damping Factor
$\check{S}_{ncl}$	Closed loop desired frequency
INTLAB	Interval Laboratory
HIL	Hardware In the Loop
SIL	Software In the Loop
RCP	Rapid Control Prototyping

List of Figures

List of Figures

List of Tables

Chapter 1

Introduction

1.0 Introduction

Induction motors have gained popularity in industrial applications and elsewhere due to their high reliability, reduced power consumption, lower maintenance cost, reduced electromagnetic radiation and most importantly, higher efficiency. A host of factors like nonlinearity arising out of saturation, parametric variation due to factors like temperature rise and complex dynamics make their application difficult. As a result, control techniques for induction motors have become increasingly complex while the motor control industry becomes more and more competitive.

The present dissertation attempts to develop a local control loop for controlling the speed of an induction motor driving a tractive load such as a single wheel of a 4 wheel driven electric vehicle driven by battery. The control scheme assumes load variations which cause sudden application of torque, for example, while negotiating a bump or a slope. The need for an optimal controller arises because of the need to restrict the current drawn from the battery as input to the motor. The relevant established technology modules that can be used for achieving these goals are first introduced in this dissertation and than verified through credible real-time simulation.

While established techniques in optimal control produce acceptable solutions [1] that guarantee acceptable stability robustness, it is equally important to ensure commensurate parametric robustness. This dissertation explores the feasibility of application of interval techniques to achieve a control solution that couples the advantages of an optimal controller with added parametric robustness.

1.1 Literature Survey and Options

Of the various control strategies available, Field Oriented Control provides high performance control and enables independent control of flux and torque. Field Oriented Control was first proposed by Technical University Darmstadt's K. Hasse and Siemens' F. Blaschke in the year 1968. In 1970, Hasse proposed Indirect Vector Control and Blaschke proposed Direct Vector Control.   This work was further developed by Technical

University Braunschweig's Werner Leonhard and as a result, ac drives could now give competition to dc drives [2].

Previous to Vector Control, other methods that existed for control of asynchronous machines can be termed collectively as scalar control. Scalar control of induction machines provided good steady state response, but failed to provide satisfactory dynamic response [3]. Scalar control uses only the magnitude and frequency of stator phase current, but does not consider the phase. As a result, phase and magnitudes of air gap flux deviate from their set values. Vector Control provides phase, frequency and magnitude control of currents. As this control is achieved in field coordinates, it is known as Field Oriented Control. Since this method of control is actually phasor control of flux linkages pertaining to the rotor, it is also called Vector Control.

The works of Robert H. Park in 1929 (Parks Transformation) enable transformation of a set of linear differential equations for any electric machine from a time varying coefficient to a time invariant coefficient. This greatly helped in understanding of the concepts of Field Oriented Control. Basically Vector Control represents an induction motor in a manner similar to a dc motor. Here, the field flux and armature flux produced by the field poles and the armature currents respectively, act orthogonally and therefore enable control of field flux and torque irrespective of each other i.e. independent control of field and torque is achieved. Vector Control can be of two types.

1. Direct Vector Control - Here, the desired flux is obtained directly by the use of some sense coils or, is calculated from voltage and current measurements at the terminals. Since it is not practically possible to directly obtain flux position, the rotor flux oriented system has to be designed such that it can calculate, compute and estimate the desired values from a directly sensed signal [4].

2. Indirect Vector Control – This method aims at calculating the flux positions by using the slip relation. Here, the rotor position is sensed and the flux and torque commands are generated. From these commands, the slip is calculated. Finally the flux position is obtained from this slip [4]. Indirect Field Oriented Control can be designed using any one of the three flux orientations, namely the stator, rotor and the air gap flux. Out of these the rotor flux orientation is widely accepted due to its simplicity.

Indirect Field Oriented Control provides several advantages over Direct Field Oriented Control (DFOC) and is as follows:

1. It does not suffer from inherent low speed problems and thus can be used for all such purposes where near zero speed operation is essential [4].
2. This method avoids the requirements of flux acquisition by using known machine parameters [4].
3. Minimization of the number of transducers and feedback loops. [5]

The advantages above make Indirect Field Oriented Control simpler and hence it is widely used over Direct Field Oriented Control.

In order to implement the vector control of induction machines, it is important to first develop dynamic model of an induction motor in the stationary reference frame. The works of Edith Clarke (Clarkes Transformation) is used for required transformations that convert the three phase quantities into two phase stationary quantities. Kron's Primitive Model representation, along with Clarkes Transformation and Parks' Transformation forms a basis for developing the dynamic model of an induction motor. Vector controller for the machine is developed in synchronously rotating reference frame and all quantities have to be converted to synchronous frame using suitable transformations. This has been described extensively in [6]

Block diagram for the entire plant consisting of the induction machine along with the Field Oriented Controller has been presented in [3]. Field oriented control is a control structure comprising of two loops. The inner loop is the current control loop and the outer loop is the speed control loop [7]. The function of the inner current control loop is to provide efficient tracking of the motor current. The motor current is made to track the reference current. The outer speed loop provides efficient tracking of speed such that the motor can track and follow any speed input applied as a reference. The dynamics of the two loops vary such that the inner loop is much faster than the outer one. Thus while designing the inner current loop, the dynamics of the speed control loop can be neglected and suitable controllers for this loop can be designed. But since the inner control loop of the vector controlled induction machine is a MIMO structure, it becomes quite difficult to design the controllers for this inner loop with conventional methods [8]. Classical control strategies that include PI/PID controller tuning has been effectively used in this regard. L. Umanand in [8] have presented the induction motor drive system as a linear quadratic

(LQ) tracker problem as an output feedback. In this paper, a current controller is designed for torque dynamics and for this controller, digital control has been adopted. In [9], the objective of decoupled controller for high speed operation has been worked upon by Jinhwan Jung et.al. Debayan Bose in his master's thesis analysed and designed the inner current control loop using Relative Gain Array (RGA) [10].

While designing the speed control loop, the conventional PI controllers are used. The integral component ensures minimal or zero deviation of the actual speed from the reference speed. In [11], Speed controller for the outer speed control loop has been designed with anti-windup scheme using conditional integration method. In [12] a sliding mode controller has been designed for the outer speed control loop for FOC. In order to implement any control strategy for designing the outer speed loop, the essential prerequisite is to develop corresponding suitable dynamic equations that represent the entire system including the motor and controller. This has been demonstrated in [3] by which the entire block diagram can be effectively reduced to a second order system. Design of suitable PI controllers has also been demonstrated in the book but such a controller does not guarantee optimal control of the system.

System order reduction techniques where a system of any order can be reduced to a lower order system can be found in extensive tutorials on Model Order Reduction. Dr. S. Janardhanan in his tutorial [13] demonstrates some methods on model order reduction. Davison method of model order reduction, Chidambara model and his suboptimal control and Marshall technique are few such methods. Use of aggregation methods in model order reduction ensures efficient reduction in system order [13]. Aggregation methods were initially developed in economics literature to address the appropriateness of the analogy between microeconomic and macroeconomic relationships. It was Aoki who first proposed aggregation in control systems [13]. Later, modal aggregation techniques were developed. A more popular method in model order reduction is 'Aggregation by continued fraction method', introduced first by Chen and Shieh. Later this method was extended by many others.

Induction machines provide many advantages over their dc counterparts but suffer from one major problem. i.e. bounded uncertainty or parametric sensitivity. Due to various operating conditions and external factors, parameters of an induction motor are subject to change. Operating conditions that affect parameters of a machine include temperature rise

and saturation [3]. External factors include occurrences of inappropriate instrumentation of parameters in vector controller. Some operating conditions that induce parametric uncertainties are controllable, but external factors are beyond control. The result is coupling between the flux and torque components of the machine and a nonlinear relationship between reference torque and actual torque. Also, a change in machine parameters affects the total system comprising of the motor and the controller. The resulting transfer function obtained after suitable block diagram reduction and model order reduction depends on the machine parameters. Therefore a change in machine parameters causes a change in the transfer function. The transfer function obtained represents the entire system and the optimal controller for the outer speed loop is designed on this mathematical representation. Therefore any change in transfer function might cause the designed controller to fail to maintain optimal stability of the system. Therefore the need arises to develop a robust controller that can handle such bounded uncertainties and maintain optimal control of the outer speed loop. Interval mathematics has been developed to handle such uncertainties. Ramon E. Moore et. al [14] in their book present detailed analysis of interval mathematics. Here, upper bounds and lower bounds are considered for all such parameters which vary. The upper bound denotes the maximum value with maximum variation, while the lower bound shows the minimum value with minimum variation. For this purpose, INTLAB [15] has been developed which can be used as a toolbox with MATLAB. INTLAB performs mathematical calculations based on intervals and provides results in terms of bounded interval sets. Thus INTLAB can be effectively used for design of robust controllers.

Design of robust PI controllers for suspension systems with parametric uncertainty have been presented by Rahul Mittal in [16]. Here, graphical methods for comput*in*g PI controller parameters for various gain margin and phase margins have been used. But this approach does not use interval mathematics for controller design. Milan Hladik et.al in their work [17] have discussed about symmetric and unsymmetric interval matrices and deduced theorems for bounds on interval matrices. These results can be applied in control theory to design robust controllers that can guarantee optimal control over an interval given by interval matrices. This has been established in [18] where an optimal PID controller has been designed for a PHWR with parametric uncertainties. In [18], a nominal system is first deduced for a PHWR from corresponding dynamic equations and then an optimal controller has been designed for this nominal system. Next, bounded

parametric uncertainties have been introduced and the effect of such variations has been represented in the form of interval matrices. Now, the controller gain for the nominal system is used and suitable calculations are made to find Q and P matrices according to LQR method given by J. B. He et. al. [19]. The theorems of [17] are then used to prove that the controller guarantees optimality throughout the interval.

Since the advent of modern computers, simulation tools have been widely used by technologists to design, analyse and modify physical systems according to specific requirements. With the development of high end computing technologies, simulation tools have seen marked improvement in terms of performance, and have dramatically decreased in cost. This has increased acceptance of simulation tools as they can now be used by more and more researchers. Real time simulation has now been developed which provide marked improvement in performance and speed. In offline simulation, the computation time may be shorter or longer than the fixed time step. [20] A real time simulator computes the mathematical operations and produces the internal variables and outputs of the simulation within a similar length of time that would have been produced by its corresponding physical system. Here, the time required to compute a mathematical operation needs to be shorter than the actual wall clock duration of the time step. Any idle time after computation is over for the time step, is lost in real time simulation. Finally the duration of simulation is exactly equal to real wall clock, as would have been given by the actual process. State of the art simulators can perform various type of simulations. Some such simulation techniques are Hardware In the Loop (HIL), Software In the Loop (SIL), and Rapid Control Prototyping (RCP). In HIL, a physical controller is connected to a virtual plant and the virtual plant is simulated in real time simulators. SIL simulation is carried out by designing both the plant and the controller in the same real time simulator. SIL provides an advantage over other simulations as here, no inputs and outputs are used and signal integrity is maintained. RCP simulations consist of a controller simulated in a real time simulator, and connected to a physical plant. These different types of simulations provide various advantages. Controllers can be tested without connecting them to real plants and thus can be designed even before the actual plant has been set up. This method ensures safety of the plant in case the controller fails to provide desired response. Plants and controllers both can be simulated and tested before they are physically built. Various real time simulators have evolved, of which OPAL –RT series simulators need special mention. OPAL RT OP 4500 comes with a powerful processor

Intel 4 core CPU and can perform simulations at step size of a few nanoseconds. OPAL RT real time simulator has several advantages

❖ Has an advanced powerful new generation processor that is capable of executing high performance simulations.

❖ OPAL RT has FPGA chips that can perform simulations at very small time steps, of the order of a few nanoseconds.

❖ It can be applied for Hardware In the Loop (HIL), Software In the Loop (SIL), and Rapid Control Prototyping (RCP) simulations.

As real time simulation is executed according to real physical clock, complex and rigorous simulations can be carried out much faster

1.2 Objective of the Thesis:

Field oriented control is an effective and widely accepted vector control strategy of induction machine. Such control is essentially a cascaded control where there are two loops -The inner current loop and the outer speed loop. The inner current loop is much faster in dynamics than the outer speed loop and therefore the current loop can be designed without considering the speed loop. The design of controllers for the inner speed loop has been taken up in [10]. The design of the PI controllers for the outer speed loop has been given by various other researchers. Some of them ensure robust control with parametric sensitivity.

The objective of this thesis is to design PI controllers for the outer speed loop such that two aims are achieved.

❖ First, the controller should ensure efficient tracking of the reference speed by the actual speed.

❖ Secondly, the controller should guarantee optimal performance throughout the interval of bounded parametric uncertainties. i.e. the controller should be robust, such that parametric uncertainties can be handled by it.

The conditions of maximum temperature rise and operating zones of the machine have been considered here and the effects of these two on the machine parameters have been represented by interval mathematics. Next, a robust optimal controller using Linear Quadratic Regulator (LQR) technique has been taken up for the controller design. The final outcome is an optimal controller that is robust throughout the range of the interval matrix for parametric uncertainty

1.3 Outline of the thesis:

The thesis consists of 5 chapters. Results and Discussion have been provided with each chapter and section as deemed necessary. Therefore this dissertation does not contain a separate chapter on results and discussions:

❖ Chapter 1: This chapter introduces the dissertation and provides extensive discussion on the literature survey as a prerequisite to this work. Literature survey is followed by objective of the thesis where the aim of this work is presented.

❖ Chapter 2: Second chapter of the thesis deals with dynamic modelling of an induction machine and discusses some elementary related concepts. This chapter is subdivided into two sections.

2.0 The first section introduces local loop control of induction machines.

2.1   The second section discusses the basic enabling concepts that are a pre-requisite for Field Oriented Control and thereafter, demonstrates the dynamic modelling of an induction motor in the stationary reference frame and presents the response curves of the various performance parameters through the use of MATLAB/Simulink. Mathematical relations are also derived and presented.

❖ Chapter 3: Third chapter of this thesis introduces Field Oriented Control and extensively discusses implementation of IFOC in induction machines. Finally with the help of Block Diagram Reduction and Model Order Reduction techniques, a corresponding first order system is obtained that represent the IFOC structure.

3.0   This section introduces Field oriented Control.

3.1 The second section of this chapter presents Theory and Structure of IFOC. All necessary mathematical derivations are explained and discussed.

3.2 Third section of the third chapter briefly presents Pulse Width Modulation (PWM) and Sinusoidal PWM technique

3.3 Fourth section of this chapter presents Simulation of IFOC, produces the results obtained and offers a discussion on the results.

3.4 The entire IFOC structure is identified as an integrated Block diagram and thereafter, Block Diagram Reduction Techniques are applied and finally this section presents a reduced form of the entire IFOC structure as a second order system.

3.5 The last section of the third chapter discusses Model Order Reduction techniques and applies such techniques to obtain the IFOC structure as a reduced first order system.

❖ Chapter 4: This chapter presents the design of an Optimal Controller for the nominal system. Optimal Control concepts are presented and then design and implementation of the controller is discussed. This chapter has the following sections:

4.1 The first section introduces Optimal control.

4.2 This section discusses Optimal Control and the LQR problem. Basic theory on performance indices and Algebraic Ricatti Equation are presented.

4.3 Controller design is discussed in this section of the third chapter. Using the concepts and theory of the previous section, an Optimal Controller is designed using LQP technique. Derivations and implementation is presented and finally, the controller gains are obtained through the use of MATLAB/Simulink.

4.4 This section concludes chapter 3 and presents the MATLAB Simulations and discusses the results obtained. For this purpose, the designed controller is added to the first order nominal system and responses are studied. Later, the controller is added to the original simulation and the results are studied. This is followed by a discussion

❖ Chapter 5: Parametric Robustness is studied in this chapter and the entire IFOC system is identified as an Interval system. Thereafter, INTLAB is introduced and an interval system is obtained. This chapter has the following sections:

5.0   The first section introduces bounded parametric uncertainties and robust control along with discussions on Interval Laboratory.

5.1   The second section presents theories on bounded parametric uncertainties and discusses the types of bounded parametric uncertainties- temperature rise and saturation as has been considered in this dissertation.

5.2   This section provides theories and concepts on Interval mathematics and INTLAB, a toolbox that can be used with MATLAB. Finally a reduced order transfer function considering parametric variation is presented.

5.3   Design of a robust control is presented in this section. First the theory of robust control is discussed and then the results of implementation of such a controller with the use of INTLAB/MATLAB are provided. Finally robustness of the designed controller is verified.

5.4   Results of using the Robust controller with the IFOC structure is studied through Matlab and discussions are presented on the results.

❖   Chapter 6: The 5th chapter presents an overview of Real Time Simulation using Opal Rt OP 4500. This chapter has the following sections:

   6.0 An overview of Real Time Simulation is presented in this section

   6.1 An overview of Real Time Simulation is presented in this section

   6.2 Various types of simulation like RCP, HIL and SIL are discussed in this section of chapter 5.

   6.3 The third section of the 5th chapter provides a brief description of the state of the art Real Time Simulator Opal Rt OP 4500.

   6.4 Simulation using Opal Rt OP 4500 is presented in this section along with the results.

   6.5 The last section of this thesis presents discussion on the results obtained

❖   Chapter 7: The last chapter of the dissertation provides concluding remarks for the entire dissertation along with scope of future work.

CHAPTER 2

Enabling Concepts and Modeling

In this Chapter the basic enabling concepts associated with control of an Induction Motor for a variable speed-torque scenario are first introduced . These concepts are then used to present a model of an Indcution Motor which is verified with credible simulation.

2.0 Introduction:

In 1920 Park formulated a change of variables concept, which brought revolutionary changes in electric machine analysis. Parks Transformation has a unique property of removing all time varying inductances that are present in voltage equation of synchronous machines. Such time varying inductances occur due to

1. Relative motion of electric circuits.
2. Variable magnetic reluctance of electric circuits. [21]

In 1930s, H.C. Stanley formulated a change of variables for analysis of induction machines. He concluded that all time varying inductances could be effectively eliminated by transforming the variables associated with the rotor windings, to variables that are associated with any fictitious stationary winding. According to Stanley, the rotor variables are transformer transformed to frame that is fixed on the rotor. Later, Kron introduced a change of variables by which all stator and rotor variables could be transformed to a reference frame that rotates with synchronous speed with the rotating magnetic field. This is commonly known as the "synchronous reference frame". This work was in reference to symmetrical induction machines [21].

Later, D.S. Brereton formulated another scheme of change of variables by which all stator variables could be transformed along a reference frame fixed to the rotor. This was Parks Transformation applied to induction machines.

Brereton, Kron and Clarkes work laid the path to study dynamic equations of induction machines. A dynamic model of induction machine is useful to study dynamic response of induction machines, can be used as a teaching tool in electric machine and power electronic courses and can be used in various motor control techniques [22]. In this work, a D-Q or

dynamic model of an induction motor in the stationary reference frame has been made and necessary assumptions are made.

2.1 D-Q modelling of Induction motor and simulation:

The simplified per phase equivalent circuit representation of Induction machines is helpful in the analysis of steady state response, but fails to provide effective insight into dynamic response. Therefore in order to study dynamic analysis of machines, a dynamic model is a necessity.

Now, as we transform balanced three phase currents to balanced two phase currents, tit is seen that the mmf produced by both the systems is identical. Also, the transformations are made such that per phase impedances are also same. Thus, the constants per phase for an equivalent 2 phase induction machine can be obtained from the study and conducted on three phase induction machine. Therefore it can be concluded that a three phase induction machine can be studied on a two phase induction machine and can be transformed back to a three phase induction machine [4]. Before this transformation is carried out, a discussion on reference frame transformation is presented.

2.2 a) Reference Frame Theory and Transformations:

Dynamic modelling of induction motor can carried out in a synchronously rotating reference frame (as proposed by Park), or in stationary reference frame as proposed by Stanley, or in a reference frame that rotates at any arbitrary speed, i.e. the arbitrary reference frame as proposed by Krause [21]. Therefore before a dynamic model and its derivations and calculations are presented, it is essential to have discussions on the various Transformations.

1. Clarkes' Transformation (($ d^S - q^S $) Transform):

Clarkes Transform converts all quantities in three phase reference frames to quantities in two axis orthogonal reference frame as shown in figure 1. Here a 3 phase system of currents have been represented as phases a, b and c that are 120 degrees apart from each other. This

stationary three phase system on the left is transformed to a stationary two phase reference frame ($d^S - q^S$). Here, I_d^S is considered to be aligned along I_a. I_d^S and I_q^S are of same magnitude. The relation between the two reference frames that follow is valid for both voltages and currents.
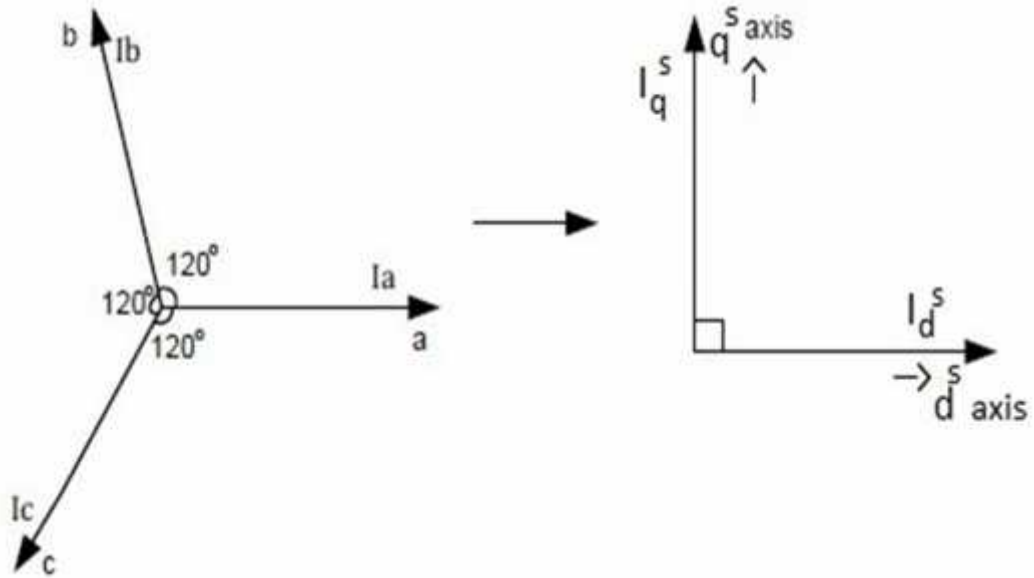
Figure 1) Clarkes Transform from three phase to two phase.
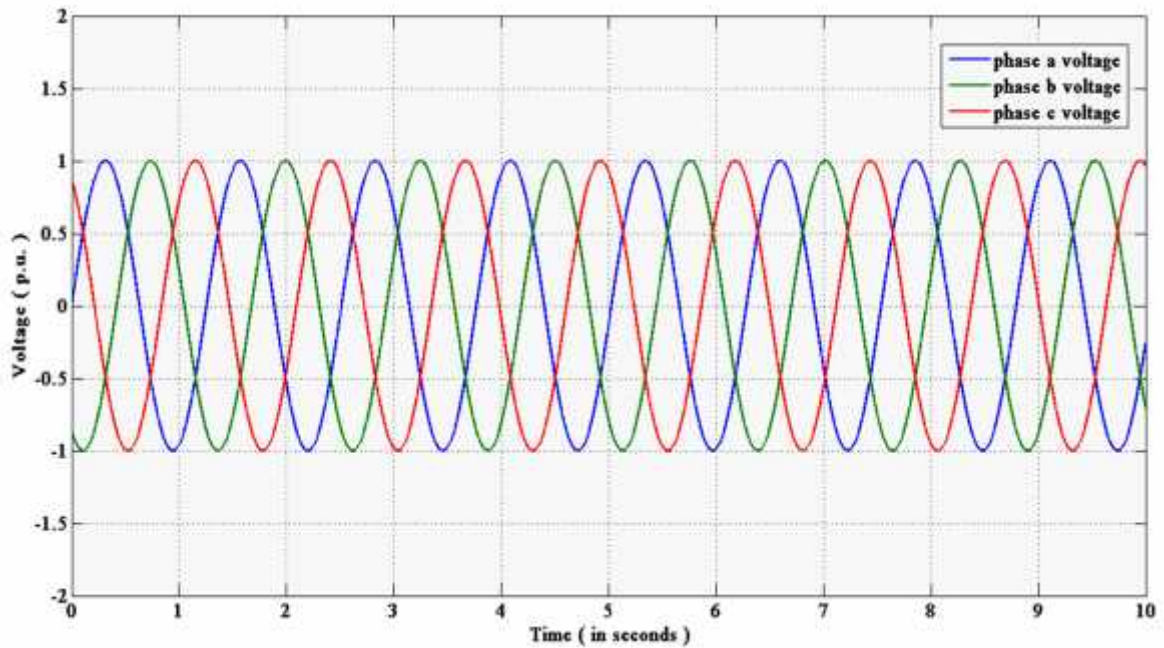
Figure 2. a) Three phase voltage waveforms
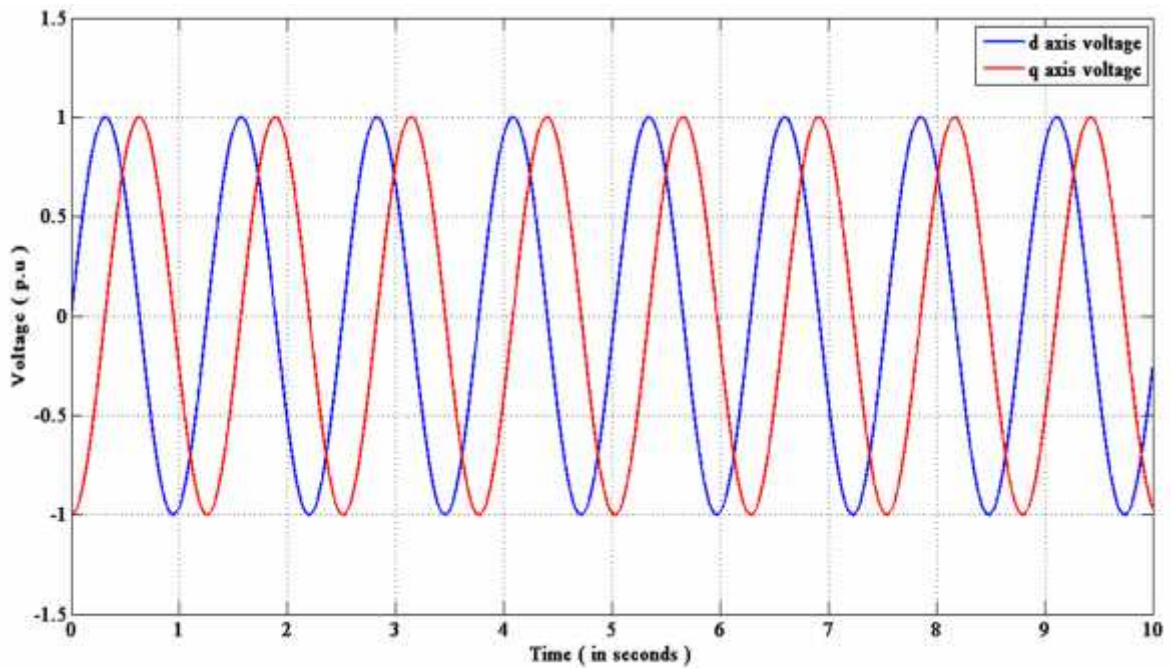
Figure- 2. b) Two phase voltage waveforms

The transformation of three phase balanced system of currents to a two phase system can be obtained with the following relation-

$$
\begin{pmatrix} V_d^s \\ V_q^s \end{pmatrix} = \frac{2}{3} \begin{pmatrix} 1 & -\frac{1}{2} & -\frac{1}{2} \\ 0 & \frac{\sqrt{3}}{2} & -\frac{\sqrt{3}}{2} \\ \frac{1}{2} & \frac{1}{2} & \frac{1}{2} \end{pmatrix} \begin{pmatrix} V_a \\ V_b \\ V_c \end{pmatrix}
\tag{2.1}
$$

Transformation from a two phase system to a three phase system can be carried out by having inverse of the transformation matrix and the final relation can be obtained as:

$$
\begin{pmatrix} V_a \\ V_b \\ V_c \end{pmatrix} = \begin{pmatrix} 1 & 0 & 1 \\ -\frac{1}{2} & \frac{\sqrt{3}}{2} & 1 \\ -\frac{1}{2} & -\frac{\sqrt{3}}{2} & 1 \end{pmatrix} \begin{pmatrix} V_d^s \\ V_q^s \\ V_0 \end{pmatrix}
\tag{2.2}
$$

Here, $V_0 = \frac{1}{3}(V_a + V_b + V_c)$ which is the zero sequence component of voltage.

2. Park's Transformation ((d^e-q^e) transform:

Parks Transformation transforms three phase quantities lying in a stationary reference frame (a, b, c) to two phase quantities in a rotating reference frame (d^e-q^e). The equations that lead to Parks Transformation are given as:

$$
\begin{pmatrix} V_d^e \\ V_q^e \\ V_0 \end{pmatrix} = \frac{2}{3} \begin{pmatrix} \cos\theta_e & \cos(\theta_e - \frac{2\pi}{3}) & \cos(\theta_e + \frac{2\pi}{3}) \\ -\sin\theta_e & -\sin(\theta_e - \frac{2\pi}{3}) & -\sin(\theta_e + \frac{2\pi}{3}) \\ 1/2 & 1/2 & 1/2 \end{pmatrix} \begin{pmatrix} V_a \\ V_b \\ V_c \end{pmatrix}
\tag{2.3}
$$

Here, θ_e is the angle between the two reference frames. i.e. the rotating reference frame makes an angle θ_e with the stationary reference frame at each instant.

Inverse of Parks transform converts a two phase rotating system to a three phase system and the corresponding equation is:

$$
\begin{pmatrix} V_a \\ V_b \\ V_c \end{pmatrix} = \begin{pmatrix} \cos\theta_e & -\sin\theta_e & 1 \\ \cos(\theta_e - \frac{2\pi}{3}) & -\sin(\theta_e - \frac{2\pi}{3}) & 1 \\ \cos(\theta_e + \frac{2\pi}{3}) & -\sin(\theta_e + \frac{2\pi}{3}) & 1 \end{pmatrix} \begin{pmatrix} V_d^e \\ V_q^e \\ V_0^e \end{pmatrix}
\tag{2.4}
$$

The figure above in 3 shows Parks Transformation. The component V_0 is the same as that used for Clarkes Transform.
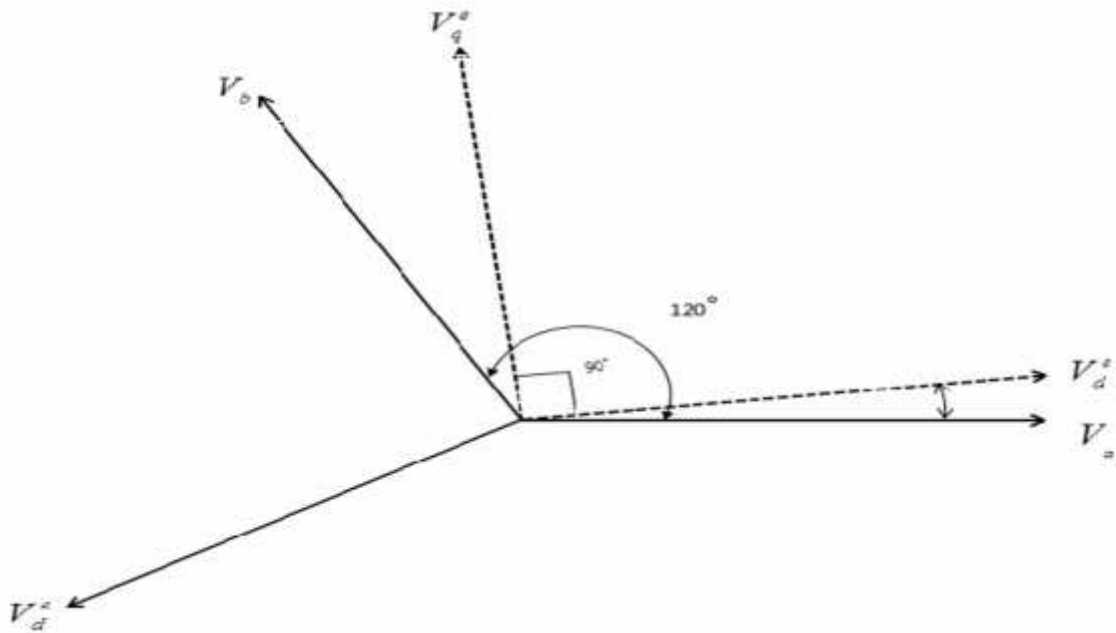
Figure 3- Parks Transformation (Three phase to Two phase Rotating Reference Frame)

2.2b Dynamic Modelling of Induction motor:

Before a dynamic model for an induction motor is presented n detail, it is necessary discuss some of the assumptions that have been used for the derivations [6].

i. Mmf distribution along periphery of air gap is assumed to be sinusoidal. Thus space harmonics are efffectively neglected. The effects of space harmonics on torque and induced voltages are therefore not taken into consideration.

ii. Hysterisis and saturation are not considered. Therefore, the concept of linear coupled circuit theory is considered valid.

iii. We have assumed the mutual inductances to be equal.

iv. There is no consideration of slots causing variation of inductances with relative movement between stator and rotor. Therefore to conclude, the self and mutual inductances vary sinusoidally as the rotor rotates.

Considering the above assumptions, dynamic modelling has been caried out for an induction motor and has been presented in the subsequent section.

Aleck W. Leedy in [20] has presented a dynamic model of an induction motor in the rotating reference frame. But for this thesis, a stationary reference frame has been chosen to represent the dynamic equations of the machine.

The voltage equations for the Stator d and q axis has been given by [4]:

$$V_{ds}^s = R_s i_{ds}^s + \frac{d}{dt} \lambda_{ds}^s \tag{2.5}$$

And,

$$V_{qs}^s = R_s i_{qs}^s + \frac{d}{dt} \lambda_{qs}^s \tag{2.6}$$

Similarly the voltage equations for the rotor d and q axis have been given by [4] as follows:

$$V_{dr}^s = R_r i_{dr}^s + \frac{d}{dt} \lambda_{dr}^s + \omega_r \lambda_{qr}^s \tag{2.7}$$

And,

$$V_{qr}^s = R_r i_{qr}^s + \frac{d}{dt} \lambda_{qr}^s - \omega_r \lambda_{dr}^s \tag{2.8}$$

Now, for an induction machine with squirrel cage rotor, the rotor bars are short circuited and hence the rotor voltages become zero.

Therefore, $V_{dr}^s = V_{qr}^s = 0$

Hence, eq (7) becomes

$$0 = R_r i_{dr}^s + \frac{d}{dt} \lambda_{dr}^s + \omega_r \lambda_{qr}^s \tag{2.9}$$

And eq (8) becomes

$$0 = R_r i_{qr}^s + \frac{d}{dt} \lambda_{qr}^s - \omega_r \lambda_{dr}^s \tag{2.10}$$

The equations for the various flux linkages for the stator and rotor are as follows:

$$\lambda_{ds}^s = L_{ls} i_{ds}^s + L_m(i_{ds}^s + i_{dr}^s) \tag{2.11}$$

$\Rightarrow \quad {}^{s}_{qs} = L_{ls}i^{s}_{qs} + L_m(i^{s}_{qs} + i^{s}_{qr})$ \hfill (2.12)

$\Rightarrow \quad {}^{s}_{dr} = L_{lr}i^{s}_{dr} + L_m(i^{s}_{ds} + i^{s}_{dr})$ \hfill (2.13)

$\Rightarrow \quad {}^{s}_{qr} = L_{lr}i^{s}_{qr} + L_m(i^{s}_{qs} + i^{s}_{qr})$

(2.14)

The flux linkage for air gap flux is given by:

$${}^{s}_{dm} = L_m(i^{s}_{ds} + i^{s}_{dr}) \hfill (2.15)$$

$\Rightarrow \quad {}^{s}_{qm} = L_m(i^{s}_{qs} + i^{s}_{qr})$ \hfill (2.16)

$$_{m} = \sqrt{{}^{2}_{dm} + {}^{2}_{qm}}$$

Inductances for the stator and rotor can be calculated as:

$$L_s = L_{ls} + L_m$$

$$L_r = L_r + L_m$$

Where, $L_m = \dfrac{3}{2}L_{ms}$

Putting the values (11) - (14) in equations (5), (6), (9) and (10) we get:

$$V^{s}_{ds} = R_s i^{s}_{ds} + \frac{d}{dt}(L_{ls}i^{s}_{ds} + L_m(i^{s}_{ds} + i^{s}_{dr}))$$

$\Rightarrow \quad V^{s}_{ds} = R_s i^{s}_{ds} + \dfrac{d}{dt}((L_{ls} + L_m)i^{s}_{ds} + L_m i^{s}_{dr}))$

$\Rightarrow \quad V^{s}_{ds} = R_s i^{s}_{ds} + \dfrac{d}{dt}(L_s i^{s}_{ds} + L_m i^{s}_{dr})$

$\Rightarrow \quad V^{s}_{ds} = R_s i^{s}_{ds} + L_s \dfrac{d}{dt}i^{s}_{ds} + L_m \dfrac{d}{dt}i^{s}_{dr}$ \hfill (2.17)

And,

$$V_{qs}^s = R_s i_{qs}^s + \frac{d}{dt}(L_{ls} i_{qs}^s + L_m(i_{qs}^s + i_{qr}^s))$$

$$\Rightarrow \quad V_{qs}^s = R_s i_{qs}^s + \frac{d}{dt}((L_{ls} + L_m)i_{qs}^s + L_m i_{qr}^s)$$

$$\Rightarrow \quad V_{qs}^s = R_s i_{qs}^s + \frac{d}{dt}(L_s i_{qs}^s + L_m i_{qr}^s)$$

$$\Rightarrow \quad V_{qs}^s = R_s i_{qs}^s + L_s \frac{d}{dt} i_{qs}^s + L_m \frac{d}{dt} i_{qr}^s \qquad (2.18)$$

And, we have the rotor equations as :

$$0 = R_r i_{dr}^s + \frac{d}{dt}(L_{lr} i_{dr}^s + L_m(i_{ds}^s + i_{dr}^s)) + \quad_r(L_{lr} i_{qr}^s + L_m(i_{qs}^s + i_{qr}^s))$$

$$\Rightarrow \quad V_{dr}^s = R_r i_{dr}^s + \frac{d}{dt}(L_r i_{dr}^s + L_m i_{ds}^s) + \quad_r(L_r i_{qr}^s + L_m i_{qs}^s)$$

$$\Rightarrow \quad 0 = R_r i_{dr}^s + L_r \frac{d}{dt} i_{dr}^s + L_m \frac{d}{dt} i_{ds}^s + \quad_r L_r i_{qr}^s + \quad_r L_m i_{qs}^s$$

$$\Rightarrow \quad 0 = L_m \frac{d}{dt} i_{ds}^s + \quad_r L_m i_{qs}^s + R_r i_{dr}^s + L_r \frac{d}{dt} i_{dr}^s + \quad_r L_r i_{qr}^s \qquad (2.19)$$

Also,

$$0 = R_r i_{qr}^s + \frac{d}{dt}(L_{lr} i_{qr}^s + L_m(i_{qs}^s + i_{qr}^s)) - \quad_r(L_{lr} i_{dr}^s + L_m(i_{ds}^s + i_{dr}^s))$$

$$\Rightarrow \quad 0 = R_r i_{qr}^s + \frac{d}{dt}(L_r i_{qr}^s + L_m i_{qs}^s) - \quad_r(L_r i_{dr}^s + L_m i_{ds}^s)$$

$$\Rightarrow \quad 0 = R_r i_{qr}^s + L_r \frac{d}{dt} i_{qr}^s + L_m \frac{d}{dt} i_{qs}^s - \quad_r L_r i_{dr}^s - \quad_r L_m i_{ds}^s$$

$$\Rightarrow \quad 0 = - \quad_r L_m i_{ds}^s + L_m \frac{d}{dt} i_{qs}^s - \quad_r L_r i_{dr}^s + R_r i_{qr}^s + L_r \frac{d}{dt} i_{qr}^s \qquad (2.20)$$

The equations (17), (18), (19) and (20) give the relations according to which the simulation for dynamic modelling of an induction machine is carried out in MATLAB. These equations can be represented in the form of a matrix by the following relation:

$$\begin{pmatrix} V_{ds}^{s} \\ V_{qs}^{s} \\ 0 \\ 0 \end{pmatrix} = \begin{pmatrix} R_S + L_S p & 0 & L_m p & 0 \\ 0 & R_S + L_S p & 0 & L_m p \\ L_m p & rL_m & R_r + L_r p & rL_r \\ -rL_m & L_m p & -rL_r & R_r + L_r p \end{pmatrix} \begin{pmatrix} i_{ds}^{s} \\ i_{qs}^{s} \\ i_{dr}^{s} \\ i_{qr}^{s} \end{pmatrix} \qquad (2.21)$$

The torque equation is developed by the interaction of two fluxes i.e. the air gap flux and the rotor mmf. Thus in stationary reference frame, the torque equations appear as:

$$T_e = \frac{3}{2}\left(\frac{P}{2}\right)(\,{}^{s}_{dm}i_{qr}^{s} - {}^{s}_{qm}i_{dr}^{s}\,) \qquad (2.22)$$

$$\Rightarrow \quad T_e = \frac{3}{2}\left(\frac{P}{2}\right)(\,{}^{s}_{dm}i_{qs}^{s} - {}^{s}_{qm}i_{ds}^{s}\,) \qquad (2.23)$$

$$\Rightarrow \quad T_e = \frac{3}{2}\left(\frac{P}{2}\right)(\,{}^{s}_{ds}i_{qs}^{s} - {}^{s}_{qs}i_{ds}^{s}\,) \qquad (2.24)$$

$$\Rightarrow \quad T_e = \frac{3}{2}\left(\frac{P}{2}\right)L_m (i_{qs}^{s}i_{dr}^{s} - i_{ds}^{s}i_{qr}^{s}\,) \qquad (2.25)$$
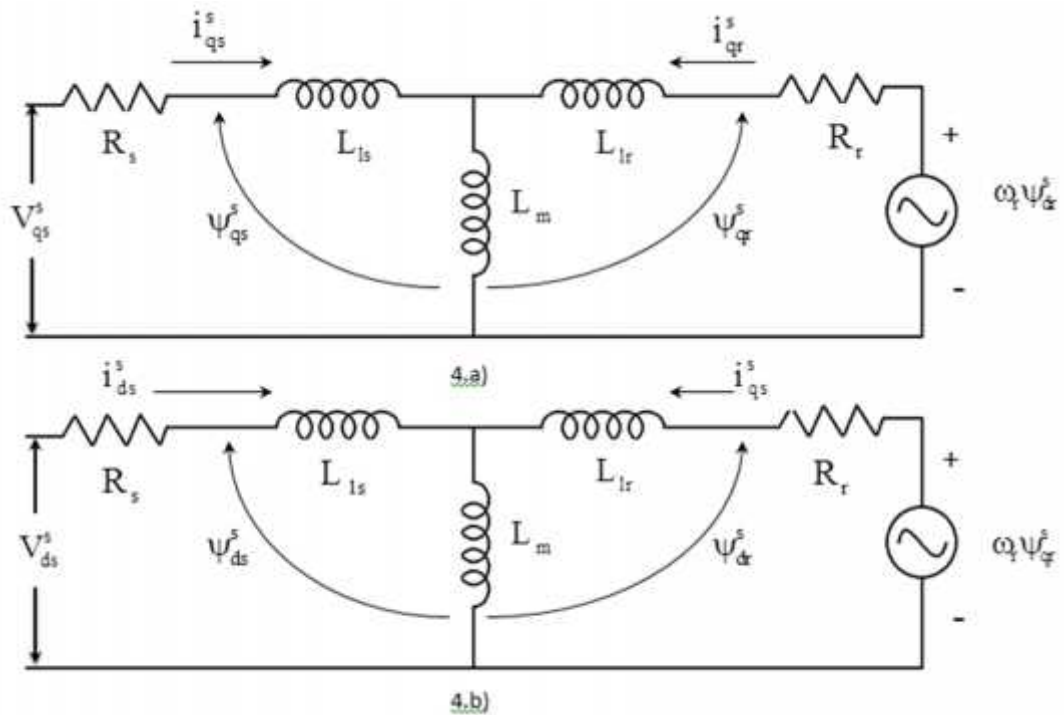
Figure 4.a) q^s circuit and **4.b)** d^s circuit of equivalent stationary reference frame model of induction machine

The electromechanical equation for an induction motor is given by the following relation:

$$T_e = T_l + \frac{2}{P}\left(J\frac{d\omega_r}{dt} + B\omega_r \right)$$

(2.26)

Figure 4 represents the simplified dynamic model of an induction motion.

2.2c Simulation and results:

The machine was simulated using MATLAB and corresponding torque, speed and flux responses were seen. For simulation of induction motor, the various parameters that were used are tabulated as follows:

Table 1- Parameters of IM used for simulation

Parameter of the motor	Symbol	Values chosen
Voltage per phase	V_m (volts)	40 volts (peak)
Frequency	F (Hz)	69 hertz
Per phase Stator resistance	R_s (ohms)	1.627 e-3
Per phase Rotor resistance	R_r (ohms)	1.364 e-3
Stator leakage inductance per phase	L_{ls}	19.42 e-6 H
Rotor leakage inductance per phase	L_{lr}	19.42 e-6 H
Air gap leakage inductance (magnetising) per phase	L_{ms}	320 e-6 H
No. of poles	P	4

Moment of Inertia	J (kg-m^2)	0.03
Frictional Coefficient	B (N-m-s)	0.07
Simulation step size	sec	1 e-5

The MATLAB simulation for dynamic modelling of an induction motor is shown in figure 5. A 3 phase sinusoidal voltage is given as input which is then converted to a two phase system of voltages in the stationary reference frame by using Clarkes Transform. After this, simulating the equations (17), (18),(19),(20), the currents have been derived. From the currents, the corresponding fluxes have been derived by simulating equations (11),(12),(13),(14). From the currents that were obtained, the electromagnetic torque is obtained by simulating equation (25). From the electromechanical relation of the motor, the speed of the machine is derived by simulating equation (26). Finally the d and q axis currents are transformed to three phase stator and rotor currents using inverse of Clarkes transform.

Results of simulation of induction machine in MATLAB Simulink:

➢ Case 1- when the machine runs at no load:

The machine is run without any external Load and the various responses are noted.
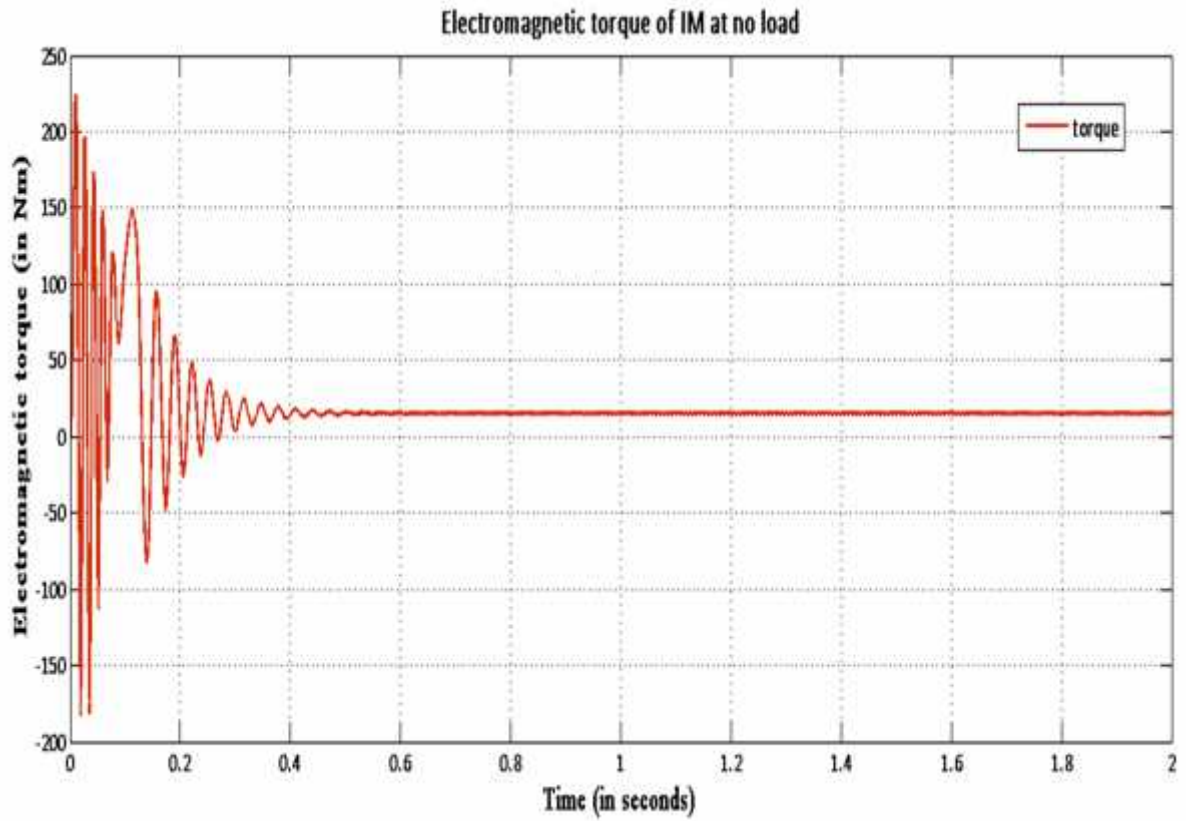
Figure 5. Electromagnetic torque of the machine at no load (in Nm)
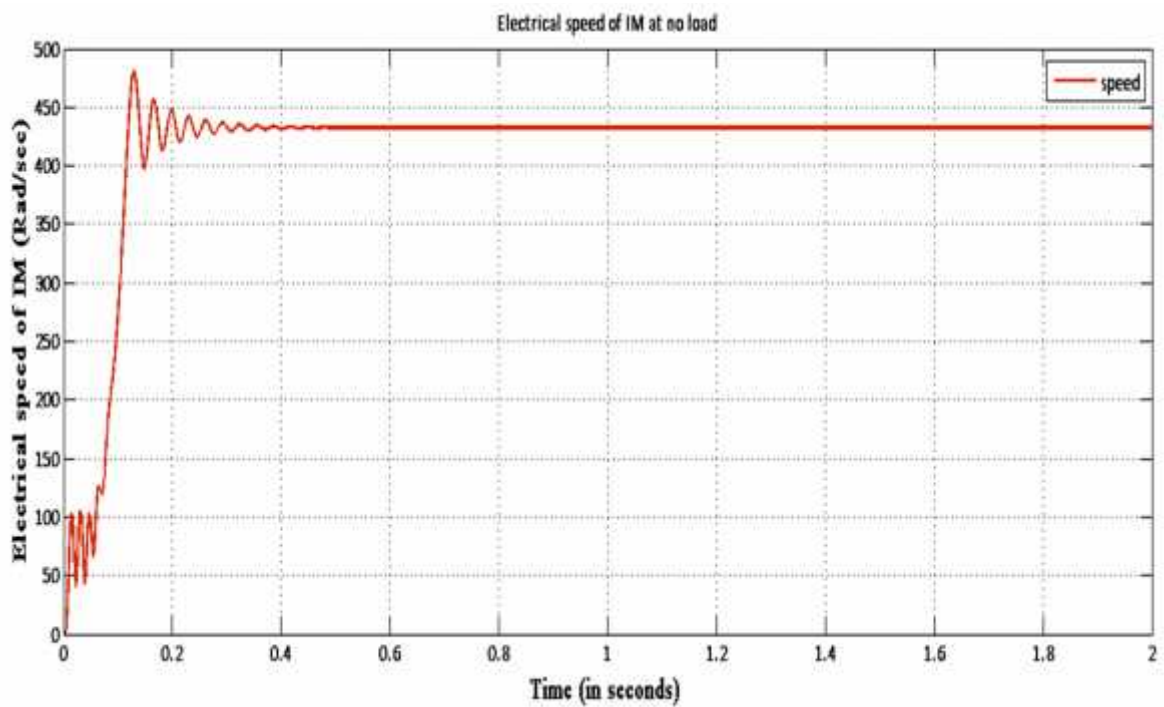
Figure 6. Electrical speed of the machine at No-Load (in Rad/sec)
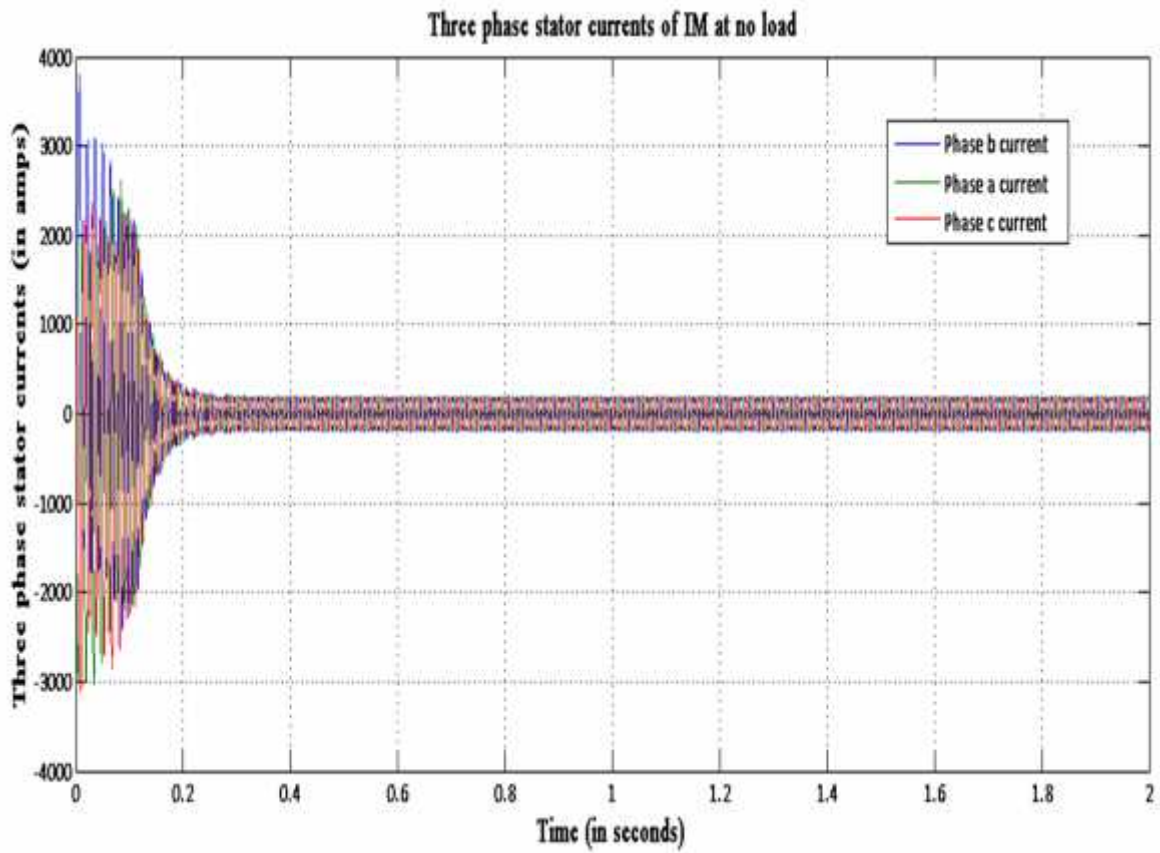
Figure 7. Three phase Stator currents of the machine at no load. (in amps)
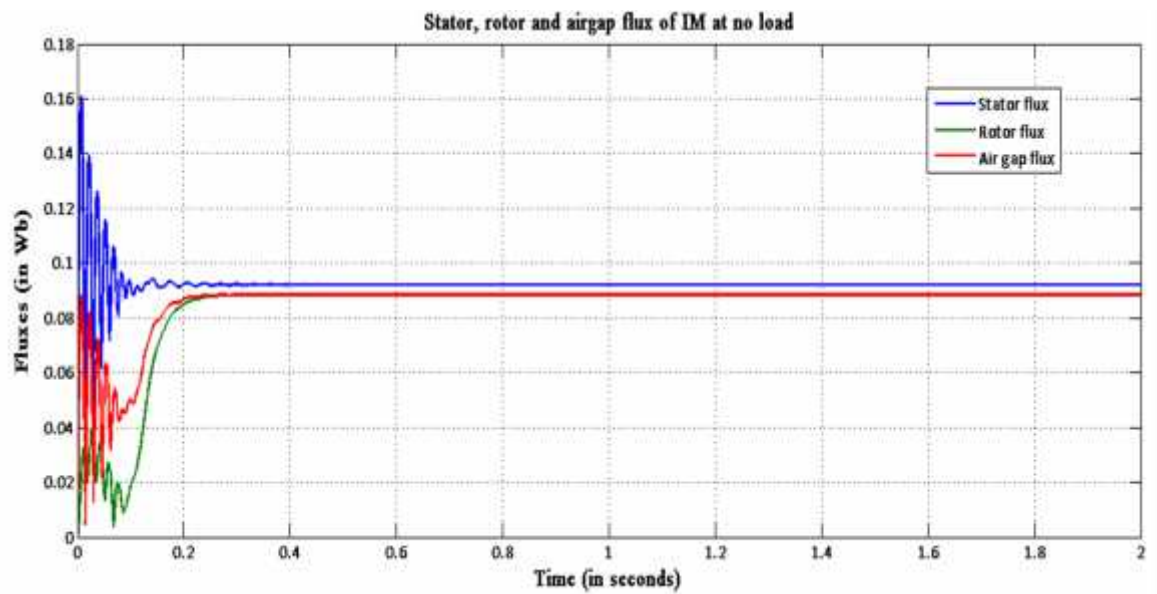
Figure 8. Stator, rotor and Air gap magnetising fluxes for the machine at no load (in Wb)

➢   <u>Case 2</u>- when a load torque of 35Nm is applied at 1 second:

The machine is made to run initially at no load and then after 1 second, a load torque of 35Nm is applied. The various responses are then noted.
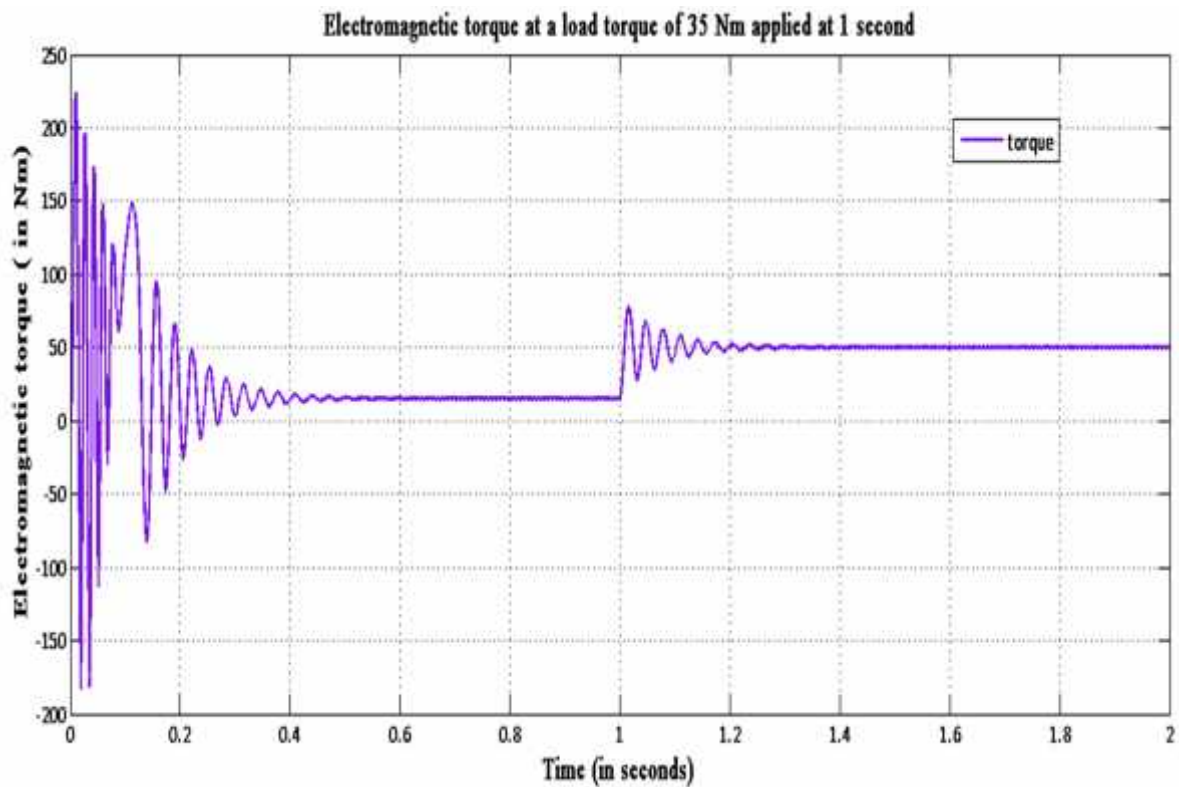
Figure 9. Electromagnetic torque of the machine at a load torque of 35Nm applied at 1 second (in Nm)
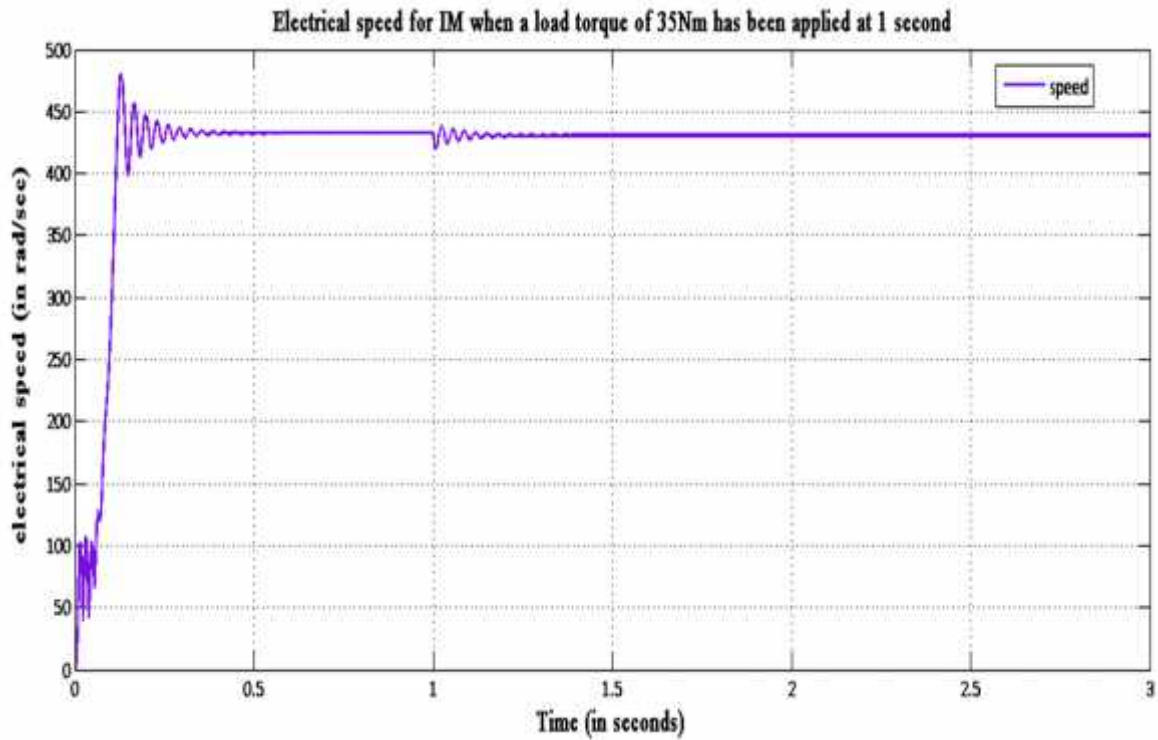
Figure 10. Electrical speed of the machine at a Load torque of 35Nm applied at 1 second (in Rad/sec)
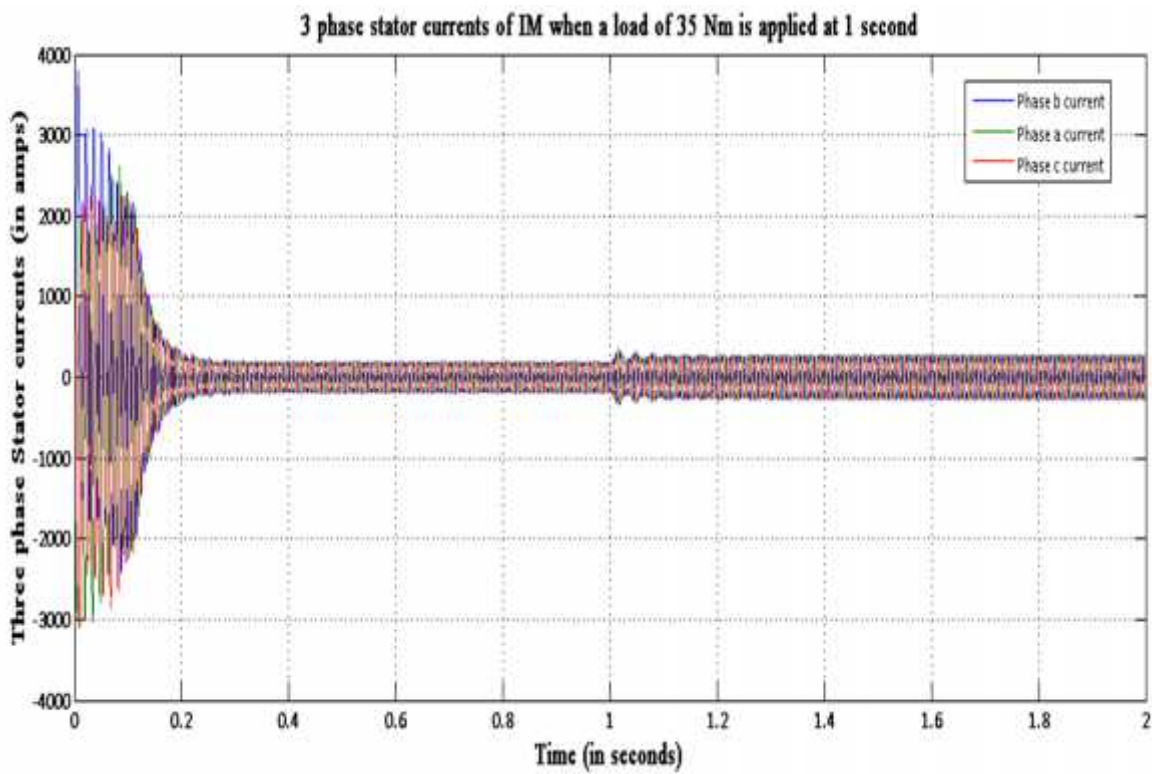
Figure 11. Three phase Stator currents of the machine at load torque of 35Nm applied at 1 second
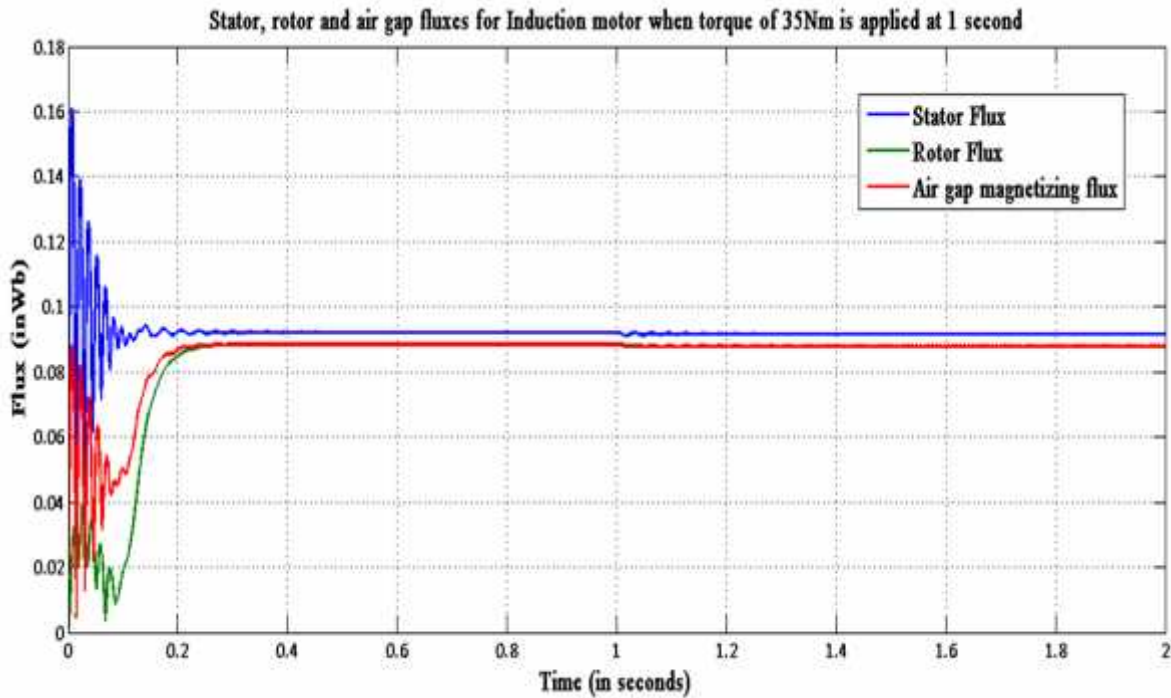
Figure 12. Stator, rotor and Air gap magnetising fluxes for the machine at a load torque of 35 Nm applied at 1 second (in Wb)

Discussions on results:

➢ Case 1- when the machine runs at no load

The simulation is first made to run with no load and the responses of corresponding currents, fluxes, electromagnetic torque and speed are seen. It is observed that the speed increases from zero to about 430 Rad/sec and settles in about 0.45 seconds after an initial overshoot. The torque initially rises to 225 Nm and settles to about 15 Nm at 0.5 seconds. Now as the speed of the machine increases, the torque increases rapidly and oscillates. During this period the torque is oscillating. As the speed of the motor reaches a steady value, the torque reduces and becomes almost stable. The 15 Nm steady state electromagnetic torque provides the motor with the frictional and windage torque. This frictional component has been introduced in the simulation as B.

➢ Case 2- when a load torque of 35 Nm is applied at 1 second

The simulation is made to run initially without the application of external load. After 1 second into the motor operation, an external load of 35 Nm is applied. Initially the speed of the motor

increases from zero to about 430 Rad/sec and settles in about 0.4 seconds. Initial overshoot is present. As speed increases, we find that the torque increases and becomes oscillatory. As the speed settles, torque also becomes steady at about 14 Nm. Now with the application of external load, there is a speed transient for 0.2 seconds and after this the speed falls by 2 rpm. Electromagnetic torque rises to meet the external applied torque and finally settles to a value of 50 Nm. The current response in this case increases slightly after load torque is applied, because now the electromagnetic torque has to increase to meet the new total torque demand.

We find from the flux responses that the rotor magnetic flux is less than the stator magnetic flux. Air gap magnetising flux is more than rotor flux but less than stator flux.

Chapter 3

Field Oriented Control

3.0 Introduction:

Field oriented or vector control is a technique in which a separately excited dc motor like approach is adopted. In a dc motor, the field flux is perpendicular to the armature flux and these phasors are orthogonal to each other and stationary in space. This implies that when armature current is controlled to control torque of the machine, the flux remains unaffected. Also, then field flux is varied, it does not affect the armature flux. This inherent decoupling of torque and flux provides fast transient response in dc machines. An induction machine suffers from a coupling effect and therefore high transient performance is difficult to achieve [21]. Such an approach as is practical with a dc machine can be extended to an induction machine by considering all the quantities of the induction motor in a synchronously rotating reference frame. Such a frame ensures that the sinusoidal variables appear as dc quantities. Here the stator current is transformed into two axes, the d^e, and the q^e axes i.e. i_{ds}^e and i_{qs}^e. These are the direct axis and quadrature axis currents and are orthogonal to each other. Vector control ensures that the i_{ds}^e component is similar to the field current i_f of a dc motor, and i_{qs}^e is similar to armature current i_a of a dc motor. Therefore the torque can be expressed as:

$$T_e = K_t \Xi_r i_{qs}^e \qquad\qquad\qquad (3.1)$$

This dc machine like analysis is possible only if i_{ds}^e is directed along the flux component and i_{qs}^e is in quadrature to it. Here, i_{ds}^e is the flux component and i_{qs}^e is the torque component.

3.1 Theory and structure of Indirect Field Oriented Control:

A. <u>THEORY:</u>

Field Oriented Control can be of two types.

1. Direct Field Oriented Control (DFOC)
2. Indirect Field Oriented Control (IFOC)

Due to various advantages over DFOC, IFOC is preferred as a control technique for an induction motor. These advantages include:

1. It does not suffer from inherent low speed problems and thus can be used for all such purposes where near zero speed operation is essential [4].
2. This method avoids the requirements of flux acquisition by using known machine parameters [4].

In this work, Indirect Field Oriented Control has been adopted and therefore it will now be discussed in detail. To explain IFOC, a phasor diagram representing the control technique is given in figure 13 below.
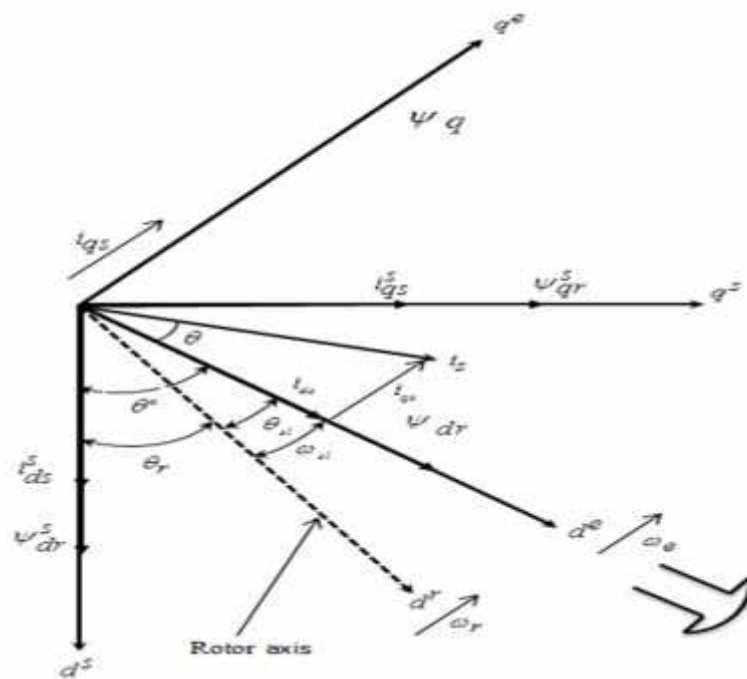
Figure 13- Indirect Field Oriented Control Phasor

In the above figure, the $(d^e - q^e)$ frame is rotating at synchronous speed of $\check{S}_e$. The $(d^s - q^s)$ Axis is fixed on the stator. The $(d^r - q^r)$ axis is fixed to the rotor and rotates at a speed of $_r$. The synchronously rotating axis rotate ahead of the rotor axis by a positive slip angle of $_{sl}$ which corresponds to slip frequency $_{sl}$. From figure 13, we can see that:

$$\check{S}_e = \check{S}_r + \check{S}_{sl} \tag{3.2}$$

$$\therefore {}_{\shortmid\shortmid} e = \int \check{S}_e \, dt = \int \left(\check{S}_r < \check{S}_{sl} \right) dt = {}_{\shortmid\shortmid} r + {}_{\shortmid\shortmid} sl \tag{3.3}$$

Now, for decoupling control, the flux component of stator current i.e. i_{ds} must be aligned

along d^e axis and the torque component i_{qs} must be aligned along the q^e axis.

In order to explain the theory of Indirect Field Oriented Control, the following figure of a simplified representation of an induction motor in the synchronous reference frame is presented.
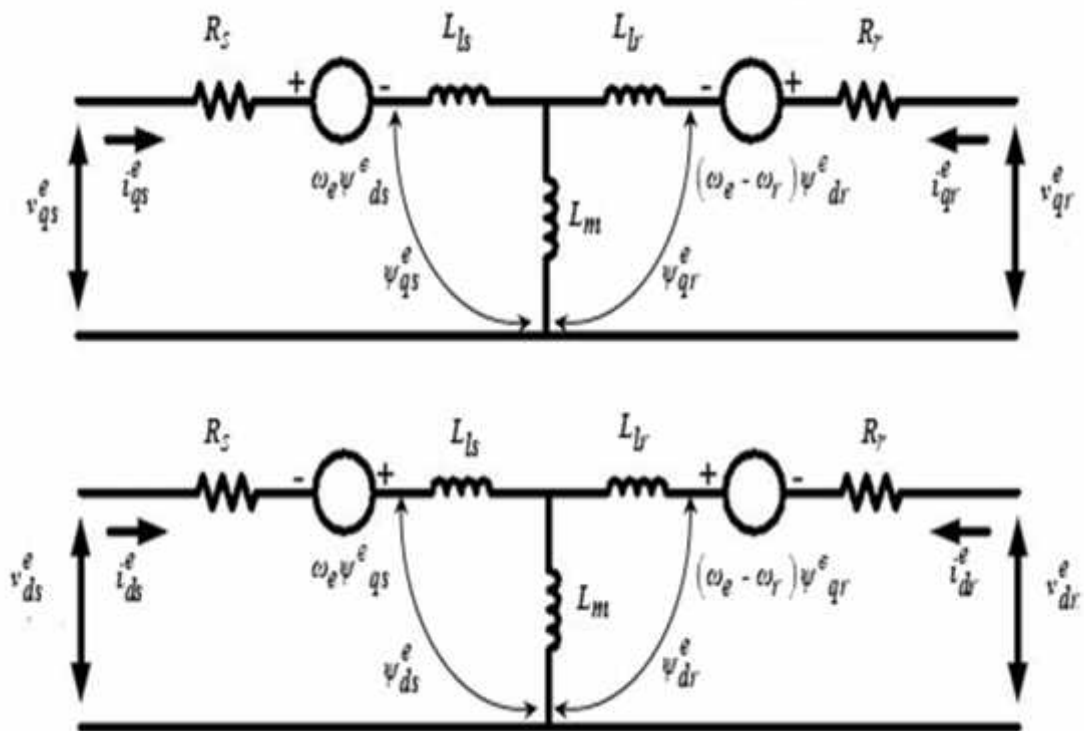
Figure-14 Synchronous Reference Frame

The rotor circuit equations can be written from figure 14 as:

$$\frac{d\Psi^e_{dr}}{dt} + R_r i^e_{dr} - (\check{S}_e > \check{S}_r)\Psi^e_{qr} = 0 \tag{3.4}$$

$$\frac{d\Psi^e_{qr}}{dt} + R_r i^e_{qr} + (\check{S}_e > \check{S}_r)\Psi^e_{dr} = 0 \tag{3.5}$$

The rotor flux linkages expression can be given as:

$$\lambda^e_{dr} = L_r i^e_{dr} + L_m i^e_{ds} \tag{3.6}$$

$$\lambda^e_{qr} = L_r i^e_{qr} + L_m i^e_{qs} \tag{3.7}$$

From above equations, we can infer:

$$i^e_{dr} = \frac{1}{L_r}\lambda^e_{dr} - \frac{L_m}{L_r}i^e_{ds} \tag{3.8}$$

$$i^e_{qr} = \frac{1}{L_r}\lambda^e_{qr} - \frac{L_m}{L_r}i^e_{qs} \tag{3.9}$$

The rotor equations of (3.4) and (3.5) can be rewritten using (3.8) and (3.9) as:

$$\frac{d\lambda^e_{dr}}{dt} + \frac{R_r}{L_r}\lambda^e_{dr} - \frac{L_m}{L_r}R_r i^e_{ds} - \omega_{sl}\lambda^e_{qr} = 0 \tag{3.10}$$

$$\frac{d\lambda^e_{qr}}{dt} + \frac{R_r}{L_r}\lambda^e_{qr} - \frac{L_m}{L_r}R_r i^e_{qs} + \omega_{sl}\lambda^e_{dr} = 0 \tag{3.11}$$

We know slip frequency= synchronous frequency – Rotor frequency

Now, indirect field oriented control ensures decoupled control of torque and flux. Hence the entire rotor magnetic flux is directed along the d_e axis. i.e. λ_r is directed along d_e axis.

Therefore:

$$\lambda_{qr} = 0 \text{ which implies } \frac{d\lambda_{qr}}{dt} = 0 \tag{3.12}$$

Substituting these values in (3.10) and (3.11) we get:

$$\frac{d\lambda_r}{dt} + \frac{R_r}{L_r}\lambda_r - \frac{L_m}{L_r}R_r i_{ds} = 0$$

$$\Rightarrow \frac{L_r}{R_r}\frac{d\lambda_r}{dt} + \lambda_r = L_m i_{ds} \tag{3.13}$$

Now, as is the usual case, rotor flux is constant. Hence $\frac{d\psi_r}{dt} = 0$

Hence at steady state,

$$\therefore \quad \psi_r = L_m i_{ds} \tag{3.14}$$

Therefore we can conclude that the rotor flux is directly proportional to current i_{ds}.

Also, we have

$$\omega_{sl} \psi_{dr} = \frac{L_m}{L_r} R_r i_{qs}$$

$$\therefore \quad \omega_{sl} = \frac{L_m R_r}{\psi_r L_r} i_{qs} \tag{3.15}$$

The slip speed is added to the rotor speed to obtain the synchronous speed as

$$\check{S}_e = \check{S}_r + \check{S}_{sl}$$

We see from equation (3.13), in laplace domain, the equation becomes:

$$\psi_r \left(\frac{L_r}{R_r} s + 1 \right) = L_m i_{ds} \quad \text{where s = Laplace transform of derivative term}$$

$$\Rightarrow \quad \psi_r = \frac{L_m i_{ds}}{1 + \tau s} \quad \text{or} \quad \psi_{dr} = \frac{L_m i_{ds}}{1 + \tau s} \tag{3.16}$$

Where $\tau = \frac{L_r}{R_r}$ is the rotor time constant.

The electromagnetic torque can be shown as:

$$T_e = \frac{3}{2} \left(\frac{P}{2} \right) L_m (i_{qs}^s i_{dr}^s - i_{ds}^s i_{qr}^s) \quad \ldots\ldots\ldots \text{from equation (2.25)}$$

Putting the values of equations (3.8) and (3.9) into equation (2.25), we have:

$$T_e = \frac{3}{2} \left(\frac{P}{2} \right) \frac{L_m}{L_r} (i_{qs}^e \psi_{dr}^e - i_{ds}^e \psi_{qr}^e) \tag{3.17}$$

Now, we have $\lambda_{dr}^e = \lambda_r$ and $\lambda_{qr}^e = 0$

$$\therefore T_e = \frac{3}{2}\left(\frac{P}{2}\right)\frac{L_m}{L_r}\left(i_{qs}^e \lambda_r\right) \tag{3.18}$$

Therefore from equation (3.18) it can be seen that Electromagnetic torque is directly proportional to the torque component of stator current i_{qs}^e provided the rotor flux is considered to be constant. Again, from equation (3.14) we see that the rotor flux is proportional to the flux component of stator current i_{ds}^e. Therefore we find that the flux and the torque can be varied independently without any coupling effect.

Figure 15 below shows the schematics of the control structure for Indirect Field Oriented Control. In order to implement IFOC, it is necessary to generate the reference current components for torque and flux i.e. i_{qs}^* and i_{ds}^* respectively.

From the figure we can see that a reference value of rotor flux $\lambda_{dr}^{e*}\left(\text{or }\lambda_r^*\right)$ is given an input. This value is the desired value of rotor flux. From this reference flux, the d axis component of stator current i_{ds}^{e*} is calculated according to the following equation:

$$\lambda_{dr}^{e*} = \frac{L_m i_{ds}^{e*}}{1+\tau_r s}$$

Now the desired value of electromagnetic torque T_e^* can be obtained from the PI controller output of the outer speed loop for a chosen value of rotor flux. Then the reference value of q axis component i_{qs}^{e*} can be further calculated as:

$$\therefore T_e^* = \frac{3}{2}\left(\frac{P}{2}\right)\frac{L_m}{L_r}\left(i_{qs}^{e*} \lambda_r^*\right) \tag{3.19}$$
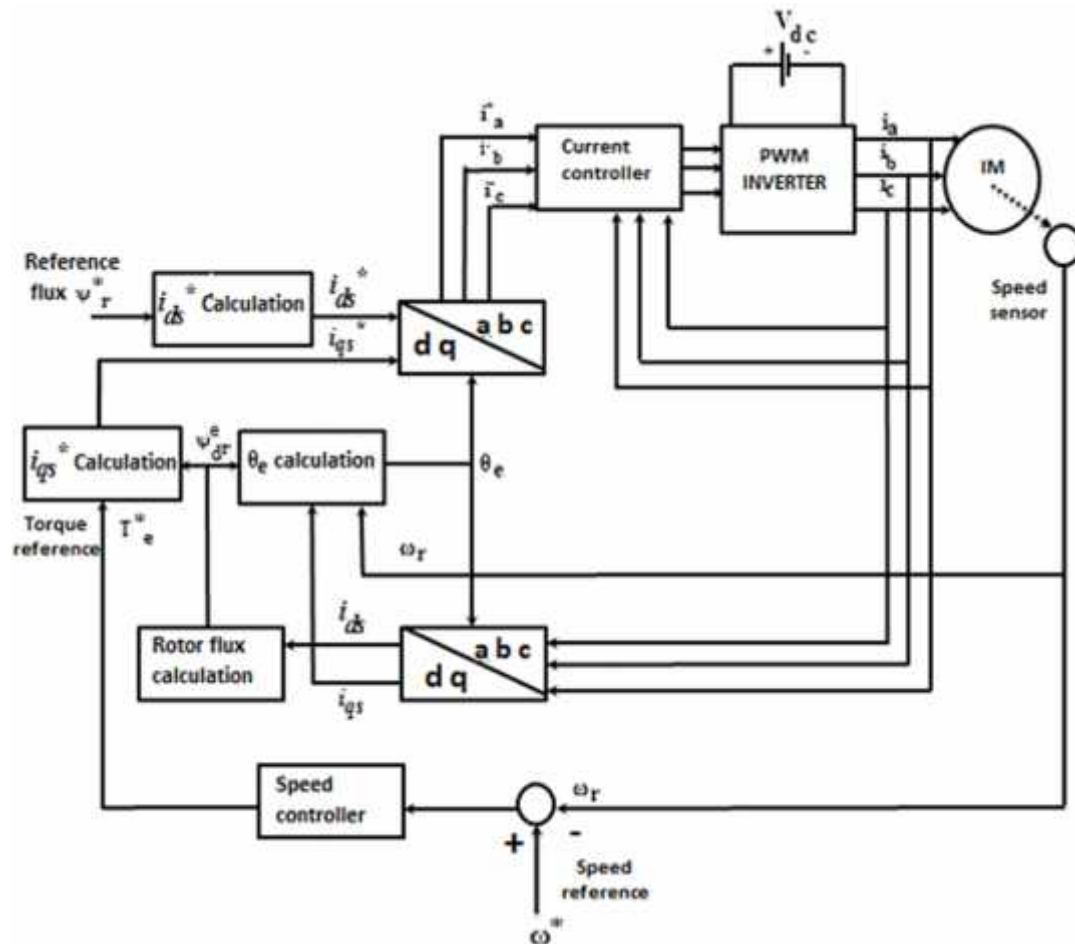
Figure 15. Indirect Field Oriented Control Structure

B. <u>INTERNAL STRUCTURE OF INDIRECT FIELD ORIENTED CONTROL :</u>

IFOC consists of two loop:

1. Inner current loop
2. Outer speed loop

The entire structure is an IFOC is cascaded control. i.e. the outer loop of the control structure generates an output which is used as input for the inner control loop. The Induction motor is fed through a sine PWM (in our case) which ensures a three phase alternating supply to the motor. The actual speed of the motor is sensed and sent back to a controller where it is compared to a reference speed and the error is subjected to a PI controller to produce a torque command. This controller which produces torque output while having speed error as an input

is the speed controller. The output from this controller, i.e. the torque command is used to generate the reference q axis component of stator current according to the equation

$$i_{qs}^{e*} = \frac{4L_r}{3PL_m \ _{dr}^e} \qquad (3.20)$$

After the q axis current component has been calculated, it is compared to the actual measured i_{qs}^e and the error signal is passed through a PI type controller. Output from this PI controller is used to generate the necessary voltages to be fed to the PWM inverter.

For the flux component of the stator current, the reference value is calculated from the equation :

$$_{dr}^{\ *} = \frac{L_m i_{ds}^{\ *}}{1+ \ s}$$

In steady state, s=0, hence

$$i_{ds}^{\ *} = \frac{_{dr}^{\ *}}{L_m} \qquad (3.21)$$

The actual value of d axis component of stator current i_{ds}^e is compared to the value of the reference $i_{ds}^{\ *}$ and the error signal generated is fed to a PI controller. The output of this PI controller along with the output of the PI controller for the q axis component is used to generate the required voltages for the sinusoidal PWM.

INNER CURRENT LOOP

The inner current loop consists of the d axis and q axis current controllers and is used to control the torque dynamics of the system. The reference torque as generated by the outer loop is transformed to actual electromagnetic torque by this loop. The voltage equations of an induction motor is presented in [23] as

$$\begin{pmatrix} V_{ds}^e \\ V_{qs}^e \\ 0 \\ 0 \end{pmatrix} = \begin{pmatrix} R_s + L_s p & -\omega_e L_s & L_m p & -\omega_e L_m \\ \omega_e L_s & R_s + L_s p & \omega_e L_m & L_m p \\ L_m p & -(\omega_e - \omega_r)L_m & R_r + L_r p & -(\omega_e - \omega_r)L_r \\ (\omega_e - \omega_r)L_m & L_m p & (\omega_e - \omega_r)L_r & R_r + L_r p \end{pmatrix} \begin{pmatrix} i_{ds}^e \\ i_{qs}^e \\ i_{dr}^e \\ i_{qr}^e \end{pmatrix} \tag{3.22}$$

These voltage equations can be written in synchronous reference frame as [8] :

$$V_{ds}^e = R_s i_{ds}^e + \sigma L_s \frac{d}{dt} i_{ds}^e + \frac{L_m}{L_r} \frac{d}{dt} \psi_{dr}^e - \omega_e \sigma L_s i_{qs}^e - \omega_e \frac{L_m}{L_r} \psi_{qr}^e \tag{3.23}$$

$$V_{qs}^e = R_s i_{qs}^e + \sigma L_s \frac{d}{dt} i_{qs}^e + \frac{L_m}{L_r} \frac{d}{dt} \psi_{qr}^e - \omega_e \sigma L_s i_{ds}^e - \omega_e \frac{L_m}{L_r} \psi_{dr}^e \tag{3.24}$$

Where $\sigma = \left(1 - \frac{L_m^2}{L_r L_s} \right)$ is the leakage coefficient. The third term of the two equations can be neglected as the rotor flux dynamics is very slow with respect to the current dynamics. Now when the d axis is aligned with the rotor flux, the q axis flux becomes zero. Therefore $\psi_{qr}^e = 0$ also the entire rotor flux is aligned along the d axis. Therefore from equation (3.16),

$$\psi_{dr} = \frac{L_m i_{ds}}{1 + \tau_r s}$$

As the rotor flux dynamics is slow compared to the current dynamics, the above equation can be written as:

$$\psi_{dr} = L_m i_{ds} \tag{3.25}$$

Putting this value in equations (3.23) and (3.24) and equating $\psi_{qr}^e = 0$, we get

$$V_{ds}^e = R_s i_{ds}^e + \sigma L_s \frac{d}{dt} i_{ds}^e - \omega_e \sigma L_s i_{qs}^e \tag{3.26}$$

And,

$$V_{qs}^e = R_s i_{qs}^e + \sigma L_s \frac{d}{dt} i_{qs}^e - \omega_e L_s i_{ds}^e \tag{3.27}$$

OUTER SPEED LOOP:

The electromechanical equation pertaining to IFOC is given by :

$$T_e = T_L + J\frac{d\omega_m}{dt} + B\omega_m \tag{3.28}$$

Where B is the coefficient of friction and ω_m is the mechanical speed of the motor.

If speed is presented as an electrical quantity in rad/sec, the equation becomes:

$$T_e = T_L + \frac{2}{P}\left(J\frac{d\omega_r}{dt} + B\omega_r\right) \tag{3.29}$$

The above equation can be represented in the form of a block diagram by:
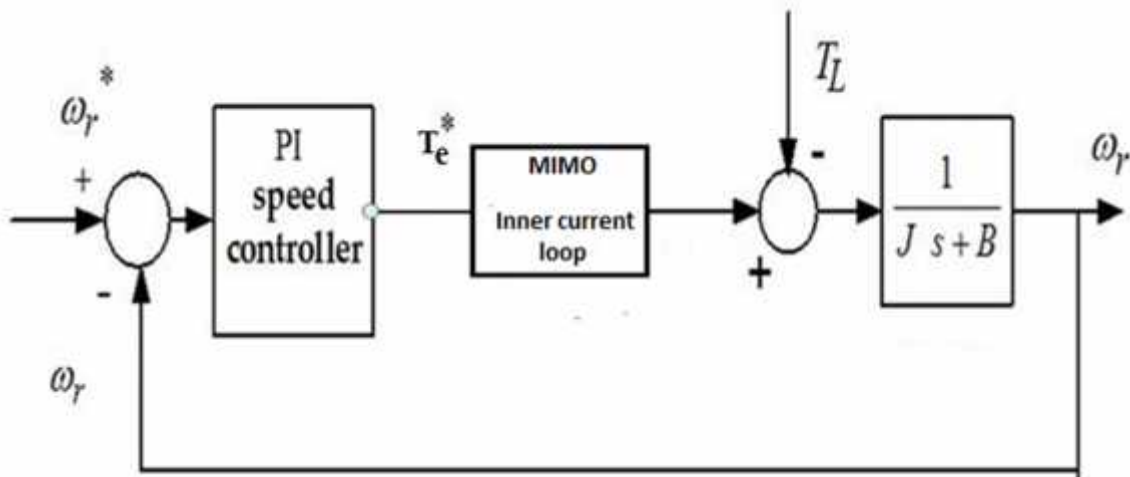
Figure 16. Block diagram depicting the outer speed loop

The outer speed loop is much slower than the inner current loop can be treated as a block with unity gain. This is because the electrical time constant of the Inner current controller structure is much less than the mechanical time constant of the outer speed loop. i.e. the mechanical system of the speed loop is much slower compared to the electrical system of the inner speed loop.

3.2 Sinusoidal Pulse Width Modulation (SPWM):

Variable speed operation is now popular and desirable for three phase alternating current machines such as induction machines. For efficient variable speed operation, supply to the machine should be a balanced set of three phase voltages with variable frequency. Traditionally the most popular and widely used method for generating such voltages is the Pulse Width Modulation Technique [24].

Basically the Pulse Width Modulation Technique is a method where the output signals are constructed through comparison between two control signals- a carrier signal and a modulation signal. This is known as Carrier based PWM. The carrier waveform is essentially a high frequency triangular waveform while the modulation waveform can be of any shape. When peak of the modulation signal becomes less than the peak of the carrier signal, the output waveform follows the shape of the modulation waveform. If instantaneous value of the modulation waveform is greater than the carrier signal for any interval of time, then for that time interval, the output gets connected to the positive side of DC link. Else, the output is connected to the negative terminal of the D C Link [25] .

By using this approach the output waveform can be made to follow any desired wave shape.

Sinusoidal pulse width modulation is a type of carrier based PWM technique. Here, the peak of the modulation signal is always less than the peak of the carrier signal. Realization of SPWM is achieved by having a high frequency triangular carrier wave V_c compared with a sinusoidal reference wave V_r of desired frequency. The intersection of the two waveforms gives the switching instant and commutation of the modulated phase. The two waveforms are fed to a comparator. During the time period when the modulating sinusoid has a peak value greater than the triangular carrier wave, the comparator output is high. Else, it is low. When triangular carrier wave has its peak coincident with zero of the reference sinusoid there are

$N = \dfrac{f_c}{2f}$ pulses per half cycle. In case the zero of the triangular wave coincides with the zero of the reference sinusoid, there are (N-1) pulses per cycle [26].
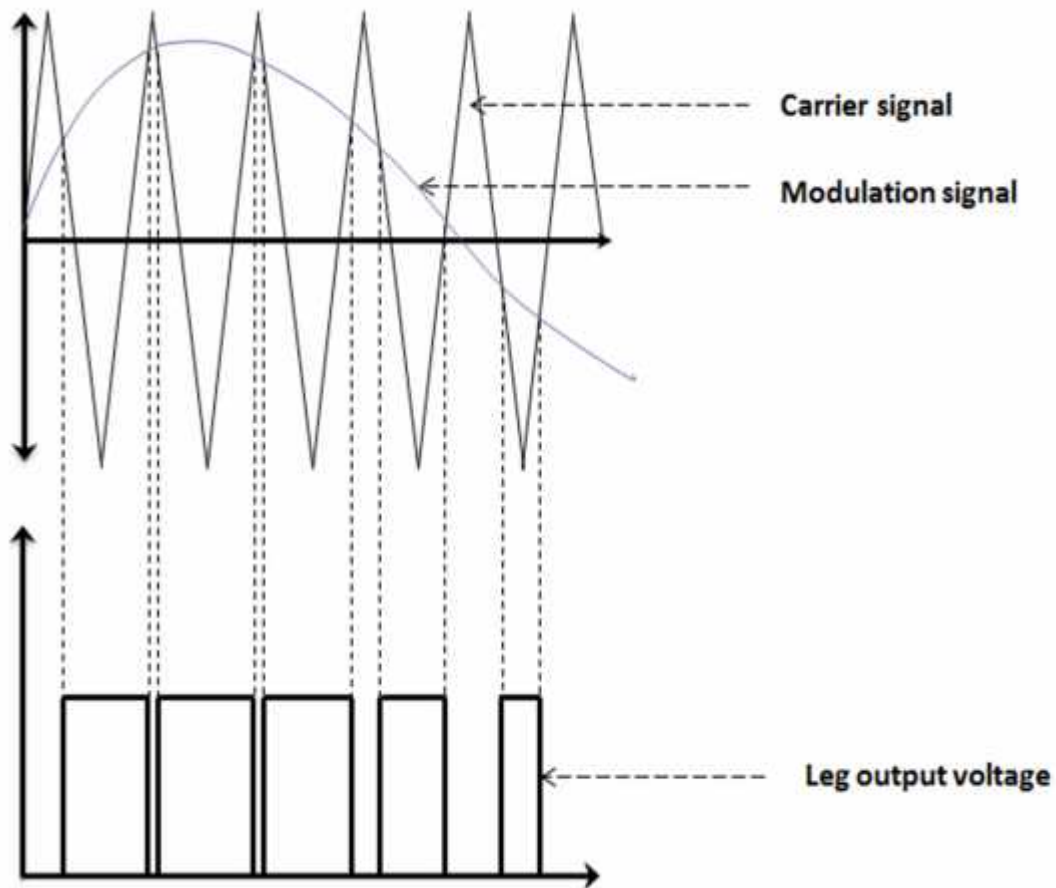
Figure 17. 1 phase Sinusoidal Pulse Width Modulation.

Modulation index:

Modulation index is the ratio of the peak magnitude of the modulating waveform and the carrier waveforms. It relates the inverters dc link voltage and the magnitude of the pole voltage output by the inverter. If the modulating signal is $V_m \sin(\omega t)$ and the magnitude of the carrier wave ranges between $+V_c$ and $-V_c$ then the ratio of the peak magnitude of the modulating signal to the peak magnitude of the carrier waveform is the modulation index.

$$m = \frac{V_m}{V_c}$$

Normally the modulation index is maintained below 1. i.e. $0 < m < 1$

OVERMODULATION:

When the modulating waveform has a peak magnitude greater than the peak magnitude of the carrier wave, i.e. when *m>1* the PWM inverter operates under over-modulation mode. During over modulation, the fundamental component of pole voltage increases slightly with increase in modulation index but the linear relation between them no longer exists. Also there is introduction of lower frequency harmonics in the pole-output waveform. The fact that over-modulation introduces lower order harmonics makes their use very rare [27].

THREE PHASE SPWM:

Three phase PWM can be used for obtaining a three phase sine modulated pole voltage pulses. Switches in each of the three poles of the inverters are individually controlled. For a balanced three-phase output voltage from the inverter poles, the three sinusoidal modulating signals (one for each pole) must also be balanced three-phase signals. The carrier waveform for all the three poles may remain identical. The fundamental components of individual pole output voltages (for 0<<1) will then be proportional to the corresponding modulating signals.
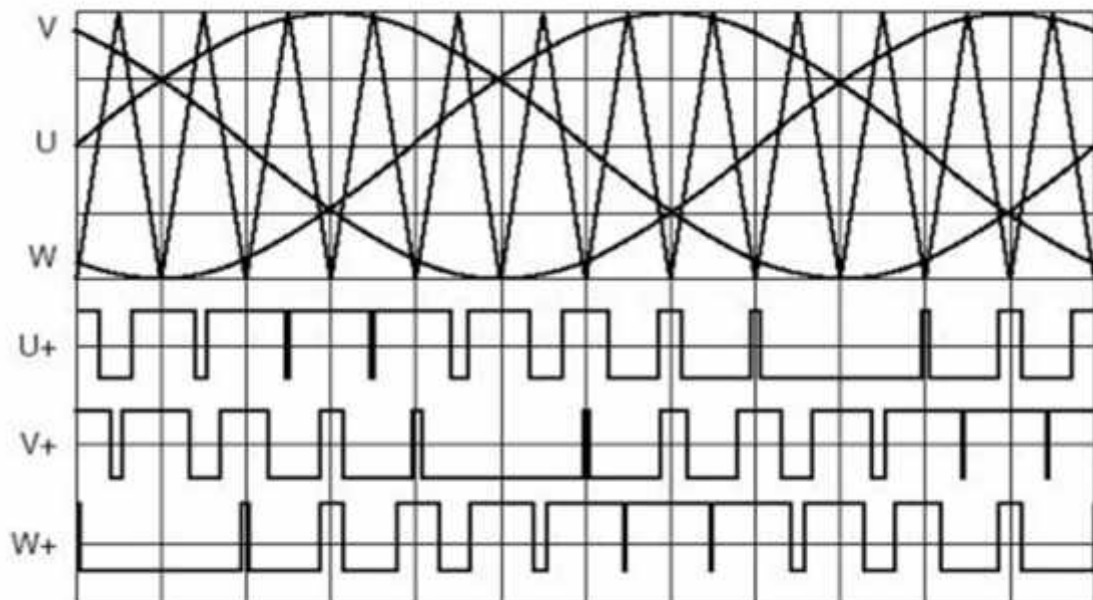
Figure 18. Three phase Sine Pulse Width Modulation

3.3 Simulation of IFOC, Results and Discussion on results:

A.   <u>Simulation of IFOC:</u>

Simulation of the field oriented control for the induction machine is carried out in MATLAB Simulink. The machine used is the one for which dynamic modelling was presented in section 2.2b. For the simulation, the equations used are in accordance to the derivations presented in section 3.2. Tuning of the controller parameters is the main objective of the thesis and it has been presented in the next chapter. As of now, it is essential to provide the controller parameters in order to run the simulation. Therefore here, the control parameters of the PI controllers in the speed loop and the current loop have been assigned arbitrary values. All values that have been taken for the simulation have been presented in table 2.

Table 2. Parameters for IFOC of Induction machine

PARAMETER OF THE MOTOR	SYMBOL	VALUES CHOSEN
Voltage per phase	V_m (volts)	60 volts (peak)
Frequency	F (Hz)	69 hertz
Per phase Stator resistance	R_S (ohms)	1.627e-3
Per phase Rotor resistance	R_r (ohms)	1.364e-3
Stator leakage inductance per phase	L_{ls}	19.42e-6 H
Rotor leakage inductance per phase	L_{lr}	19.42e-6 H
Air gap leakage inductance (magnetising) per phase	L_{ms}	320e-6 H
No. of poles	P	4

Moment of Inertia	J (kg-m^2)	0.03
Frictional Coefficient	B (N-m-s)	0.07
Rotor flux (reference)	Wb	0.075
Upper limit of speed controller		+40
Lower limit of speed controller		-40
$\mathbf{K_p}$ of speed controller		10
Қ of speed controller		100
$\mathbf{K_p}$ of current controller		150
Қ of current controller		0.01
Simulation step size	sec	1e-5

A load torque of 35 Nm was applied at 2 seconds as a step input.

B. **Results:**

The simulation was run at a time step of 1e-5 seconds and the following responses were obtained:

1. Reference and actual speed of the motor
2. Zoomed view of the reference and actual speeds
3. Stator currents of the motor
4. Electromagnetic torque of the motor
5. D axis rotor flux i.e. $\overset{e}{}_{dr}$

The responses obtained after running the simulation for 50 seconds have been given below:
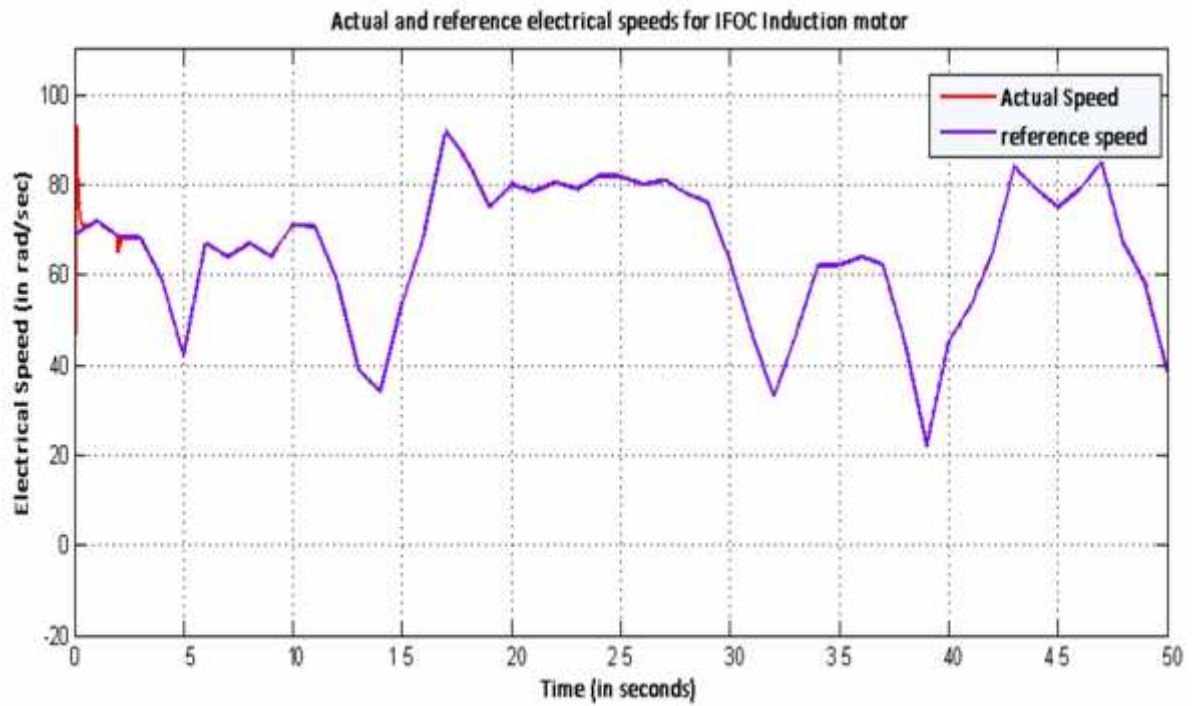
Figure 19- Actual and Reference electrical speeds for IFOC induction motor
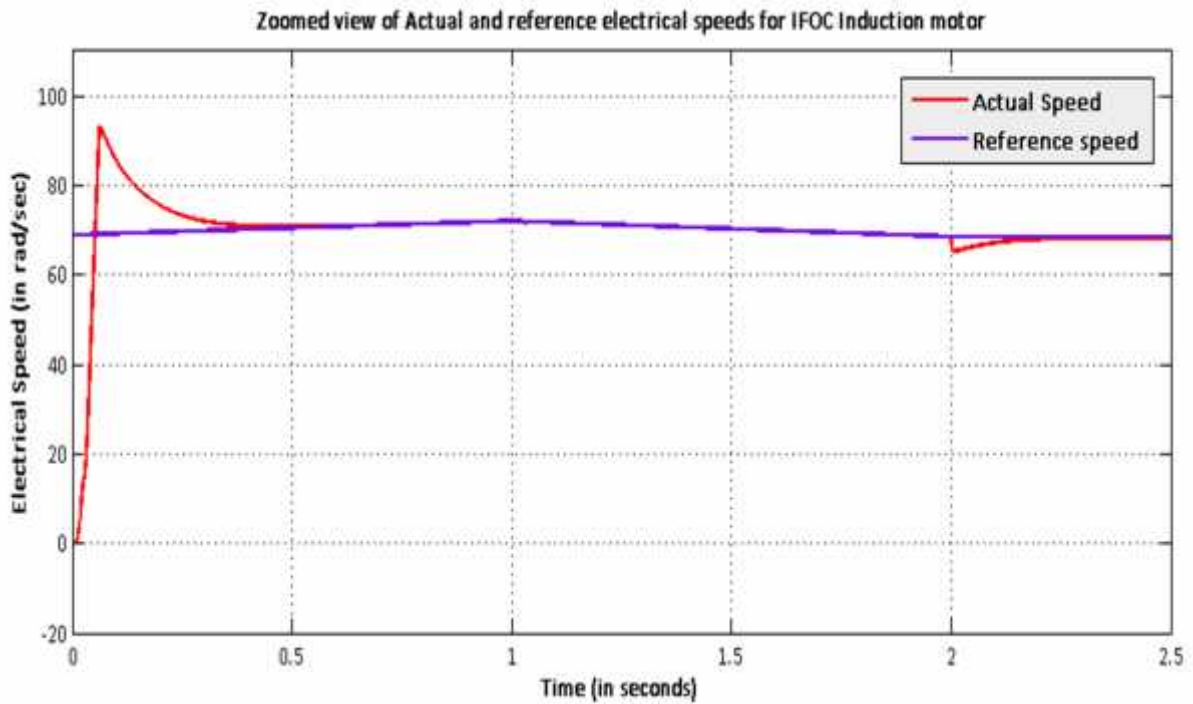
Figure 20- Zoomed view of reference and actual electrical speeds for IFOC Induction machine
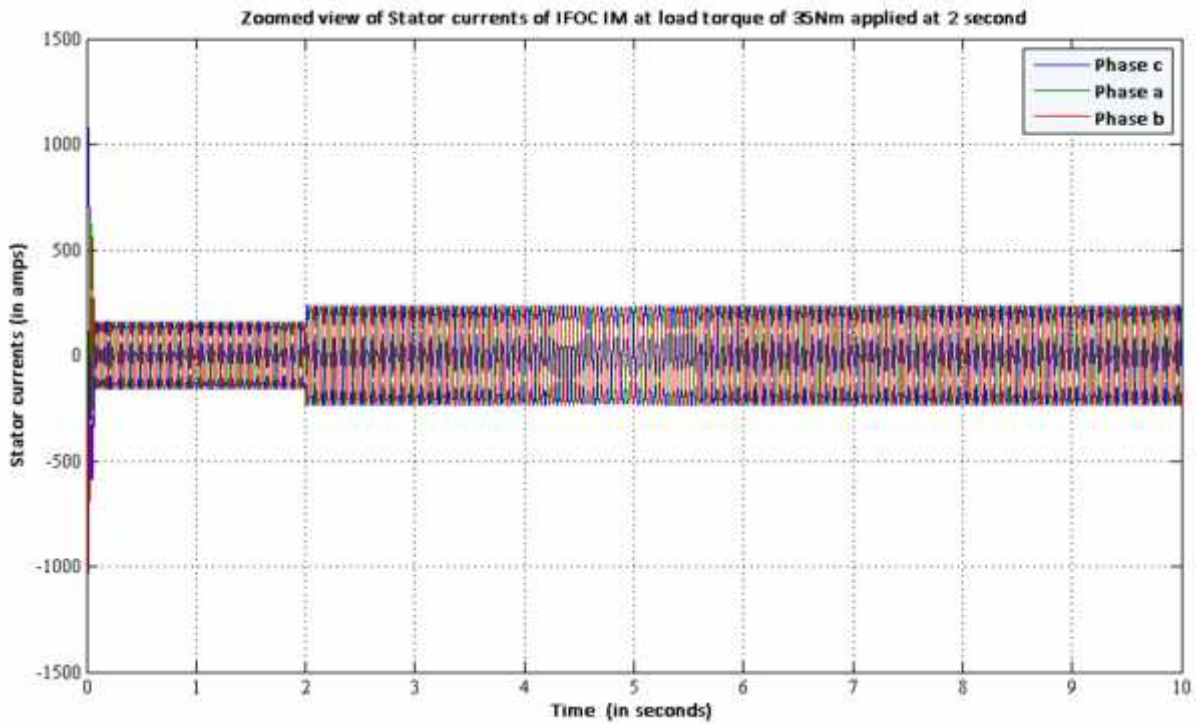
Figure 21- Zoomed view of the stator currents of IFOC Induction machine when a load torque of 35 Nm is applied at 2 seconds
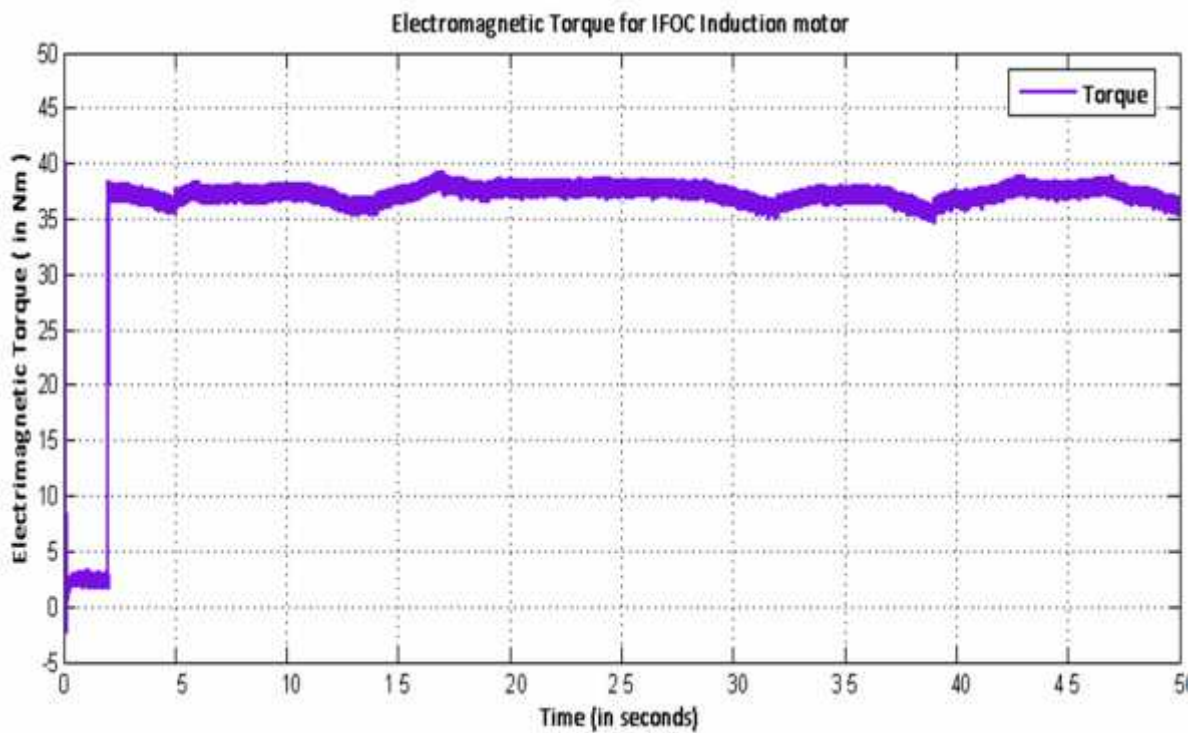
Figure 22- Electromagnetic torque variation for IFOC Induction motor
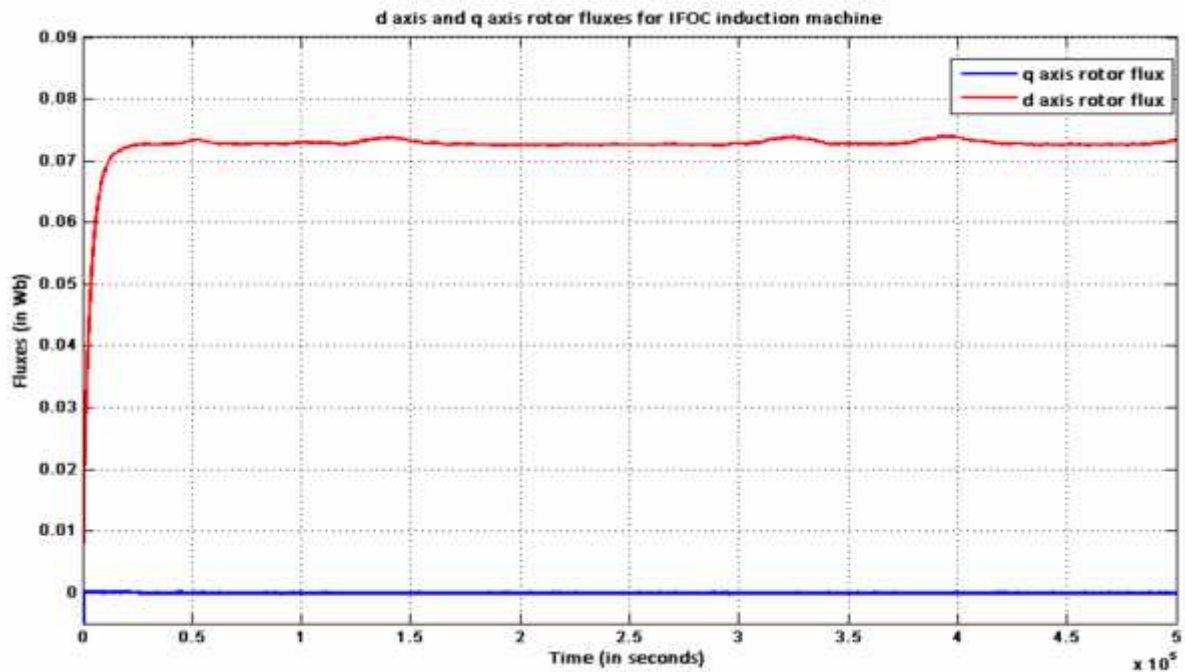
Figure 23- d-axis and q axis rotor flux for IFOC Induction machine where reference given is 0.075 Wb

C.   Discussion on results:

It can be observed from figure 19 that after an initial overshoot the actual speed of the motor effectively starts tracking the reference speed input. At 2 seconds a load torque of 35Nm has been applied. Therefore at 2 seconds the speed of the motor dips by about 2 rpm after which it again starts tracking the reference speed. The initial overshoot and thereafter settling of the actual speed to track the reference speed can be observed in figure 20. The same figure shows the effect of load torque (applied at 2 seconds) on the actual speed of the motor.

After application of load torque, there is an increase in the stator current as the motor now draws more current from the supply in order to meet the additional torque. This increase in current has been observed in figure 21.

The variation of electromagnetic torque can be observed from figure 22. Initially the motor runs at no load. During this time the torque of the machine should ideally be zero, but the presence of some friction and windage torque affects the electromagnetic torque such that at

no load, it has some minimal value in order to meet the frictional torque. After the application of load torque, the electromagnetic torque increases to meet the new torque demand. The torque response is somewhat oscillatory because of the presence of a varying speed profile. As speed varies considerably, some variations in torque response is observed.

We find from figure 23 that the d axis flux gradually increases and becomes equal to the reference flux set at 0.075 Wb. The q axis flux remains zero. This figure shows the two primary objectives of Field Oriented Control-

1.   The entire rotor flux is aligned along axis and the d axis flux exactly tracks threference rotor flux (set to 0.075 Wb).

2.   The q axis rotor flux is equal to zero.

Therefore we can conclude that satisfactory results for an Indirect Field Oriented Control scheme for an Induction machine have been achieved.

The methodologies for design of the controllers for the inner and the outer loops are presented in the next sections.

3.4 Block Diagram Reduction :

Before we continue to block diagram reduction, it is necessary to deduce mathematical dynamic equations of each of the components of the plant and then form transfer functions of each of those individual blocks. Figure 24 represents the entire system in the form of a block diagram.

A.   Derivations for block diagram representation of IFOC :

For designing speed controller of IFOC induction machines, the primary assumption is constant rotor flux linkages. Thus the following relation can be presented:

$$_r = a \tag{3.30}$$

$$\therefore \frac{d}{dt}{}_r = 0 \tag{3.31}$$

Now the stator equations of the motor can be written as :

$$V_{ds}^e = -{}_s L_s i_{qs}^e + (R_s + L_s p) i_{ds}^e - {}_s L_m i_{qr}^e + L_m p i_{dr}^e \tag{3.32}$$

$$V_{qs}^e = (R_s + L_s p)i_{qs}^e + {}_s L_s i_{ds}^e + L_m p i_{qr}^e + {}_s L_m i_{dr}^e \tag{3.33}$$

From equation (3.6), we have :

$$i_{dr}^e = \frac{r}{L_r} - \frac{L_m}{L_r} i_{ds}^e \tag{3.34}$$

And from equation (3.7) we have :

$${}^e{}_{qr} = L_r i^e{}_{qr} + L_m i^e{}_{qs} \tag{3.35}$$

As ${}^e{}_{qr} = 0$,

We have $i_{qr}^e = -\frac{L_m}{L_r} i_{qs}^e$

Substituting the above equations in (3.32) and (3.33), we have:

$$V_{ds}^e = (R_s + {}_s L_s p)i_{ds}^e - L_s {}_s i_{ds}^e + \frac{L_m}{L_r} p {}_r \tag{3.36}$$

$$V_{qs}^e = (R_s + {}_s L_s p)i_{qs}^e + L_s {}_s i_{ds}^e + {}_s \frac{L_m}{L_r} {}_r \tag{3.37}$$

Where † is the leakage coefficient, $= 1 - \frac{L_m^2}{L_r L_s}$

We know from Vector Control that the flux producing component of the stator current is constant (in steady state). As the d axis stator current is the flux producing component, therefore, it is constant and hence the derivate of this cmponent is zero. $i_f = i_{ds}^e$

$$\therefore \frac{d}{dt} i_{ds}^e = 0$$

From FOC, we also know that the q axis component of the stator current is the torque component. $i_T = i_{qs}^e$

Substituting these in equation for the q axis voltage we have

$$V_{qs}^e = (R_s + L_a p)i_T + \omega_s L_a i_f + \omega_s \frac{L_m}{L_r}\lambda_r \tag{3.38}$$

Where L_a is: $L_a = \sigma L_s$ (3.39)

$$\therefore L_a = L_s - \frac{L_m^2}{L_r} \tag{3.40}$$

Substituting $\lambda_r = L_m i_f$ gives q axis stator voltage as:

$$V_{qs}^e = (R_s + L_a p)i_T + \omega_s L_a i_f + \omega_s \frac{L_m^2}{L_r}i_f$$

$$\Rightarrow \quad V_{qs}^e = R_s + L_a p i_T + \omega_s L_s i_f \tag{3.41}$$

Now we obtain the frequency as :

$$\omega_e = \omega_r + \omega_s = \omega_r + \frac{i_T}{i_f}\left(\frac{R_r}{L_r}\right)$$

Electrical equation of the motor is obtained by substituting for ω_s. Substituting and simplifying, we get :

$$V_{qs}^e = \left(R_s + \frac{R_r L_s}{L_r} + L_a p\right)i_T + \omega_r L_s i_f \tag{3.42}$$

From the above equation, i_T can be calculated as:

$$i_T = \frac{V_{qs}^e - \omega_r L_s i_f}{R_s + \frac{R_r L_s}{L_r} + L_a p}$$

$$\Rightarrow \quad i_T = \frac{K_a}{(1 + sT_a)}\left\{V_{qs}^e - \omega_r L_s i_f\right\} \tag{3.43}$$

Where,

1. $R_a = R_s + \dfrac{L_s}{L_r} R_r$ (3.44)

2. $K_a = \dfrac{1}{R_a}$ (3.45)

3. $T_e = K_t i_T$ (3.46)

4. $T_a = \dfrac{L_a}{R_a}$ (3.47)

5. $K_t = \dfrac{3PL_m^2}{4L_r} i_f$ …. (torque constant) (3.48)

Also, the electromagnetic torque is represented as :

$$J \frac{d\check{S}_m}{dt} + B\check{S}_m = T_e - T_l = K_t i_T - B_l \check{S}_m \qquad (3.49)$$

In the above equation, converting mechanical speed to electrical speed by multiplying throughout by a pair of poles, we have

$$J \frac{d\check{S}_r}{dt} + B\check{S}_r = \frac{P}{2} K_t i_T - B_l \check{S}_r \qquad (3.50)$$

Therefore the transfer function between the speed and torque producing currents is given by:

$$\frac{I_T(s)}{\check{S}_r(s)} = \frac{K_m}{1 + sT_m} \qquad (3.51)$$

Here, $K_m = \dfrac{PK_t}{2B_t}$ (3.52)

$B_t = B + B_l$ and $T_m = \dfrac{J}{B_t}$

INVERTER MODEL-

The inverter supplies the q axis voltage to the motor with a command input which is the error between the torque current reference and the torque current feedback. The inverter is

modeled as a gain K_{in} and a time lag T_{in}. The gain is obtained from the dc link voltage to the inverter V_{dc} and maximum control voltage

$$K_{in} = 0.65 \frac{V_{dc}}{V_{cm}} \qquad (3.53)$$

The factor 0.65 has been introduced such the maximum peak fundamental voltage obtainable from the inverter with a given dc link voltage is accounted for. Time lag in the inverter is equal to the average carrier switching cycle time, i.e. half the period. This is expressed in terms if the PWM switching frequency as :

$$T_{in} = \frac{1}{2 f_c} \quad [3]$$

SPEED CONTROLLER MODEL:

There is a controller that processes the error between the speed reference and actual speed feedback signal. This is a PI (Proportional-Integrator) type controller that has a transfer function of the form:

$$G_s(s) = K_p + \frac{K_i}{s} \qquad (3.54)$$

Where K_p is the proportional gain and K_i is the integral gain
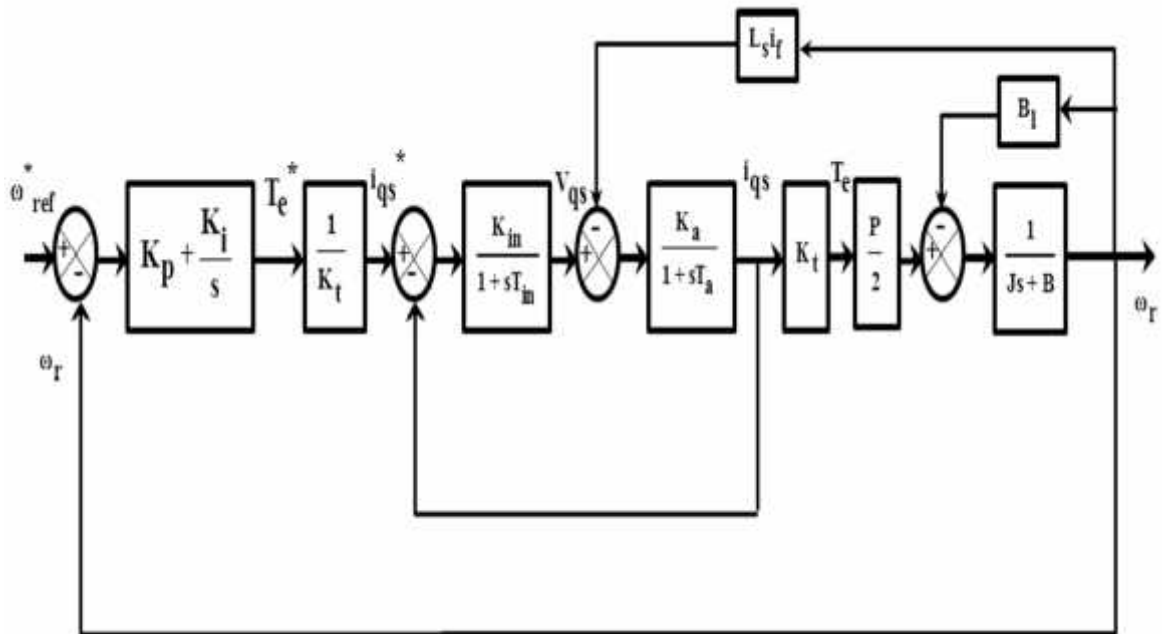
Figure 24. Block diagram representation of the IFOC Induction Machine system

Block diagram reduction techniques are applied on the above block diagram and finally a system is obtained as given in figure 25.
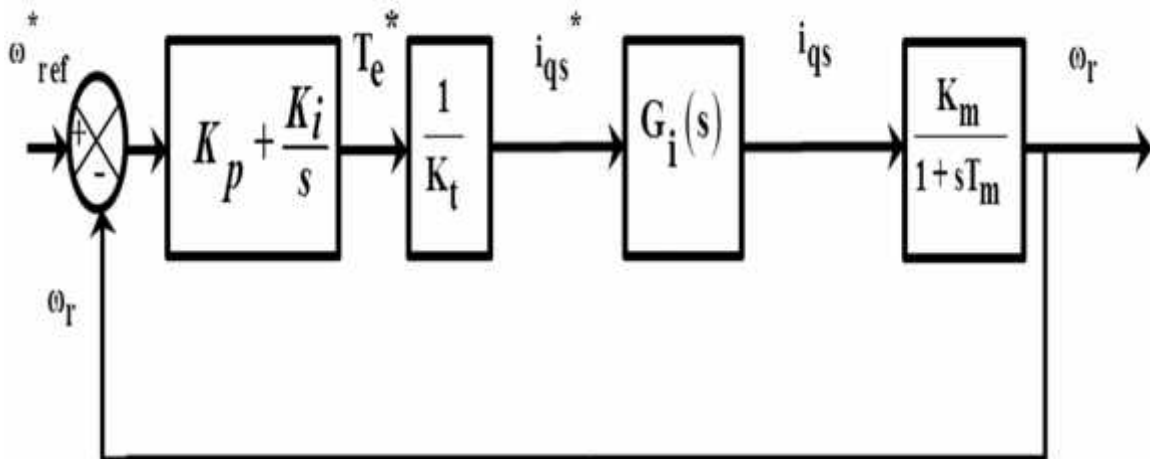
Figure 25. Reduced Block Diagram of IFOC induction machine

Here, we have $G_i(s)$ as is given in figure 26:
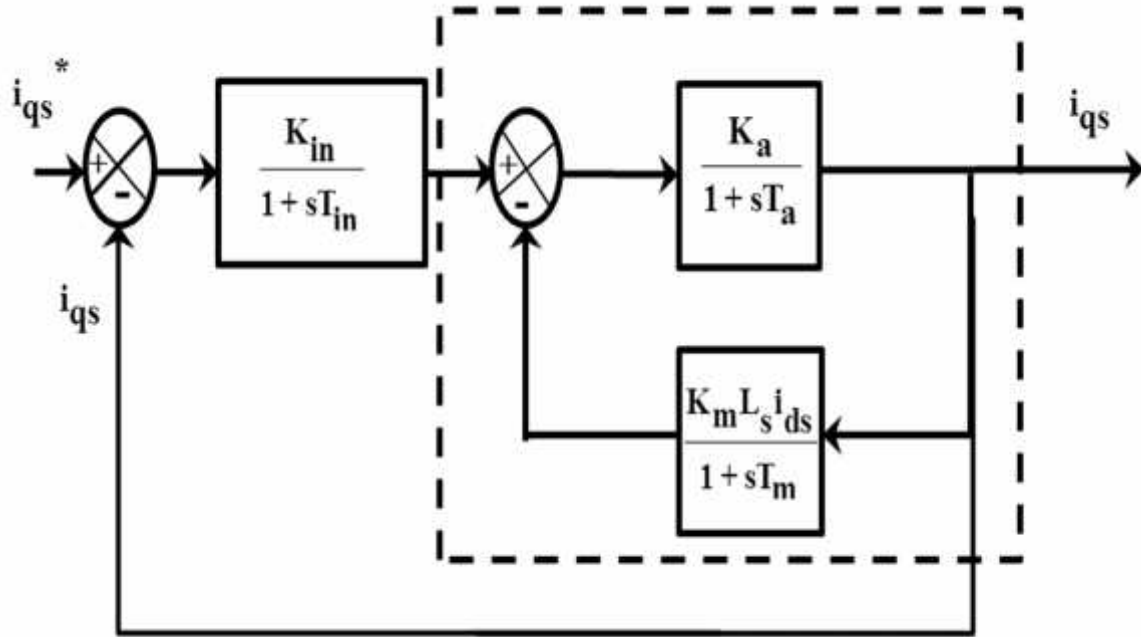
Figure 26. Block Diagram of $G_i(s)$ - The Electrical dynamics of the plant

The dotted portion of the block diagram can be represented in transfer function form as:

$$\frac{\dfrac{K_a}{(1+sT_a)}}{1+\dfrac{K_aK_mL_si_{ds}^{e}}{(1+sT_a)(1+sT_m)}}$$

$$\Rightarrow \qquad \frac{K_a(1+sT_m)}{(1+sT_a)(1+sT_m)+K_aK_mL_si_{ds}^{e}}$$

Therefore open loop tranfer function $G_{iol}(s)$ can be represented as:

$$G_{iol}(s)=\frac{K_aK_{in}(1+sT_m)}{(1+sT_{in})(1+sT_a)(1+sT_m)+K_aK_mL_si_{ds}^{e}(1+sT_{in})} \qquad (3.55)$$

Hence, the electrical dynamics of the plant can be represented in the form of a transfer function $G_i(s)$ as:

$$G_i(s)=\frac{K_aK_{in}(1+sT_m)}{(1+sT_{in})(1+sT_a)(1+sT_m)+K_aK_mL_si_{ds}^{e}(1+sT_{in})+K_aK_{in}(1+sT_m)} \qquad (3.56)$$

This current transfer function $G_i(s)$ can be approximated to a first order transfer function as:

T_{in} is usually negligible compared to T_m and in the vicinity of the crossover frequency, the following approximations are valid [3]:

1. $\quad 1 + sT_{in} \cong 1$ $\hfill (3.57)$

2. $\quad \left(1 + sT_a\right)\left(1 + sT_{in}\right) \cong 1 + s\left(T_a + T_{in}\right) \cong 1 + sT_{ar}$ $\hfill (3.58)$

Where $T_{ar} = T_a + T_{in}$

$\therefore G_i(s)$ becomes:

$$G_i(s) = \frac{K_a K_{in}}{\left(1 + sT_{ar}\right)\left(1 + sT_m\right) + K_a K_b + K_a K_{in} sT_m + K_a K_{in}} \qquad (3.59)$$

Where $K_b = K_m L_s i_{ds}^e$

$\Rightarrow \quad \dfrac{K_a K_{in}\left(1 + sT_m\right)}{s^2 T_a T_m + s\left(T_a + T_m\right) + 1 + K_a K_b + K_a K_{in} sT_m + K_a K_{in}}$

$\Rightarrow \quad \dfrac{K_a K_{in}\left(1 + sT_m\right)}{s^2 T_a T_m + s\left[T_a + T_m + K_a K_{in} T_m\right] + \left[1 + K_a K_b + K_a K_{in}\right]}$

$\Rightarrow \quad \dfrac{K_a K_{in}}{T_a T_m}\left[\dfrac{1 + sT_m}{s^2 + As + B}\right]$ $\hfill (3.60)$

Where $A = \dfrac{T_a + T_m + K_a K_{in} T_m}{T_a T_m}$ $\hfill (3.61)$

And

$B = \dfrac{1 + K_a K_b + K_a K_{in}}{T_a T_m}$ $\hfill (3.62)$

Now, we write the demoninator part of the equation separately as:

$$s^2 + As + B = \left(s + T_1\right)\left(s + T_2\right)$$

$\Rightarrow \quad s^2 + As + B = s^2 + \left(T_1 + T_2\right)s + T_1 T_2$

Hence we have $A = T_1 + T_2$

And $B = T_1 T_2$

$\Rightarrow \quad T_2 = \dfrac{B}{T_1}$ (3.63)

$\Rightarrow \quad A = T_1 + \dfrac{B}{T_1}$

$\Rightarrow \quad A T_1 = T_1^2 + B$

$\Rightarrow \quad T_1^2 - A T_1 + B = 0$ (3.64)

From equation (3.64) we obtain:

$$T_1 = \frac{A \pm \sqrt{A^2 - 4B}}{2}$$ (3.65)

$$\therefore \; T_2 = \frac{B}{T_1}$$ (3.66)

$$=> T_2 = \frac{2B}{A \pm \sqrt{A^2 - 4B}}$$

Now, putting the above values in equation (3.60), we have:

$$G_i(s) = \frac{K_a K_{in}\left(1 + sT_m\right)}{T_a T_m \left(1 + sT_1\right)\left(1 + sT_2\right)}$$ (3.67)

The above transfer function can be simplified using the fact that $T_1 > 1$

$1 + sT_1 \cong sT_1$ (3.68)

Also, near the vicinity of the crossover frequency [3], we have

$1 + sT_m = sT_m$ (3.69)

Thus equation (3.67) can be simplified as:

$$G_i(s) = \frac{K_a K_{in} s T_m}{T_a T_m s T_1 \left(1 + s T_2\right)}$$

$$\Rightarrow \quad G_1(s) = \frac{K_a K_{in}}{T_a T_1 \left(a + s T_2\right)}$$

Therefore the final simplified single order transfer function of $G_i(s)$ is obtained as:

$$G_i(s) = \frac{K_i}{1 + s T_2} \tag{3.70}$$

Therefore the transfer function of the plant incusing the IFOC controller, the electrical dynamics of the system, the mechanical dynamics of the system and the Induction motor (only the speed controller has been left out) taken together can be represented as $P(s)$ by the the transfer function:

$$P(s) = \frac{K_i K_m}{K_t (1 + s T_2)(1 + s T_m)} \tag{3.71}$$

This second order plant alongwith the speed controller is shown in the figure below.
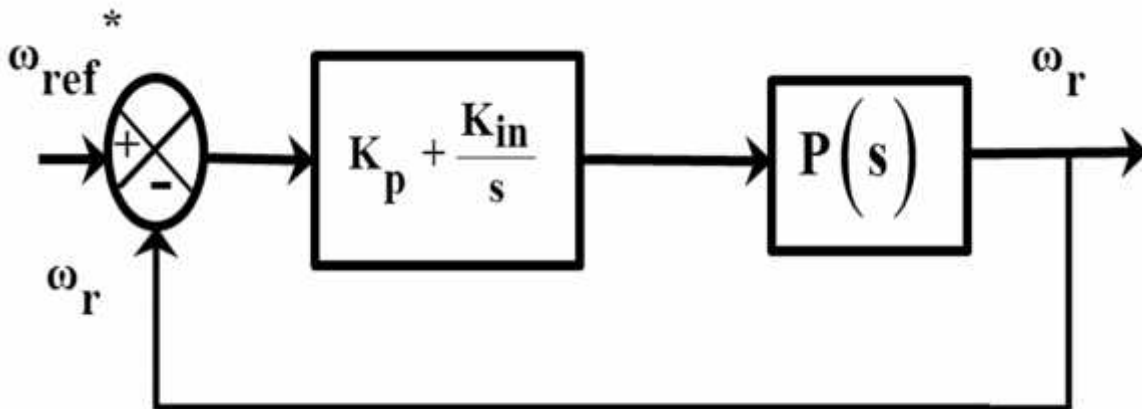
Figure 27. Final Block diagram of the Second Order Plant and the Controller- IFOC Induction Motor

B. Obtaining the nominal transfer function for IFOC induction motor:

For obtaining the nominal transfer function for the plant, the values of the parameters given in table 1 and table 2 are used. The equations presented in the last section were programmed using MATLAB Simulink and a second order plant was obtained.

Considering $\quad P(s) = \dfrac{L_0}{s^2 + a_0 s + b_0}$, $\qquad\qquad\qquad$ (3.72)

Where,

$$L_0 = \frac{K_i K_m}{K_t T_2 T_m},$$ $\qquad\qquad\qquad$ (3.73)

$$a_0 = \frac{1}{T_2} + \frac{1}{T_m}$$ $\qquad\qquad\qquad$ (3.74)

And $b_0 = \dfrac{1}{T_2 T_m}$ $\qquad\qquad\qquad$ (3.75)

From MATLAB, the results for the above values are obtained as:

$L_0 = 27.2, a_0 = 2.741,$ and $b_0 = 0.9521$

Thus, we have $P(s) = \dfrac{27.2}{s^2 + 2.741s + 0.9521}$ $\qquad\qquad\qquad$ (3.76)

Thus the final block diagram becomes:
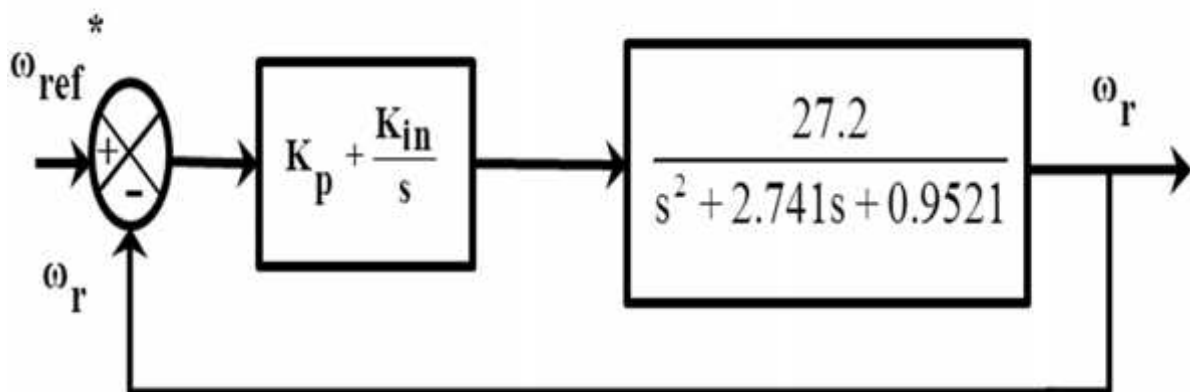
Figure 28. Nominal second order plant (IFOC induction motor) and controller

3.5 Model Order Reduction

A. Introduction:

The nominal system for the plant obtained in the previous section is a second order transfer function. For the speed control loop, the controllers used are PI type. Typically PI controllers are best suited for first order systems. Also, use of LQR technique would require augmenting the system to meet the required states. Therefore it becomes essential to reduce the system to a first order transfer function.

One of the popular methods for system order reduction is Aggregation by continued fraction. This method was first introduced by Chen and Shieh and extended by many others [13].

B. Aggregation :

The concept of aggregation was first developed for economics literature. Aggregation for control systems was first proposed by Aoki. The aggregation process is presented as [13]:

Let a large scale continuous dynamic system be represented by:

$$\dot{X} = Ax + Bu \tag{3.77}$$

$$y = Cx \tag{3.78}$$

Where $x \in R^n$ is the state vector.

$u = R^m$ is the control input vector

And $y \in R^p$ is the output vector.

The matrices A, B, and C are constants with appropriate dimensions and these are completely controllable and observable. We wish to represent this higher order model by an aggravated model of lower order given by:

$$\begin{aligned} \dot{Z} &= FZ + Gu \\ w &= HZ \end{aligned} \tag{3.79}$$

Where $Z \in R^r$ is the aggravated state vector

$w \in R^p$ is the aggravated output vector. The aggravated model can be considered to be satisfactory if for a given class of inputs $\{u\}$, the aggravated outputs $\{w\}$ are good approximations of the original output y of the original model. The aggravated model has an order r such that $m \le r \le n$

C. Aggregation by continued fraction method:

Let us consider a system

$$\dot{X} = Ax + Bu \tag{3.80}$$

$$y = C_n x \tag{3.81}$$

Without loss of generality matrix A can be written in companion form as:

$$A = \begin{pmatrix} 0 & 1 & 0 & \dots & 0 \\ 0 & 0 & 1 & \dots & 0 \\ \vdots & \vdots & \vdots & \ddots & \vdots \\ 0 & 0 & 0 & \dots & 1 \\ -a_{11} & -a_{12} & -a_{13} & \dots & -a_{1n} \end{pmatrix}$$

$$B = \begin{bmatrix} 0 & 0 & \cdots & 1 \end{bmatrix}^T , \quad C_n = \begin{bmatrix} a_{21} & a_{22} & a_{2n} \end{bmatrix}$$

The above system can be transformed to an aggravated form using a transformation matrix P corresponding to its continued fraction expansion:

$$\dot{q} = Hq + Ku$$

$$v = C_q q$$

Where the transformed vector q is

$$q = Px$$

And matrix P is obtained through the modified Routh-Hurwitz array:

$$
\begin{vmatrix}
a_{11} & & a_{12} & a_{13} & a_{14} & a_{15} & \cdots & a_{1n} & 1 \\
a_{21} & & a_{22} & a_{23} & a_{24} & \vdots & \cdots & a_{2n} & 0 \\
a_{31} & & a_{32} & a_{33} & \vdots & & \cdots & 1 & \\
a_{41} & & a_{42} & \vdots & & & \cdots & 0 & \\
a_{51} & & \vdots & & & & & & \\
\vdots & & & & & & & & \\
a_{2n-1,1} & 1 & & & & & & & \\
a_{2n,1} & 0 & & & & & & & \\
1 & & & & & & & &
\end{vmatrix}
$$

The final two rows of the above Routh array are extracted from the nth row of A and elements of output vector C_n. The remaining rows are calculated from the Routh Hurwitz iterative formula as:

$$
a_{ij} = \frac{a_{i-1,1}.a_{i-2,j+1} - a_{i-1,j+1}.a_{i-2,1}}{a_{i-1,1}}
$$

The matrix P is then extracted from the table as:

$$
P = \begin{pmatrix}
a_{31} & a_{32} & a_{33} & \cdots & \cdots & 1 \\
0 & a_{51} & a_{52} & \cdots & \cdots & 1 \\
0 & 0 & a_{71} & \cdots & \cdots & 1 \\
\vdots & \vdots & \vdots & & & \vdots \\
0 & 0 & 0 & \cdots & a_{2n-1,1} & 1 \\
0 & 0 & 0 & 0 & 0 & 1
\end{pmatrix}
\tag{3.82}
$$

The system given by equations (3.80) and (3.81) can be represented as:

$$
\dot{q} = PAP^{-1}q + PBu
$$

And so, matrices H and K become:

$$
H = PAP^{-1} \text{ and } K = PB
$$

This process of continued fraction simplification of a higher order system to a lower order system (n^{th} to l^{th} order) refers to retaining the first l variables of q. Let us call the first l elements of q as z. Then we have:

$z = Rq$

And $R = [I_l : 0]$ where I_l is identity matrix of order l

Now, $\dot{z} = R\dot{q}$

$\Rightarrow \qquad \dot{z} = R(Hq + Ku)$

$\Rightarrow \qquad \dot{z} = RHq + RKu$

Which, when compared to aggregated system state equation from equation

$\dot{z} = Fz + Gu$

$\Rightarrow \qquad \dot{z} = FRq + Gu$ $\hspace{4cm}$ (3.83)

Therefore $FR = RH = RPAP^{-1}$,

and $G = RK = RPB$

as $q = Px$ and $z = Rq$

Therefore $z = RPx$

$\Rightarrow \qquad z = Cx$ $\hspace{5cm}$ (3.84)

Where C is the $l \times n$ aggregation matrix.

Now a relation can be developed between the aggravated system output matrix C_l from the corresponding equation ($w = C_l z$) by equating y and w which gives-

$C_n = C_l C$

Now using pseudo inverses of matrices R and C, the aggravated system matrix are :

$F = RHR^+ = RPAP^{-1}R^T (RR^T)^{-1}$ $\hspace{3cm}$ (3.85)

$G = RPB$

$C_l = C_n C^+ = C_n C^T (CC^T)^{-1}$ $\quad \}$ $\hspace{3cm}$ (3.86)

With the aggregation matrix expressed as :

C=RP   (3.87)

D. Implementation of aggregation by continued fraction method and results:

We have our plant as:

$$P(s) = \frac{27.2}{s^2 + 2.741s + 0.9521}$$

Therefore, $\dfrac{Y(s)}{U(s)} = \dfrac{27.2}{s^2 + 2.741s + 0.9521}$

$\Rightarrow \quad (s^2 + 2.741s + 0.9521)Y(s) = 27.2U(s)$

Thus, $s^2 Y(s) = 27.2U(s) - 2.741sY(s) - 0.9521Y(s)$ (3.88)

Let:

$q_1(t) = y(t)$

$q_2(t) = \dot{y}(t)$

Therefore,

$Q_1(s) = Y(s)$
$Q_2(s) = sY(s)$

Thus, $\dot{Q_1} = sQ_1(s) = Q_2(s) = sY(s)$

And, $\dot{Q_2} = sQ_2(s) = Q_3(s) = s^2 Y(s)$

$\Rightarrow \quad \dot{Q_2} = 27.2U(s) - 2.741sY(s) - 0.9521Y(s)$

Therefore state space representation of the plant is as:

$$\begin{pmatrix} \dot{Q_1} \\ \dot{Q_2} \end{pmatrix} = \begin{pmatrix} 0 & 1 \\ -0.9521 & -2.741 \end{pmatrix} \begin{pmatrix} Q_1 \\ Q_2 \end{pmatrix} + \begin{pmatrix} 0 \\ 27.2 \end{pmatrix} U(s)$$

$$Y(s) = \begin{pmatrix} 1 & 0 \end{pmatrix} \begin{pmatrix} Q_1 \\ Q_2 \end{pmatrix}$$

The above system can be rewritten as:

$$\begin{pmatrix} \dot{x}_1 \\ \dot{x}_2 \end{pmatrix} = \begin{pmatrix} 0 & 1 \\ -0.9521 & -2.741 \end{pmatrix} \begin{pmatrix} x_1 \\ x_2 \end{pmatrix} + \begin{pmatrix} 0 \\ 27.2 \end{pmatrix} U(s) \tag{3.89}$$

$$Y(s) = \begin{pmatrix} 1 & 0 \end{pmatrix} \begin{pmatrix} x_1 \\ x_2 \end{pmatrix} \tag{3.90}$$

This is the state space representation of the plant.

Now, we proceed with the implementation of aggregation by continued fraction method on the above state space model. Here, we have

$$A = \begin{pmatrix} 0 & 1 \\ -a_{11} & -a_{12} \end{pmatrix} = \begin{pmatrix} 0 & 1 \\ -0.9521 & -2.741 \end{pmatrix}$$

And $C_n = \begin{pmatrix} a_{21} & a_{22} \end{pmatrix} = \begin{pmatrix} 1 & 0 \end{pmatrix}$

The Routh array to obtain the matrix P is calculated as:

$$\begin{vmatrix} 0.9521 & 2.741 & 1 \\ 1 & 0 & 0 \\ 2.741 & 1 & \\ -\dfrac{1}{2.741} & 0 & \\ 1 & & \end{vmatrix}$$

Therefore, $P = \begin{pmatrix} 2.741 & 1 \\ 0 & 1 \end{pmatrix}$

And R= [1 0]

Now, using MATLAB programming to calculate the values of F, G, and C_l from equations (3.85) and (3.86) we have:

F = -0.347307790546172

G = 27.196653072425203

C_l = 0.321941223086278

Thus, our reduced first order system becomes:

$$\dot{x} = -0.3473x + 27.2u \qquad (3.91)$$

$$y = 0.321941x \qquad (3.92)$$

This can be written in transfer function form as:

$$P(s) = \frac{8.756}{s + 0.3473}$$

Chapter 4

Optimal Controller design

4.0 Introduction:

In order that the induction motor efficiently tracks the reference speed, the error between the reference and the actual speeds need to be processed with the help of a controller. The type of controller used here is a PI controller because of its various advantages and ease of implementation. Available control strategies that include optimal control, Linear quadratic Regulator (LQR) technique and concepts of robust control can be found in extensive literature and therefore these existing control strategies are used in this dissertation. The theory and concept behind the various control strategies is discussed in this chapter, along with implementation of such techniques through Matlab.

4.1 Optimal Control and LQR Problem:

The essential element of a control problem is a means of testing the performance of any proposed control law. Whenever we say that the effectiveness of a given control strategy is "optimal", we do so with respect to some numerical index of performance called the performance index [28]. We assume that the value of the performance index decreases as the quality of the given admissible control law increases. The admissible controller that ensures the completion of the system objective and at the same time minimizes the performance index is called an optimal controller for the system.

A. Performance Indices:

Let us consider a system

$$\overset{)}{X}(t) \,X\, Ax(t)\, \Gamma\, Bu(t), \qquad x(t_0)\, X\, x_0$$

$$y(t)\, X\, Cx(t)\ ,$$

on a fixed interval $[t_0, t_f]$

A suitable performance index to be minimized can be

$$J_1 = \int_{t_0}^{t_f} x^T(t)x(t)dt$$

(Here, the term "J_1 minimizes" means components of state vector decrease.)

As J_1 is small, state vector norm $\|x(t)\|$ is small.

If the objective is to control the system such that the components of the output, y(t) are to be small, then the performance index may be:

$$J_2 = \int_{t_0}^{t_f} y^T(t)y(t)dt$$

$\Rightarrow$ $$J_2 = \int_{t_0}^{t_f} x^T(t)C^T Cx(t)dt$$

$\Rightarrow$ $$J_2 = \int_{t_0}^{t_f} x^T(t)Q\,x(t)dt$$

Where the weight matrix $Q = C^T C$ is symmetric positive semidefinite.

If we need to control the system such that the input components u(t) are small, then,

$$J_3 = \int_{t_0}^{t_f} u^T(t)u(t)dt$$

Or, $$J_3 = \int_{t_0}^{t_f} u^T(t)Ru(t)dt$$

Where the weight matrix R is symmetric positive definite.

Now, we cannot simultaneously minimize J_1 and J_3 because minimising the state vector components needs large control signals, while minimizing the output vector components needs small control signals. To solve this dilemma, we can compromise between the two objectives by minimizing the performance index that is a convex combination of J_1 and J_3

$J\,\text{X}\}J_1\,\Gamma(1\,\text{Z}\})J_3$

$$\Rightarrow \int_{t_0}^{t_f} [\;x^T(t)x(t)+(1-\;)u^T(t)u(t)]dt$$

Where $\}$ is a parameter ranging from 0 to 1. i.e. $\}$ $[0,1]$

A generalized form of J is thus,

$$J_4\,\text{X}\int_{t_0}^{t_f}[x^T(t)Qx(t)\,\Gamma\,u^T(t)Ru(t)]\,\mathrm{dt}$$

In some applications, we may wish the final state $x(t_f)$ to be as close as possible to 0. Then a possible performance measure to be minimized is:

$J_5\,\text{X}x^T(t_f)Fx(t_f)$,where F is a symmetric positive definite matrix.

Now, we can combine $J_2, J_3,$ and J_5

$$J\,\text{X}\frac{1}{2}x^T(t)Fx(t_f)\,\Gamma\frac{1}{2}\int_{t_0}^{t_f}(x^TQx(t)\,\Gamma\,u^TRu(t))\,\mathrm{dt}$$

The above performance index is to be used when our control aim is to have the state small, the control not too large and the final state to be as nearly equal to zero as possible. The factor $\frac{1}{2}$ is placed to simply subsequent algebraic manipulation. This above problem is called the Linear Quadratic Regulator problem.

B. <u>Algebraic Ricatti Equation</u>:

Let a system be [26]:

$$\overset{\jmath}{X}(t)\,\text{X}\,Ax(t)\,\Gamma\,Bu(t)\qquad x(0)\,\text{X}x_0 \tag{4.1}$$

And its associated performance index is

$$J = \int_0^\infty \left(x^T Q x + u^T R u \right) dt$$

Where $Q = Q^T \geq 0$ and $R = R^T > 0$ our goal is to design a stabilizing linear state feedback controller of the form $u = -Kx$ that minimises the performance index J. such a control law is denoted by u^*.

We now assume that a linear state feedback optimal controller exists such that the optimal closed loop system $\dot{x} = (A - BK)x$ is asymptotically stable.

This implies that there is a lyapunov function $V = x^T P x$ for the closed loop system, that is for some positive definite matrix P, the time derivative $\dfrac{dV}{dt}$ evaluated on the trajectories of the closed loop system is negative definite.

C. Theorem:

If the state feedback controller $u^* = -Kx$ is such that

$$\min_{u} \left(\frac{dV}{dt} + x^T Q x + u^T R u \right) = 0 ,$$

For some $V = x^T P x$, then the controller is optimal [28].

Therefore from the above theorem it implies that synthesis of the optimal control law involves finding an appropriate Lyapunov Function, or equivalently, the matrix P. This P matrix is found by minimising:

$$f(u) = \frac{dV}{dt} + x^T Q x + u^T R u \tag{4.2}$$

To the above equation we apply the necessary condition for unconstrained minimization,

$$\frac{\partial}{\partial u}\left[\frac{dV}{dt}\Gamma x^T Qx \Gamma u^T Ru\right]\Bigg|_{u\mathsf{X}u\mathsf{B}} \mathsf{X}0^T \quad \text{、}$$

Differentiating, we get:

$$\frac{\partial}{\partial u}\left[\frac{dV}{dt}\Gamma x^T Qx \Gamma u^T Ru\right] \mathsf{X}\frac{\partial}{\partial u}\left[2x^T P \overset{)}{x}\Gamma x^T Qx \Gamma u^T Ru\right]$$

$$\Rightarrow \qquad \frac{\partial}{\partial u}\big[2x^T PAx \Gamma 2x^T PBu \Gamma x^T Qx \Gamma u^T Ru\big]$$

$$\Rightarrow \qquad 2x^T PB \Gamma 2u^T R$$

$$\Rightarrow \qquad 0^T$$

Here the optimal control law has the form:

$$u^\mathsf{B} \mathsf{X} \mathsf{Z}R^{\mathsf{Z}1}B^T Px \mathsf{X} \mathsf{Z}Kx \qquad\qquad\qquad (4.3)$$

Where $K \mathsf{X} R^{\mathsf{Z}1}B^T P$ therefore

$$\frac{\partial^2}{\partial u^2}\left[\frac{dV}{dt}\Gamma x^T Qx \Gamma u^T Ru\right] \mathsf{X}\frac{\partial^2}{\partial u^2}\big[2x^T PAx \Gamma 2x^T PBu \Gamma x^T Qx \Gamma u^T Ru\big]$$

$$\Rightarrow \qquad \frac{\partial}{\partial u}\big[2x^T PB \Gamma 2u^T R\big]$$

$$\Rightarrow \qquad 2R$$

$$\Rightarrow \qquad > 0$$

Thus the second order sufficiency condition for u^B to minimize equation (4.2) is satisfied.

We now try to find an appropriate P. The optimal closed loop system has the form

$$\overset{)}{x} \mathsf{X}\big[A \mathsf{Z}BR^{\mathsf{Z}1}B^T P\big]x \quad, \quad x(0) \mathsf{X}x_0$$

And our optimal controller satisfies the equation:

$$\frac{dV}{dt}\Bigg|_{u\mathsf{X}u\mathsf{B}}\Gamma x^T Qx \Gamma u^{\mathsf{B}T} Ru^\mathsf{B} \mathsf{X}0$$

Therefore, $\quad 2x^T PAx \Gamma 2x^T PBu^\mathsf{B}\Gamma x^T Qx \Gamma u^{\mathsf{B}T} Ru^\mathsf{B} \mathsf{X}0$

Putting the value of u^B from eq (4.3) in above equation, we get

$$x^T \int A^T P \Gamma PA \big| x \, Z2x^T PBR^{Z1} B^T Px \Gamma x^T Qx \Gamma x^T PBR^{Z1} B^T Px \, X0$$

Factoring out x gives:

$$x^T \int A^T P \Gamma PA \Gamma Q \, Z PBR^{Z1} B^T P \big| x \, X0 \tag{4.4}$$

The above equation holds for any x and for this to be true, we must have

$$\boxed{A^T P \Gamma PA \Gamma Q \, Z PBR^{Z1} B^T P \, X0} \tag{4.5}$$

The above equation is called the **Algebraic Ricatti Equation (ARE).** Therefore for designing an optimal controller for the system given in equation (4.1), it is necessary to solve the ARE given by the above equation (4.5)

4.2 Controller Design and implementation:

A. Controller design

We consider our first order plant to be

$$P(s) \, X \frac{b}{s \Gamma a} \tag{4.6}$$

$$\Rightarrow \quad \frac{Y(s)}{U(s)} \, X \frac{b}{s \Gamma a}$$

$$\Rightarrow \quad sY(s) \Gamma aY(s) \, XbU(s) \tag{4.7}$$

In time domain,

$$\overset{\jmath}{y}(t) + ay(t) = bu(t) \tag{4.8}$$

Now, let $y(t) \, Xx_1(t)$ \hfill (4.9)

And $\overset{\jmath}{y}(t) \, X\overset{\jmath}{x}_1(t) \, Xx_2(t)$ \hfill (4.10)

thus,

$$x_2 \; \Gamma a x_1 \; \mathrm{X} b u(t)$$

$$\Rightarrow \quad \overset{\jmath}{x_1}(t) \Gamma a x_1(t) \; \mathrm{X} b u(t)$$

$$\Rightarrow \quad \overset{\jmath}{x_1}(t) \; \mathrm{X} \mathbb{Z} a x_1 \; \Gamma b u(t) \tag{4.11}$$

Therefore we have:

$$[\overset{\jmath}{x_1}(t)] \; \mathrm{X} [\mathbb{Z} a][x_1] \Gamma [b] u(t) \tag{4.12}$$

And $[y(t)] \; \mathrm{X} [1] x_1(t)$ (4.13)

Thus, we have $A \; \mathrm{X} [\mathbb{Z} a] \qquad B \; \mathrm{X} [b] \qquad c \; \mathrm{X} [1] \quad$ and $\; D \; \mathrm{X} [0]$

Now for design of a PI controller, we augment our plant to a second order system:

Let $\quad y(t) dt \; \mathrm{X} x_1(t)$ (4.14)

Thus, $\; x_2(t) \; \mathrm{X} \, y(t) \; \mathrm{X} \overset{\jmath}{x_1}(t)$ (4.15)

And $\; \overset{\jmath}{y}(t) \; \mathrm{X} \overset{\jmath}{x_2}(t) \; \mathrm{X} \overset{\jmath\jmath}{x_1}(t) \; \mathrm{X} x_3(t)$ (4.16)

Now, from equation (3.70) we have

$$\overset{\jmath}{x_2}(t) \; \Gamma a x_2(t) \; \mathrm{X} b u(t)$$

$$\Rightarrow \quad \overset{\jmath}{x_2}(t) \; \mathrm{X} \mathbb{Z} a x_2(t) \; \Gamma b u(t)$$

Hence, our augmented system is:

$$\begin{matrix} \overset{\jmath}{x_1}(t) \\ \overset{\jmath}{x_2}(t) \end{matrix} \; \mathrm{X} \; \begin{matrix} 0 & 1 \\ 0 & \mathbb{Z} a \end{matrix} \; \begin{matrix} x_1(t) \\ x_2(t) \end{matrix} \; \Gamma \; \begin{matrix} 0 \\ b \end{matrix} \; u(t) \tag{4.17}$$

So, we have $A \; \mathrm{X} \; \begin{matrix} 0 & 1 \\ 0 & \mathbb{Z} a \end{matrix} \qquad B \; \mathrm{X} \; \begin{matrix} 0 \\ b \end{matrix}$

Our chosen control law is:

$$u \; \mathrm{X} \mathbb{Z} [K][x(t)] \tag{4.18}$$

Where K is the controller gain matrix

$$u \cdot XZ(K_i \quad K_p) \begin{array}{c} x_1(t) \\ x_2(t) \end{array}$$

Where K_i is the controller integral gain and K_p is the controller proportional gain

$$\therefore \; K = \begin{array}{cc} K_i & K_p \end{array} \tag{4.19}$$

$$\therefore \; K = \begin{array}{cc} K_i & K_p \end{array} \; X R^{Z1} B^T P$$

$$\Rightarrow \quad K \, X f1 A f0 \; b A \begin{array}{cc} P_{11} & P_{12} \\ P_{21} & P_{22} \end{array}$$

(considering R=1)

$$\text{Therefore } K \, X f b P_{21} \quad b P_{22} A \tag{4.20}$$

$$\underset{K_i \qquad K_p}{\Big\uparrow \qquad \Big\uparrow}$$

Thus $K_i \, X b P_{12}$ and $K_p \, X b P_{22}$

Now transfer function of the system including the controller and the plant is (OLTF):

$$P_{aol} \, X \frac{K_p \, \Gamma \dfrac{K_i}{s} \; b}{s \, \Gamma a} = \frac{b K_p \, \Gamma b K_i}{s(s \, \Gamma a)} \tag{4.21}$$

Close loop transfer function (CLTF) for the system is:

$$P_{acl} \, X \frac{b K_p s \, \Gamma b K_i}{s(s \, \Gamma a) \, \Gamma b K_p s \, \Gamma b K_i} \tag{4.22}$$

$$\Rightarrow \quad P_{acl} \, X \frac{b K_p s \Gamma b K_i}{s^2 \Gamma s(a \Gamma b K_p) \Gamma b K_i}$$

A standard second order closed loop system is now chosen as:

$$T.F. \, X \frac{\check{S}^2_{ncl}}{s^2 \, \Gamma 2 \langle \check{S}_{ncl} s \, \Gamma \check{S}^2_{ncl}} \tag{4.23}$$

Where $\check{S}_{ncl}$ and ‹ are closed loop frequency and damping factor of the standard second order system respectively. For this second order closed loop system, we have:

$$A_1 \ \text{X} \begin{bmatrix} 0 & 1 \\ \text{Z}\check{S}^2_{ncl} & \text{Z}2\text{‹}\check{S}_{ncl} \end{bmatrix} \qquad B_1 \ \text{X} \begin{bmatrix} 0 \\ \check{S}^2_{ncl} \end{bmatrix} \qquad C_1 \ \text{X} f0 \quad 1 \text{Å}$$

We also have:

$$P \ \text{X} \begin{bmatrix} P_{11} & P_{12} \\ P_{12} & P_{22} \end{bmatrix}, \qquad Q \ \text{X} \begin{bmatrix} Q_{11} & 0 \\ 0 & Q_{22} \end{bmatrix}, \qquad R \ \text{X} f1\text{Å}$$

From equation (4.22) we have the characteristic equation of our second order plant and controller system as:

$$s^2 \, \Gamma \, s(a\,\Gamma\,bK_p)\,\Gamma\,bK_i \ \text{X} 0 \tag{4.24}$$

And we have the characteristic equation of the standard second order system as:

$$s^2 \, \Gamma \, 2\text{‹}\check{S}_{ncl}s \, \Gamma \, \check{S}^2_{ncl} \ \text{X} 0 \tag{4.25}$$

Comparing the above two equations, we find:

$$K_i \ \text{X} \frac{\check{S}^2_{ncl}}{b} \ \dots\dots \ (3.88) \qquad \text{and} \qquad K_p \ \text{X} \frac{2\text{‹}\check{S}^2_{ncl}\,\text{Z}a}{b} \tag{4.26}$$

As, $K_i \ \text{X} bP_{12}$ and $K_p \ \text{X} bP_{22}$

Therefore, comparing the above relations, we have

$$P_{12} \ \text{X} \frac{\check{S}^2_{ncl}}{b^2} \tag{4.27}$$

And $\quad P_{22} \, \text{X} \dfrac{2\langle \check{S}_{ncl} \, \text{Z} a}{b^2}$ (4.28)

Now, we have the ARE as:

$A^T P \, \Gamma \, PA \, \Gamma \, Q \, \text{Z} \, PBR^{\text{Z1}} B^T P \, \text{X0}$ (4.29)

We solve for $A^T P \, \Gamma \, PA$:

$$A^T P \, \Gamma \, PA \, \text{X} \begin{bmatrix} 0 & 1 \\ 0 & \text{Z}a \end{bmatrix}^T \begin{bmatrix} P_{11} & P_{12} \\ P_{12} & P_{22} \end{bmatrix} \Gamma \begin{bmatrix} P_{11} & P_{12} \\ P_{12} & P_{22} \end{bmatrix} \begin{bmatrix} 0 & 1 \\ 0 & \text{Z}a \end{bmatrix}$$

$\Rightarrow \quad \begin{bmatrix} 0 & P_{11} \, \text{Z}aP_{12} \\ P_{11} \, \text{Z}aP_{12} & 2P_{12} \, \text{Z}2aP_{22} \end{bmatrix}$ (4.30)

Also, we solve for $PBR^{\text{Z1}} B^T P$:

$$PBR^{\text{Z1}}{}_B{}^T P \, \text{X} \begin{bmatrix} P_{11} & P_{12} \\ P_{12} & P_{22} \end{bmatrix} \begin{bmatrix} 0 \\ b \end{bmatrix} f0 \quad bA \begin{bmatrix} P_{11} & P_{12} \\ P_{12} & P_{22} \end{bmatrix} \quad \text{…….. considering R=1}$$

$\Rightarrow \quad \begin{bmatrix} P_{11} & P_{12} & 0 & 0 \\ P_{12} & P_{22} & b^2 P_{12} & b^2 P_{22} \end{bmatrix}$

As, $K_i \, \text{X} bP_{12}$ and $K_p \, \text{X} bP_{22}$, putting these values in above equation and then solving, we get:

$$PBR^{\text{Z1}}{}_B{}^T P \, \text{X} \begin{bmatrix} P_{12}bK_i & P_{12}bK_p \\ P_{22}bK_i & P_{12}bK_p \end{bmatrix}$$ (4.31)

Putting the values of equation (4.30) and (4.31) in equation (4.29) and then solving, we have:

$$\begin{bmatrix} P_{12}bK_i & P_{12} \, \text{Z} P_{11} \, \Gamma a P_{12} \\ P_{22}bK_i \, \text{Z} P_{11} \, \Gamma aP_{12} & P_{22}bK_p \, \text{Z} 2P_{12} \, \Gamma 2aP_{22} \end{bmatrix} \, \text{X} \begin{bmatrix} Q_{11} & 0 \\ 0 & Q_{22} \end{bmatrix}$$

Therefore comparing LHS and RHS we get,

$Q_{11} \, \text{X} P_{12}bK_i$ (4.32)

$$Q_{22} \text{ X} P_{22} b K_p \text{ Z} 2 P_{12} \Gamma 2 a P_{22} \tag{4.33}$$

$$P_{11} \text{ X} (1 \Gamma a) P_{12} \tag{4.34}$$

Putting the value of P_{12} and P_{22} in above eq,

$$P_{11} \text{ X} \frac{(1 \Gamma a) \check{S}_{ncl}^2}{b^2}$$

$$Q_{11} \text{ X} \quad \frac{\check{S}_{ncl}^2}{b}^2$$

$$Q_{22} \text{ X} \frac{\check{S}_{ncl}^2 \int 4 < ^2 \text{ Z} 2 \not{A} \text{Z} a^2}{b^2}$$

We now select the values of the closed loop frequency and the damping factor according to the desired response:

$< \text{ X} 0.90$

$\check{S}_{ncl} \text{ X} 10$

B. Results of controller design:

All the equations are programmed in MATLAB and the values of a and b were given. Finally MATLAB calculated the following results:

$$Q = \begin{matrix} 130.4333036084530 & 0 \\ 0 & 1.6157997135841 \end{matrix}$$

$$P \text{ X} \begin{matrix} 23.477994649521548 & 1.304333036084530 \\ 1.304333036084530 & 0.230249997860894 \end{matrix}$$

And the controller gain was obtained as:

$$K \text{ X} \quad f 11.420740063956147 \quad 2.016068981269987 \not{A}$$

Therefore Proportional gain $K_p = 2.016068981269987$

And integral gain K_i X 11.420740063956147

Therefore the optimal values of PI controller have been obtained which is to be used in the Speed Control loop of the field oriented control structure for an induction motor.

4.3 RESULTS AND DISCUSSIONS:

A. Results obtained by using the designed controller with the reduced first order system:

PI controller of the outer speed loop (that is designed using LQR technique) is used with the nominal reduced order system and the results were observed. Figure 29 shows the simulation of the said system

The simulation in figure 29 shows a response curve as given in figure 30. For this purpose, a speed reference in the form of a step signal of magnitude 60 was given as input. The error signal which is the difference of this reference speed and the actual speed is then fed to the designed optimal PI controller. Output from the optimal controller is fed to the first order system. The response of the output is then observed in figure 30.
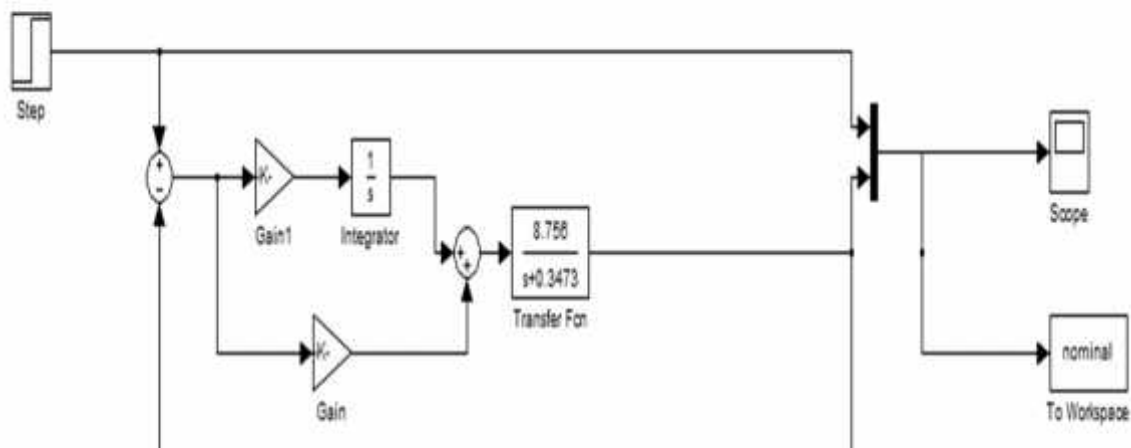

Figure 29 Simulation of Reduced First Order System response with the designed controller
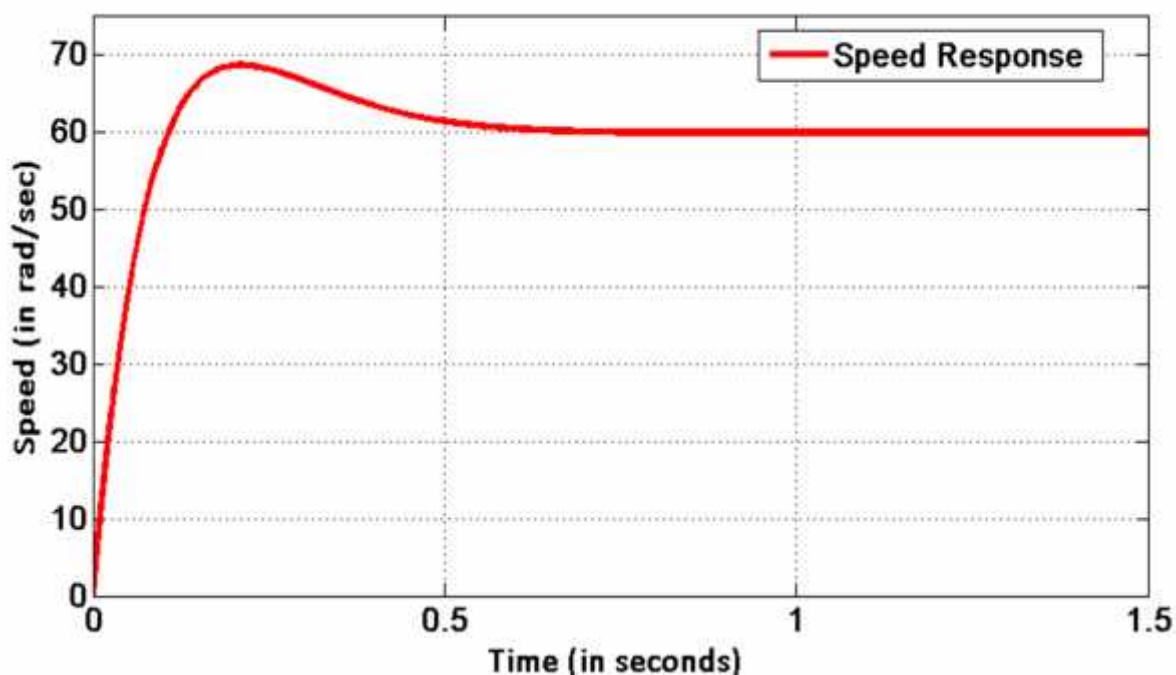
.

Figure 30 Zoomed view of the response of the first order system with the designed optimal controller

It can be stated from figure 30 that the proposed controller provides an overshoot of about 9 rad/sec and settles at about 0.5 seconds. Therefore it can be said that the rise time of the system is fast and the response is stable. Thus the system provides satisfactory transient steady state response.

B. MATLAB simulation results:

The proportional and integral gains of the controller obtained above were put in the PI controller for speed control loop of IFOC structure for induction motor. The following response curves were then observed:
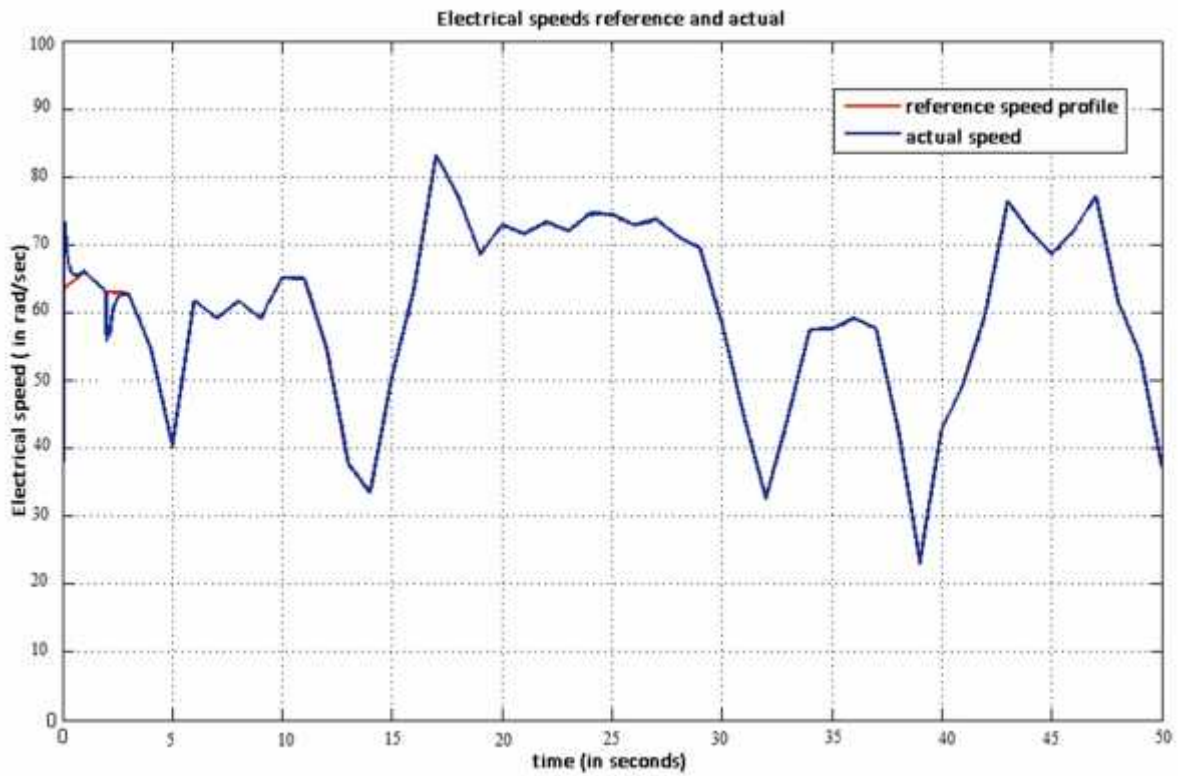
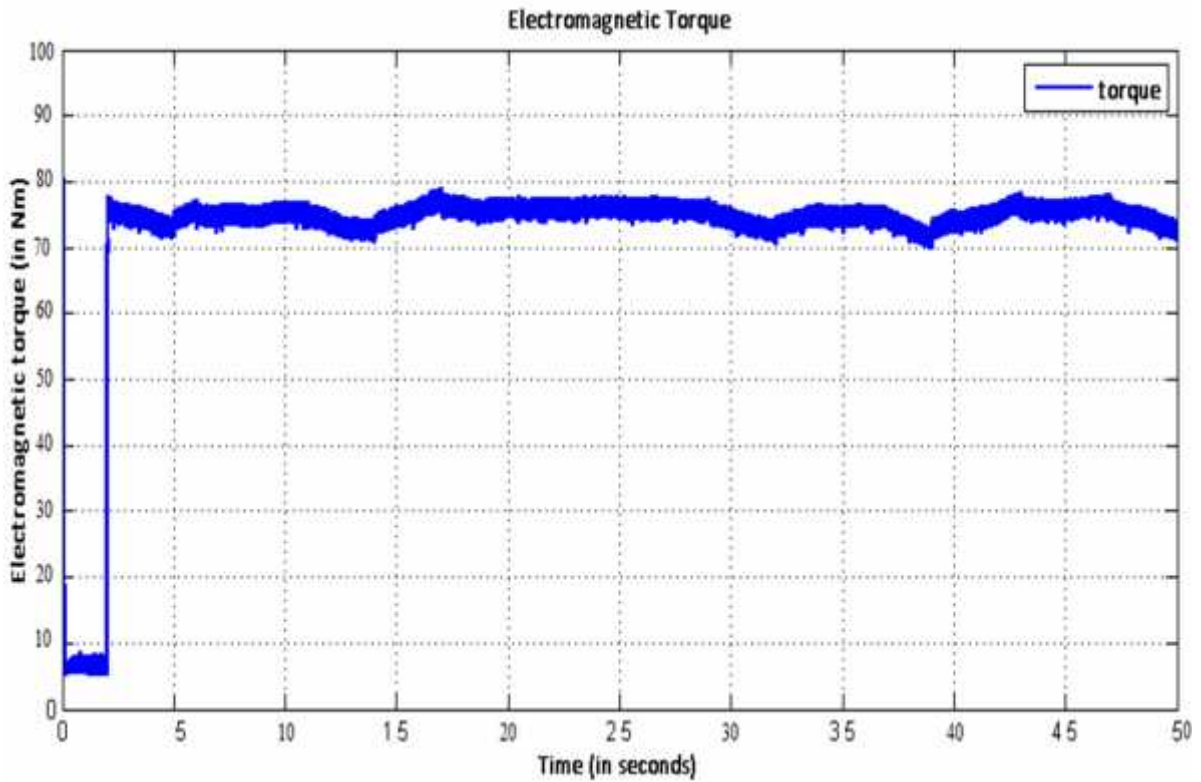**Figure 31. Reference speed profile and actual speed of optimal IFOC induction motor.**

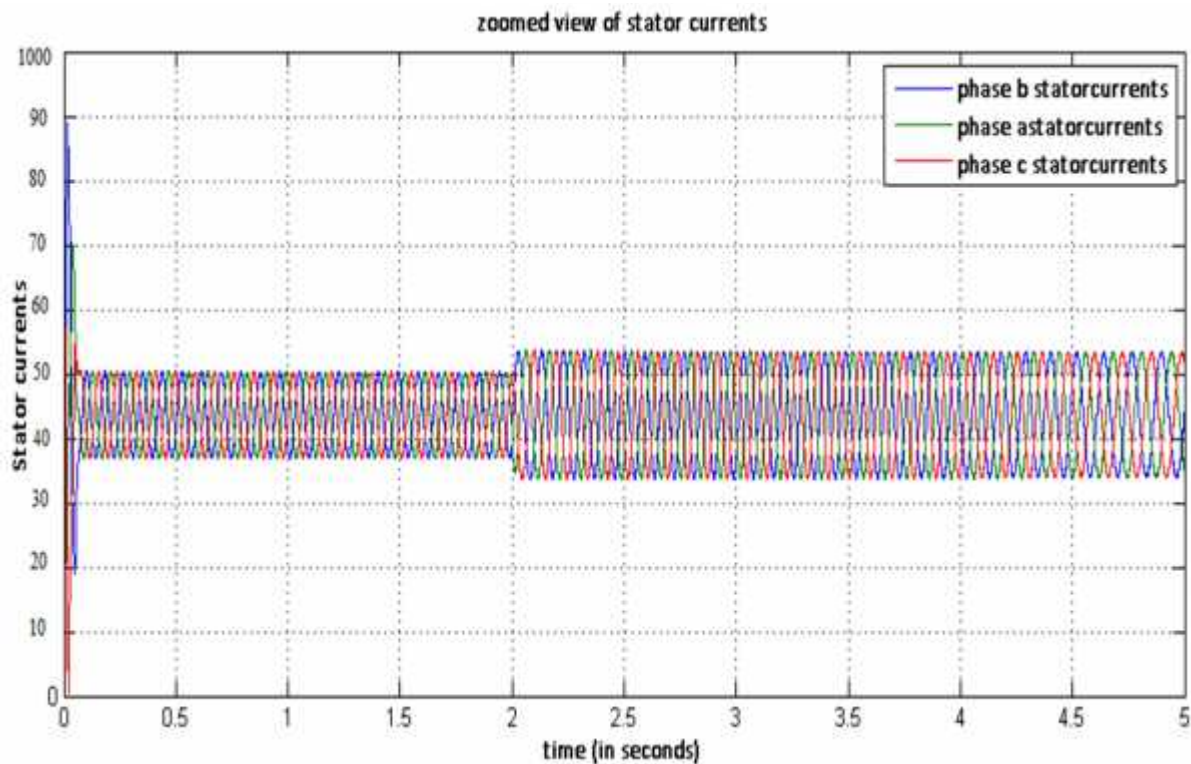**Figure 32 Electromagnetic torque of optimal IFOC induction motor.**

Figure 33 Zoomed view of the stator currents of optimal IFOC induction motor.

C. Discussions on results:

The speed controller of the IFOC induction motor produced an overshoot for the speed response as the speed increased from zero to the required value. This overshoot was of the order of 20-25rpm. Such an overshoot is undesirable for many applications. Therefore it is necessary to reduce this initial overshoot while maintaining effective tracking of reference speed by the actual speed. From figure 29 above, it can be observed, that with the use of the optimal speed controller, the initial overshoot is now greatly reduced.

The other response curves of torque and stator current were also found to be satisfactory.

Chapter 5

Parametric Robustness

5.0 Introduction

In this chapter, bounded parametric uncertainties have been considered and their results and effects have been incorporated into the IFOC induction motor system. These results have been simulated using interval laboratory and then finally a robust controller has been designed for the speed control loop of the Vector Controller

5.1 Bounded parametric uncertainties:

Indirect Field Oriented Control requires use of a machine model in order to calculate the field angle. But, the parameters of the machine model change due to various operating conditions [5]. A variation of these parameters affects the dynamic response as well as the transient response of the control scheme. Such a variation of parameters causes a mismatch between the vector controller and the induction machine. This mismatch results in a coupling between the flux and the torque producing channels of the machine. This has various consequences [3]:

❖ The rotor flux linkages deviate from the commanded values

❖ Therefore the electromagnetic torque deviates from the commanded value thereby producing a nonlinear relationship between the actual torque and the commanded torque.

❖ Oscillations are caused during torque transients, both in the rotor flux linkages and in torque responses, and have a settling time equal to the rotor time constant.

The above effects make system performance undesirable in various applications. For example in electric vehicles, deviations in electromagnetic torque and commanded torque and a nonlinear relationship between them is not acceptable. Therefore the effects of such parameter variations need to be studied.

A. Types of bounded parametric uncertainties:

There are primarily three phenomenon for parametric variations of an induction motor. They are:

❖ Changing operating conditions like temperature rise

❖ Changes in operating condition like saturation

❖ Wrong instrumentation of parameters in Vector Controller.

Of these, the last phenomenon is controllable while the former two are uncontrollable. Therefore in our study, we consider the two uncontrollable phenomenon that cause parametric uncertainties.

1. TEMPERATURE RISE:

It has been observed and stated in [3], [5] that the practical temperature excursion of the motor is approximately $130°$ above ambient. This increases the rotor resistance by 50% over its ambient or nominal value. Therefore the rotor resistance can change from their nominal value to 1.5 times of the nominal value.

2. SATURATION:

Magnetic saturation can decrease the self-inductance of the motor to 80% of the nominal value. Again, operation of the induction motor in the linear region of the B-H curve can increase the self-inductance to 1.2 times the nominal value. Thus self-inductance can change from 0.8 times of the nominal value to 1.2 times of the nominal value. i.e. 80% to 120% variation is possible in this case.

It is to be noted that the above variations were considered at stator currents not exceeding twice the rated value. Combining the above two conditions we obtain four operating points of the motor. They are:

A. When the motor is operating at linear flux region and ambient temperature. Here, R_r is equal to nominal value and L_m is equal to 1.2 times the nominal value. hence $R_r = R_r^*$, and $L_m = 1.2 L_m^*$.

B. When the motor runs in linear flux region and 130° above ambient temperature. Thus, we have $R_r = 1.2 R_r^*$ and $L_m = 1.2 L_m^*$.

C. When the motor runs in magnetic saturation region and ambient temperature. Hence we have $R_r = R_r^*$ and $L_m = 0.8 L_m^*$.

D. When the operating conditions are Magnetic saturation region and 130° above ambient temperature. We have $R_r = 1.5 R_r^*$ and $L_m = 0.8 L_m^*$

The above conditions incorporate all possible operating conditions for an induction motor upto 130° above the ambient temperature and any region of flux wave (B-H curve).

5.2 Interval Laboratory:

It is required to obtain the first order reduced model of the plant for each of the above conditions mentioned in the previous section. Thereafter, the variations of each parameter will be studied. This is a laborious job is carried out manually as each relation pertaining to all of the four scenarios needs to be considered independently. Also, the coupling between the various parameters mean minimum or maximum values of one parameter is greatly dependent on other parameters. At this juncture, INTLAB, a tool which can be used with MATLAB and has the distinct advantage of providing rigorous bounds for the exact solution [29], provides a solution to effectively calculate the effects of the variations of parameters to the actual system.

The concept of interval analysis is to compute with intervals of real numbers in place of real numbers. An application is when some parameters are not known exactly but are known to lie within a certain interval; algorithms may be implemented using interval arithmetic with uncertain parameters as intervals to produce an interval that bounds all possible results.

If the lower and upper bounds of the interval can be rounded (rounded down and rounded up respectively) then finite precision calculations can be performed using intervals to give an enclosure of the exact solution [29].

The idea of bounding rounding errors using Intervals was introduced by several people in the 1950s, but the real interval analysis and its use began with Moore's book in 1966. Siegfried M. Rump showed that by expressing intervals by the midpoint and radius, interval arithmetic can be implemented entirely using Basic Linear Algebra Subroutines (BLAS). Using these findings, Rump produced the MATLAB toolbox INTLAB.

Notations:

Intervals are represented here with brackets "[]" defined by an upper bound and a lower bound. Underscores are used to denote lower bounds of intervals and overscores are used to denote upper bounds.

A. Real Interval Arithmetic:

A real interval x is a nonempty set of real numbers

$$x = [\underline{x}, \overline{x}] = \{x \in R : \underline{x} \le x \le \overline{x}\}$$

Where $\underline{x}$ is called the *infimum* and $\overline{x}$ is called the *supremum.* The set of all intervals over R is denoted by "$\mathcal{R}$" where

$$\mathcal{R} = \{[\underline{x}, \overline{x}] : \underline{x}, \overline{x} \in R, \underline{x} \le \overline{x}\}$$

The midpoint of x,

$$\text{mid}(x) = \hat{x} = \frac{1}{2}\left(\underline{x} + \overline{x}\right)$$

And the radius of x

$$\text{rad}(x) = \frac{1}{2}\left(\overline{x} - \underline{x}\right)$$

Elementary interval arithmetic operations are implemented with:

$$x + y = [\underline{x} + \underline{y}, \overline{x} + \overline{y}]$$

$$x - y = [\underline{x} - \overline{y}, \overline{x} - \underline{y}]$$

$$x \times y = [\min\{\underline{x}\underline{y}, \underline{x}\overline{y}, \overline{x}\underline{y}, \overline{x}\overline{y}\}, \max\{\underline{x}\underline{y}, \underline{x}\overline{y}, \overline{x}\underline{y}, \overline{x}\overline{y}\}]$$

$$\frac{1}{x} = [\frac{1}{\overline{x}}, \frac{1}{\underline{x}}] \quad \text{if } \underline{x} > 0 \text{ or } \overline{x} < 0$$

$$x \div y = x \times \frac{1}{y}$$

[29]

For the elementary interval operations, division by an interval containing zero is not defined. It is often useful to remove this restriction to give what is called extended interval arithmetic.

Division rules for INTLAB using extended interval arithmetic is as follows:

$$\frac{x}{y} = \begin{cases}
[\overline{x}/\underline{y}, ¿] & \text{if } \overline{x} \leq 0 \text{ and } \overline{y} = 0 \\
[-¿, \overline{x}/\overline{y}] \, â \, [\overline{x}/\underline{y}, ¿] & \text{if } \overline{x} \leq 0 \text{ and } \underline{y} < 0 < \overline{y} \\
[-¿, \overline{x}/\overline{y}] & \text{if } \overline{x} \leq 0 \text{ and } \underline{y} = 0 \\
[-¿, ¿] & \text{if } \underline{x} \leq 0 \leq \overline{x} \\
[-¿, \underline{x}/\underline{y}] & \text{if } \underline{x} \geq 0 \text{ and } \overline{y} = 0 \\
[-¿, \underline{x}/\underline{y}] \, â \, [\underline{x}/\overline{y}, ¿] & \text{if } \underline{x} \geq 0 \text{ and } \underline{y} < 0 < \overline{y} \\
[\underline{x}/\overline{y}, ¿] & \text{if } \underline{x} \geq 0 \text{ and } \underline{y} = 0
\end{cases}$$

[29]

The addition and subtraction of infinite or semi-infinite intervals are the n defined by the following:

$$[\underline{x}, \overline{x}] + [-¿ = \overline{y}] = [-¿, \overline{x} + \overline{y}]$$

$$[\underline{x}, \overline{x}] + [\underline{y}, ¿] = [\underline{x} + \underline{y}, ¿]$$

$$[\underline{x}, \overline{x}] + [-¿, ¿] = [-¿, ¿]$$

$$[\underline{x}, \overline{x}] - [-¿, ¿] = [-¿, ¿]$$

$$[\underline{x}, \overline{x}] - [-¿, \overline{y}] = [\underline{x} - \overline{y}, ¿]$$

$$[\underline{x}, \overline{x}] - [\underline{y}, ¿] = [-¿, \overline{x} - \underline{y}]$$

B. INTLAB toolbox:

Real intervals in INTLAB are stored by the infimum and supremum, whereas complex intervals are stored by the midpoint and radius. However, this is not seen by the user. Intervals may be entered using either representation. For example the interval x= [1;1] is entered using infimum and supremum as

>> x = infsup(-1,1);

but the same interval could be entered using the midpoint and radius as

>> x = midrad(0,1);

Since complex intervals are stored as a circular region using the midpoint and radius it is more accurate to input such intervals in this way. For example the circular region with midpoint at $1 + i$ and radius 1 is entered using

>> y = midrad(1+i,1);

If a rectangular region is entered using the infimum and supremum then the region is stored with an overestimation as the smallest circular region enclosing it. The infimum is entered as the bottom left point of the region and the supremum is the top right point. The region with a infimum of $1 + i$ and a supremum of $2 + 2i$ is entered as

>> z = infsup(1+i,2+2i);

However, it is stored by the midpoint and radius notation as

>> midrad(z)
        intvalz =

<1.50000000000000+ 1.50000000000000i,0.70710678118655>

<u>C.</u> Reduced first order transfer functions considering parametric variation:

The derivation for calculating the reduced order systems and the robust controller design have been programmed in MATLAB using INTLAB toolbox. The results of reduced first order transfer function considering parametric variation are:

1. Nominal system is obtained as:

$$\frac{8.756}{s + 0.3473}$$

2. Case-1 When the motor is operating at linear flux region and ambient temperature

$$\frac{8.595}{s + 0.3412}$$

3. Case-2 When the motor runs in linear flux region and 130° above ambient temperature:

$$\frac{8.594}{s + 0.3412}$$

4. Case-3 When the motor runs in magnetic saturation region and ambient temperature:

$$\frac{8.829}{s + 0.3501}$$

5. Case-4 When the operating conditions are Magnetic saturation region and 130° above ambient temperature:

```
   8.891
 ----------
 s + 0.3525
```

5.3 Robust Controller Design:

We extend the derivations and results of the optimal controller for designing the robust controller. We consider a 10% variation in the damping factor and the closed loop frequency. Thus, we have

$$\xi' = [0.81, 0.99] \text{ ,}$$

And $\check{S}_{ncl} = [9, 11]$

Now, it is our aim to replace the nominal system by an interval system and use the optimal controller already designed such that the controller remains an optimal controller for the corresponding interval system. For this, we refer to the following theorem [18]:

Here, the nominal system is given by : $P_0(s) = \dfrac{b_0}{s + a_0}$

While the interval system is given by:

$$P = \frac{b}{s+a} \quad \text{where } a \in [\underline{a}, \overline{a}] \text{ and } b \in [\underline{b}, \overline{b}]$$

Now, we have $b = x\, b_0$ and calculating x from the results of last section, we have

$x = [0.9814984, 1.0154179]$

Form the results of the previous section, we form the intervals a and b as:

$a = [0.3412, 0.3525]$

$b = [8.594, 8.891]$

And our nominal values for a and b are:

$a = 0.3473$ and $b = 8.756$

Therefore the range of change in the values can be expressed as:

$\Delta a = [-0.0061, 0.0052]$

$\Delta b = [-0.162, 0.135]$

Thus, $\Delta A = \begin{pmatrix} 0 & 1 \\ 0 & \Delta a \end{pmatrix}$ and $\Delta B = \begin{pmatrix} 0 \\ \Delta b \end{pmatrix}$

Hence,

$$A = A_0 + \Delta A$$

$$B = B_0 + \Delta B$$

where A_0 and B_0 are the nominal values of the A and B matrix of the nominal system.

Let $P = \begin{pmatrix} P_{11} & P_{12} \\ P_{12} & P_{22} \end{pmatrix}$ be the solution to the ARE

$$A_0{}^T P + P A_0 + Q_0 - P B_0 R_0{}^{-1} B_0{}^T P = 0$$

Then we have

$$P = \begin{pmatrix} P_{11} & \dfrac{K_i}{b_0} \\ \dfrac{K_i}{b_0} & \dfrac{K_p}{b_0} \end{pmatrix}$$

Now if $\tilde{P} = P + \Delta P$ be the solution of the equation

$$A^T \tilde{P} + \tilde{P} A + Q - \tilde{P} B R^{-1} B^T \tilde{P} = 0$$

Now, if the controller is same for both the systems, then

$$R^{-1} B^T \tilde{P} = K$$

$\Rightarrow \quad \begin{pmatrix} 0 & b_0 + \Delta b \end{pmatrix} \begin{pmatrix} P_{11} & P_{12} \\ P_{12} & P_{22} \end{pmatrix} = \begin{pmatrix} K_i & K_p \end{pmatrix}$

Now, we know $b_0 + \Delta b = x\, b_0$

So, $\begin{pmatrix} 0 & x\, b_0 \end{pmatrix} \begin{pmatrix} P_{11} & P_{12} \\ P_{12} & P_{22} \end{pmatrix} = \begin{pmatrix} K_i & K_p \end{pmatrix}$

$\Rightarrow \quad \begin{pmatrix} x\, b_0 P_{12} & x\, b_0 P_{22} \end{pmatrix} = \begin{pmatrix} K_i & K_p \end{pmatrix}$

Hence, $x\, b_0 P_{12} = K_i$

$P_{12} = \dfrac{K_i}{x\, b_0}$

$P_{22} = \dfrac{K_p}{x\, b_0}$

Therefore, $\tilde{P}$ becomes:

$$\tilde{P} = \begin{pmatrix} P_{11} + \Delta P_{11} & \dfrac{K_i}{x\, b_0} \\[2ex] \dfrac{K_i}{x\, b_0} & \dfrac{K_p}{x\, b_0} \end{pmatrix}$$

Now, we calculate $A^T \tilde{P} + \tilde{P} A$

Putting the values of A and $\tilde{P}$ in the above equation, we have:

$$A^T \tilde{P} + \tilde{P} A = \begin{pmatrix} 0 & \tilde{P}_{11} + a\tilde{P}_{12} \\ \tilde{P}_{11} + a\tilde{P}_{12} & 2\tilde{P}_{12} + 2a\tilde{P}_{22} \end{pmatrix}$$

And from the ARE,

$\tilde{Q} = \tilde{P} B R^{-1} B^T \tilde{P} - (A^T \tilde{P} + \tilde{P} A)$

we obtain :

$$\tilde{Q} = \begin{pmatrix} \tilde{P}_{12} \times b_0 K_i & \tilde{P}_{12} \times b_0 K_p - \tilde{P}_{11} - a\tilde{P}_{12} \\ \tilde{P}_{22} \times b_0 K_i - \tilde{P}_{11} - a\tilde{P}_{12} & \tilde{P}_{22} \times b_0 K_p - 2\tilde{P}_{12} - 2a\tilde{P}_{22} \end{pmatrix} = \begin{pmatrix} \tilde{Q}_{11} & 0 \\ 0 & \tilde{Q}_{22} \end{pmatrix}$$

Thus,

We find $\tilde{Q}_{11} = \dfrac{\check{S}^4_{ncl}}{b^2_0}$

And, $\tilde{Q}_{22} = K_p^2 - 2a\dfrac{K_p}{x\,b_0} - 2\dfrac{K_i}{x\,b_0}$

$\Rightarrow$ $\tilde{Q}_{22} = \dfrac{\left(2\langle \check{S}_{ncl} - a_0\right)^2}{b_0} - \dfrac{2a}{x\,b_0^2}\left(2\langle \check{S}_{ncl} - a_0\right) - \dfrac{2\check{S}^2_{ncl}}{x\,b_0^2}$

From the above relations, the values of $\tilde{Q}$ are calculated.

The nominal PI controller designed for the nominal system remains an optimal controller for the interval plant and it produces a closed loop system with poles in regions of the complex plane given the intervals of $\langle$ and $\check{S}_{ncl}$, if the condition $\tilde{Q} \geq 0$ is satisfied over the entire convex box of a and b.

The positive semi definiteness of the matrix over the entire convex box of a and b can be tested by using the results established in [15]. It is established in [15] that for a symmetrical interval matrix such as $\tilde{Q}$, if

$$\tilde{Q}_c = \frac{1}{2}(\tilde{Q}^- + \tilde{Q}^+)$$

And $\tilde{Q}^\Delta = \frac{1}{2}\left(\tilde{Q}^+ - \tilde{Q}^-\right)$

Then $\tilde{Q}$ is a positive semi-definite for the interval $[\tilde{Q}^-, \tilde{Q}^+]$ if

$$\}_{min}(\tilde{Q}_c) \geq \ldots (\tilde{Q}^\Delta)$$

For a given $\tilde{Q}$, the matrices $\tilde{Q}^-$ and $\tilde{Q}^+$ are computed using the functions inf($\tilde{Q}$) and sup($\tilde{Q}$ respectively using INTLAB

5.4 RESULTS:

A. Matlab Results and proof of robustness:

The above controller design is programmed in MATLAB using INTLAB to compute the interval arithmetic involved. The following results were then obtained:

$$\tilde{Q}^+ = \begin{pmatrix} 130.433 & 0 \\ 0 & 32.86526741 \end{pmatrix}$$

$$\tilde{Q}^- = \begin{pmatrix} 130.433 & 0 \\ 0 & 32.7658343770 \end{pmatrix}$$

$$\tilde{Q}^C = \begin{pmatrix} 130.433 & 0 \\ 0 & 32.815550 \end{pmatrix}$$

$$\tilde{Q}^\Delta = \begin{pmatrix} 0 & 0 \\ 0 & 0.0497165 \end{pmatrix}$$

Also,

$$\}_{min}(\tilde{Q}_c) = 32.81$$

And

$$\ldots(\tilde{Q}^\Delta) = 0.0497$$

Thus the relation

$\}_{\min}(\tilde{Q}_c) \geq _{...}(\tilde{Q}^{\Delta})$ holds.

Hence, the optimal controller designed for the nominal system is capable of providing desired response for the entire convex box of the interval system $P = \dfrac{b}{s+a}$ where $a \in [\underline{a}, \overline{a}]$ and $b \in [\underline{b}, \overline{b}]$ and therefore it is a robust controller which can take into account the effects of bounded parametric uncertainties arising out of operating conditions of the motor.

B. Simulation results using the proposed controller taking into account the maximum and minimum parameter variations and discussions on results.

For the purpose of study of the performance of the robust controller, out of the four transfer functions for the four conditions, the minimum and the maximum, i.e. the infimum and the supremum is selected. Then the response for the nominal system, the infimum system and the supremum system is observed when the proposed controller is added. The simulation of the said scheme is given in figure 34.
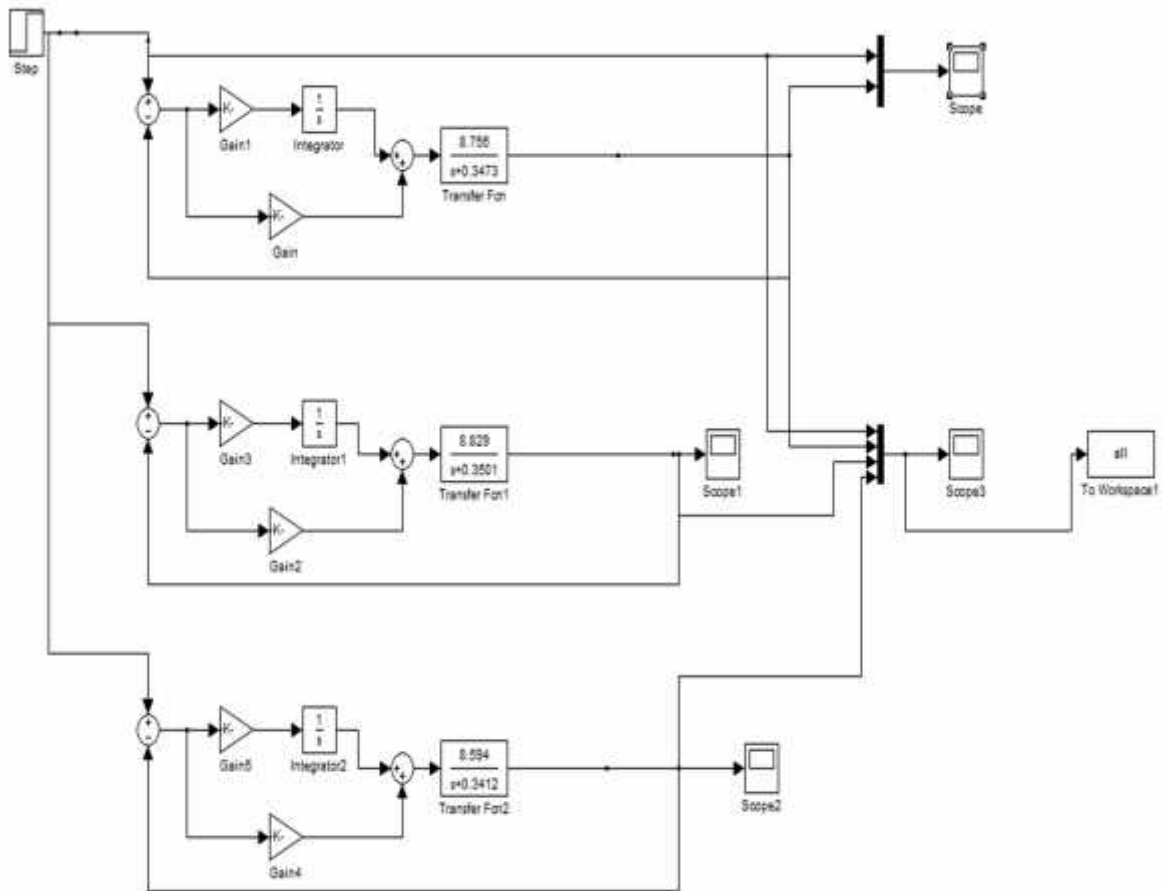
Figure 34 Simulation of the systems with minimum, zero and maximum parameter variation using the proposed controller.

The above scheme consists of each of the four transfer functions (for each condition of paramteric uncertainty considered in previous discussions) and a unity speed feedback with the proposed optimal PI controller. The outputs of the responses are then studied and presented in figure 35..
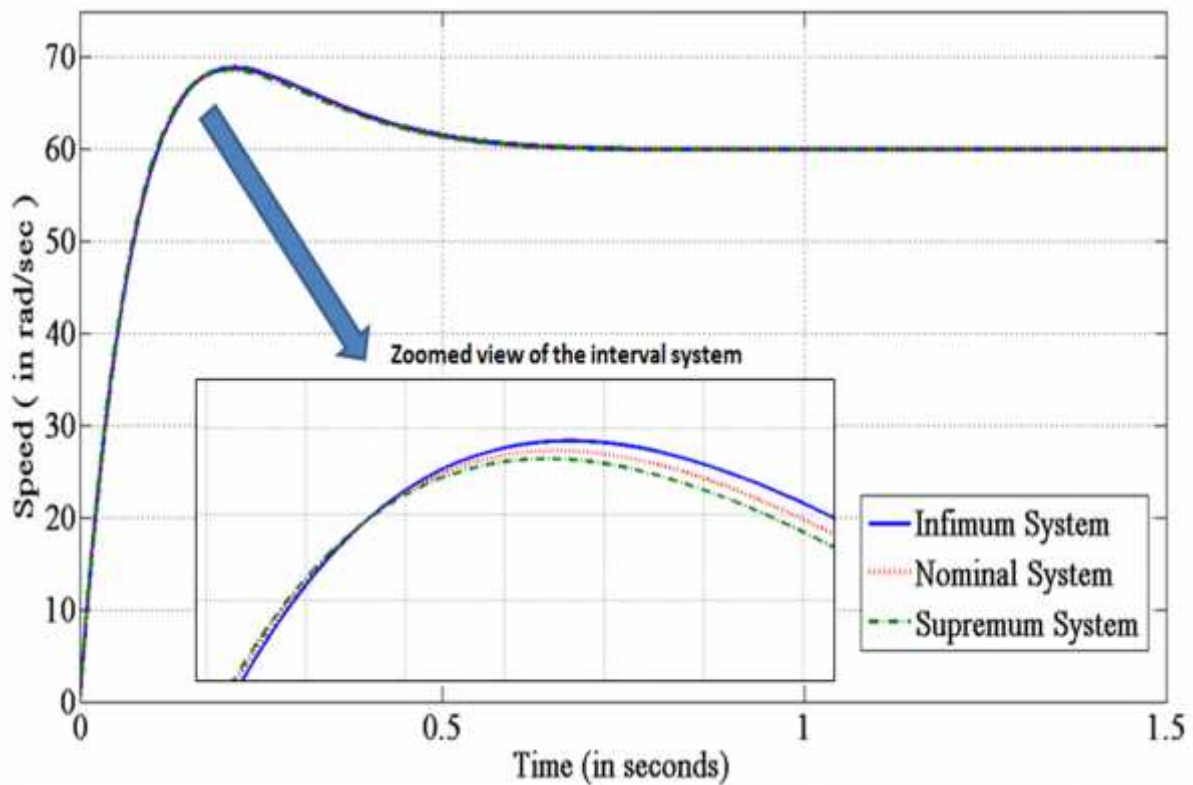
Figure 35 zoomed view of the responses of the interval system to a speed input(step) of 60 rad/sec

The above figure shows that the nominal system response lies in between the infimum and supremum system responses. All three responses are almost identical, though on magnification, each can be individually traced. The nature of the responses are same. Rise time is quite fast and the systems settle at about 0.5seconds. From this figure we can say that throughout the interval, the system response is fast and stable5

C. <u>Results obtained by subjecting the simulink of the IFOC system to paramteric uncertainties and a brief discussion.</u>

The IFOC system developed and designed in Matlab/Simulink is subjected to paramteric uncertainties. The maximum and minimum values of the parameters are put in the simulation and results are obtained. The responses are then studied.
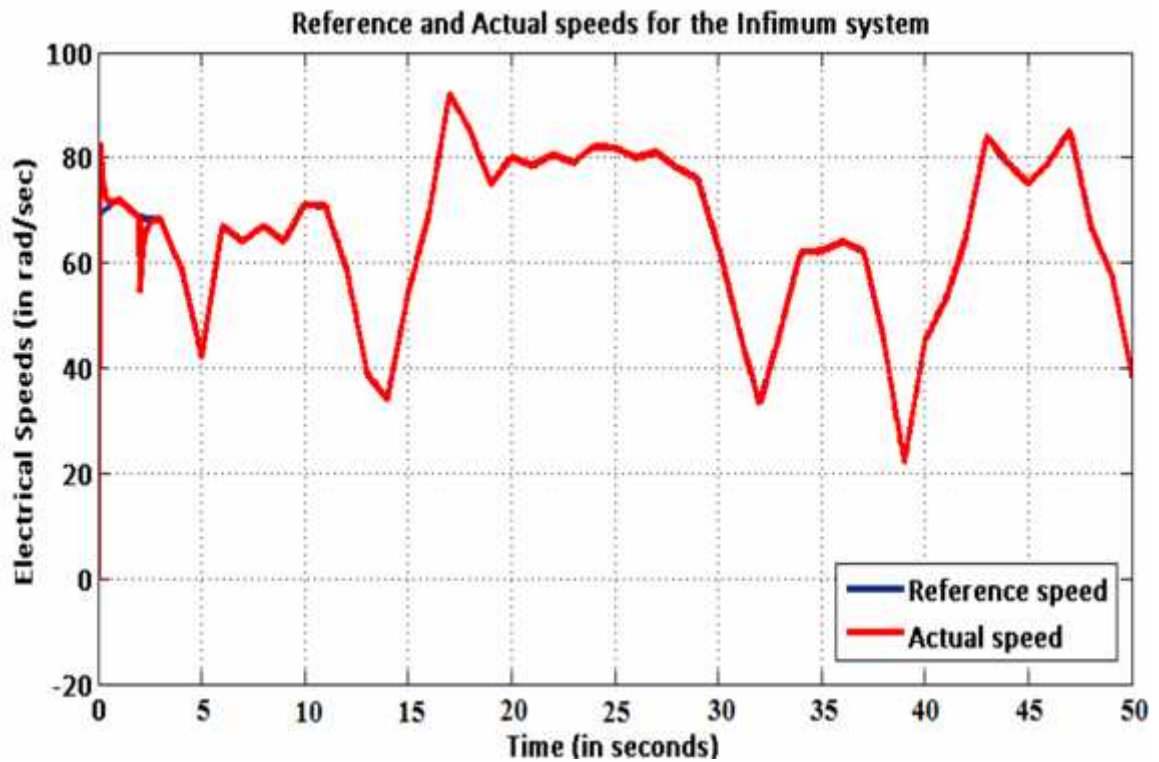
Figure 36 speed response of the IFOC system with minimum system parameters. i.e. Infimum system
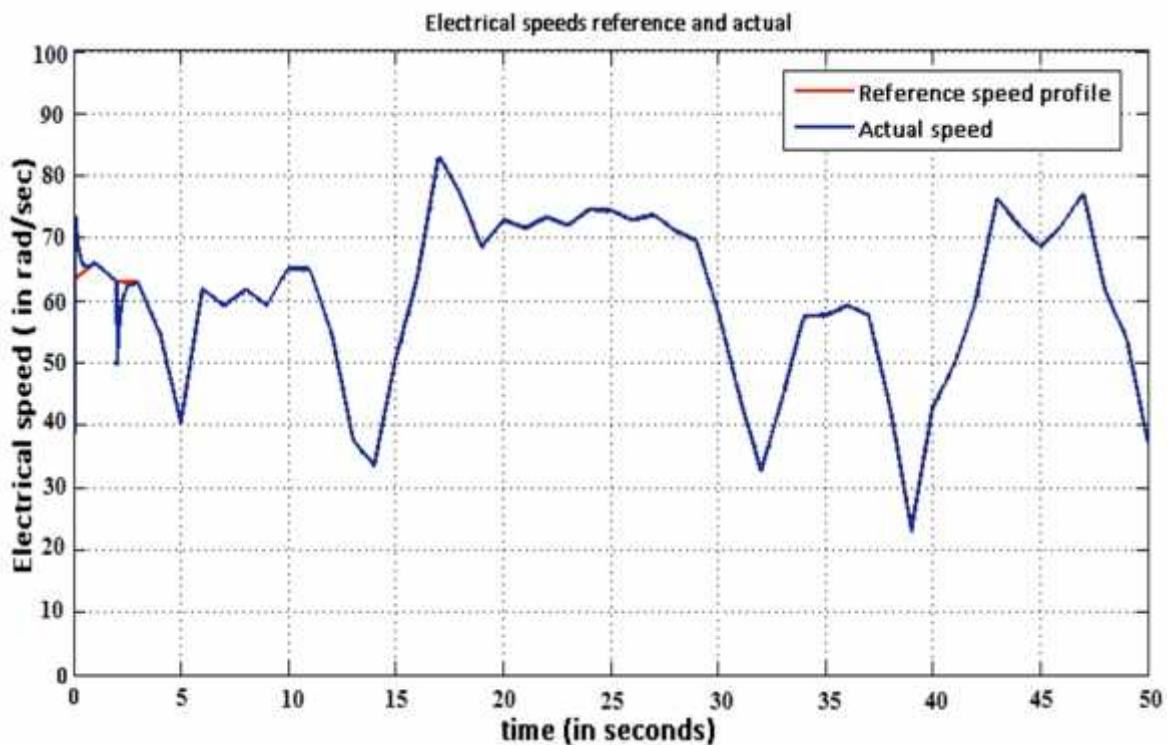

Figure 37 speed response of the IFOC system with nominal system parameters. i.e. Nominal system
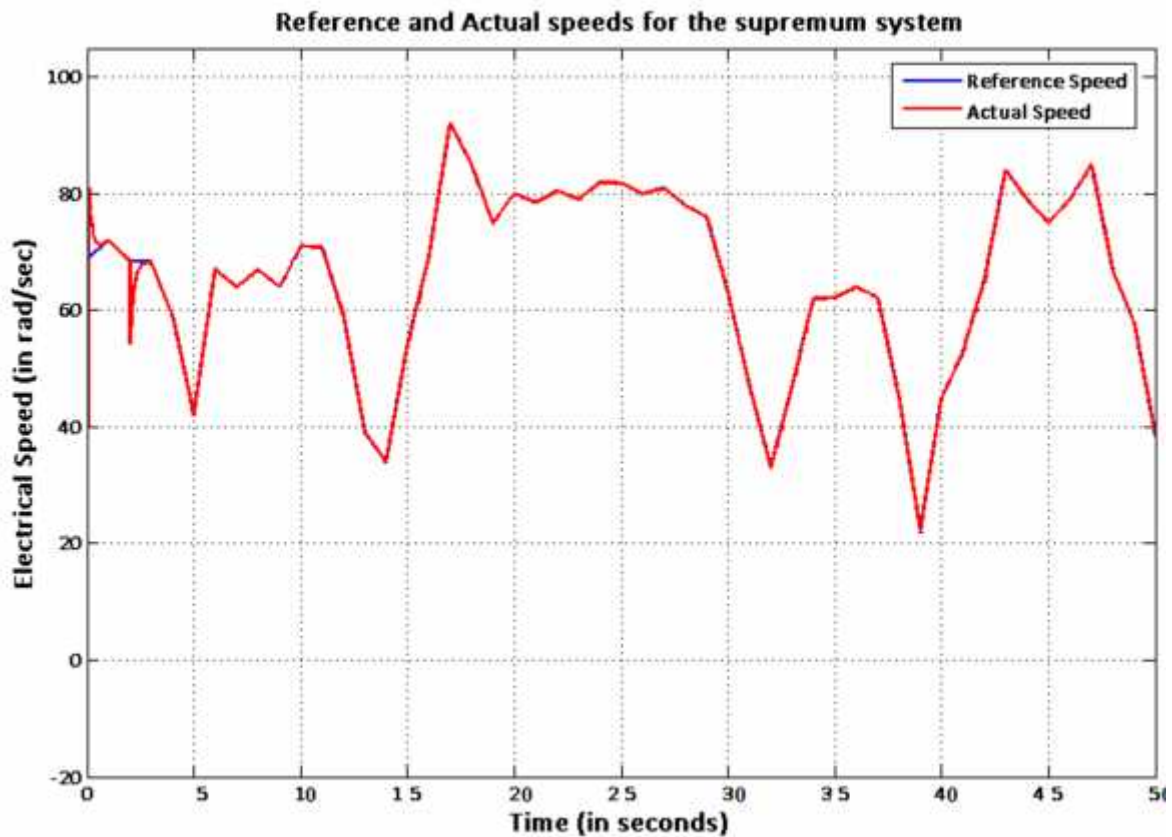
Figure 38. Speed response of the IFOC system with maximum system parameters. i.e. Supremum system

Discussions:

It can be observed and stated from the above responses that the proposed controller is capable of maintaining optimal stability throughout the interval. As the controller gives almost identical results for the infimum, the nominal as well as the supremum system, it can be concluded that the controller can be used effectively throughout the interval, even with the maximum and minimum parameter variations. Thus, the designed controller is a robust controller.

CHAPTER 6

Real Time Simulation

6.0 Introduction :

Since the advent of modern computers, simulation tools have been widely used by technologists to design, analyse and modify physical systems according to specific requirements. With the development of high end computing technologies, simulation tools have seen marked improvement in terms of performance, and have dramatically decreased in cost. This has increased acceptance of simulation tools as they can now be used by more and more researchers. Real time simulation has now been developed which provide marked improvement in performance and speed.

6.1 Real Time Simulation

A real time simulation is a representation of the operation or features of a system through the use or operation of another. During discrete time simulation, time moves forward in steps of equal duration. This is usually called fixed step simulation. In offline simulation, the moment at which a result becomes available is irrelevant. While performing offline simulation, the objective is to obtain results as fast as possible. The system solving speed depends on the available computation power and the systems mathematical model complexity.
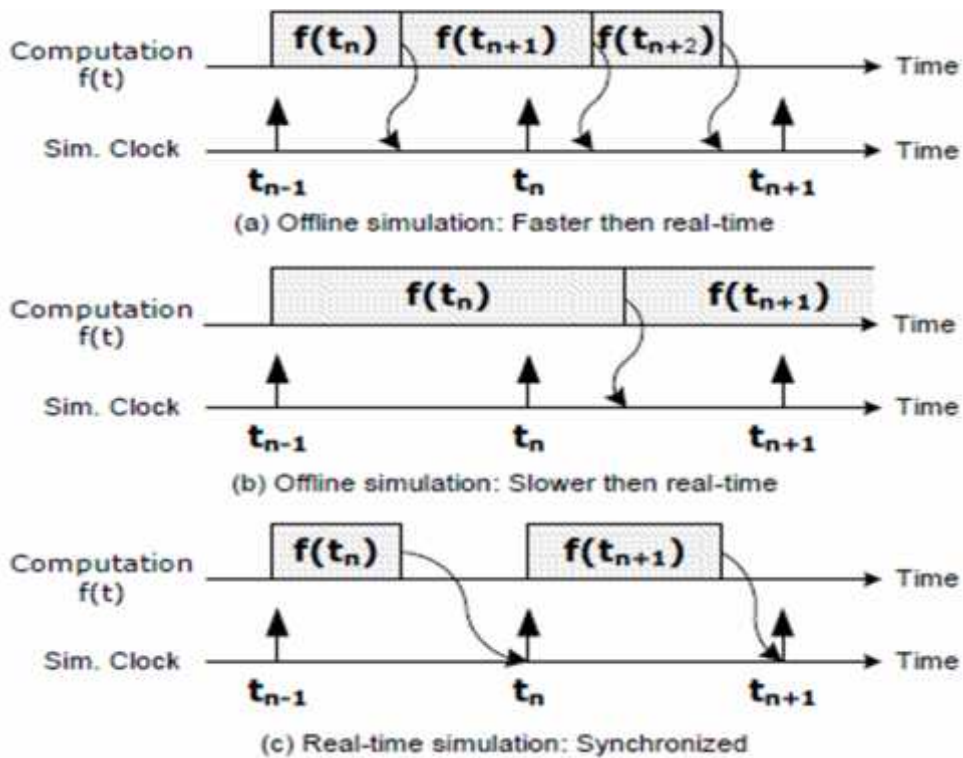
Figure 39: Real time simulation requisites and other simulation techniques

The figure above [20] shows a) and b) show two possible simulation conditions where the computation time is either shorter than a fixed time step (shown in a), or the computation time is longer than the fixed time step. These are cases of offline simulation. But in real time simulation shown in c) the real time simulator accurately produces the internal variables and outputs of the simulation within the same length of time that its physical counterpart would. Moreover, it can stated that the time required to compute the solution at a given time step must be shorter than the wall clock duration of the time step. Here any idle time preceding or following the simulator operation is lost and the simulator waits for the next time step to arrive. If in any case the simulator fails to achieve operations within the fixed time step, the real time simulation becomes erroneous and this phenomenon is termed as OVERRUN [20].

For each time step, the simulator executes a series of operations is the following order:

1. Reads inputs and generates outputs.
2. Solve model equations.
3. Exchange results with other simulation nodes.

4. Waits for the next step.

Recently, solutions to stability and timing issues have been proposed that include discrete time compensation techniques. Modern simulators are equipped with cutting edge technology advanced I/O cards that run at a much faster sampling rate than fixed step simulation. They can read state changes in between simulation steps. Then when the next time step arrives, the I/O card besides passing state information on to the simulator also passes timing information as to when the state change occurred. Finally the simulator can compensate for the time error.

6.2 Various types of Real Time simulations:

The various types of simulations that can be performed by modern simulators are:

A. Rapid Control Prototyping (RCP)

In this kind of an application, the plant controller is implemented using a real time simulator and is connected to a physical plant. Such a controller provides more flexibility, is faster to implement and easier to debug. Such a technique a controller to be tested even before it is physically made, thereby making decisions on feasibility of the controller much simpler.

B. Hardware In the Loop (HIL)

In Hardware in the Loop simulation, there is a physical controller which is to be connected to a virtual plant, while the virtual plant is executed on a real time simulator. There is absence of any physical plant. HIL possesses all the advantages of RCP with a few added benefits. HIL allows early testing of controllers when physical test benches are not available. Moreover such ta technique provides great flexibility as controllers and plants can be separately produced and testing of controller is possible with a virtual plant. It also provides for testing conditions that are unavailable on real physical plants such as extreme testing.

C. Software In the Loop (SIL):

Software in the Loop is a step beyond RCP and HIL. It requires a powerful simulator that can simulate both the controller and the plant. This has great implications on engineering and scientific domain as no inputs or outputs are used and thus signal integrity is preserved. As both the plant and the controller operate within the simulator, it can be faster or slower than real time. Thus an SIL simulation can be made to perform accelerated simulation.

6.3 OPAL RT OP 4500:

OPAL RT OP4500 is a real time simulator manufactured by OPAL RT labs. It is a state of the art simulator, a compact device with 96 fast I/O channels with signal conditioning, fast 5-Gbits fiber optics and is fully integrated with Simulink and SimPowerSystems. The integration of high end INTEL multi core processors with powerful XILINX Kintex 7FPGA allows greater simulation power and sub microsecond simulation time steps to maximise accuracy of fast power electronic systems.

Opal RT has 32 analog inputs and 16 analog output channels . the other specifications are shown below [30]:

Table 3 OPAL RT OP4500 specifications. (source: OP4500 Datasheet, OPAL RT labs)

Power supply	Universal input and active power factor correction
FPGA	Xilinx Kintex-7 FPGA, 325T, 326000logic cells, 840 DSP slice
computer	SuperMicro, 4GB RAM, One Intel 4 core CPU, 2.5 or 3.3GHz, solid state hard disk 125 GB
Fast Optical Interface	4 sockets for optional Small Form Factor Pluggable 1 to 2Gbits/s optical cable pairs
Software Compatibility	RT-LAB Multiprocessors Platform, LINUX, Simulink, RTW, SimPowerSystems, SimScape, ARTEMIS, RT-EVENT,HYPERSIM,and several third party software compatible with Simulink.

| FPGA	XILINX System Generator for Simulink, RT-LAB XSG, eHS FPGA electrical circuit solvers, library of floating point functions, resolvers and Finite-Element based motor models and converters.
Performance	Minimum time step of 8 microseconds for model subsystemsexecuted on the INTEL CPU and 250 nanoseconds for models executed on the FPGA chips, 100 nanosecond timer resolution
Dimensions	43.2(W)*27.4(D)*8.9cm(H)
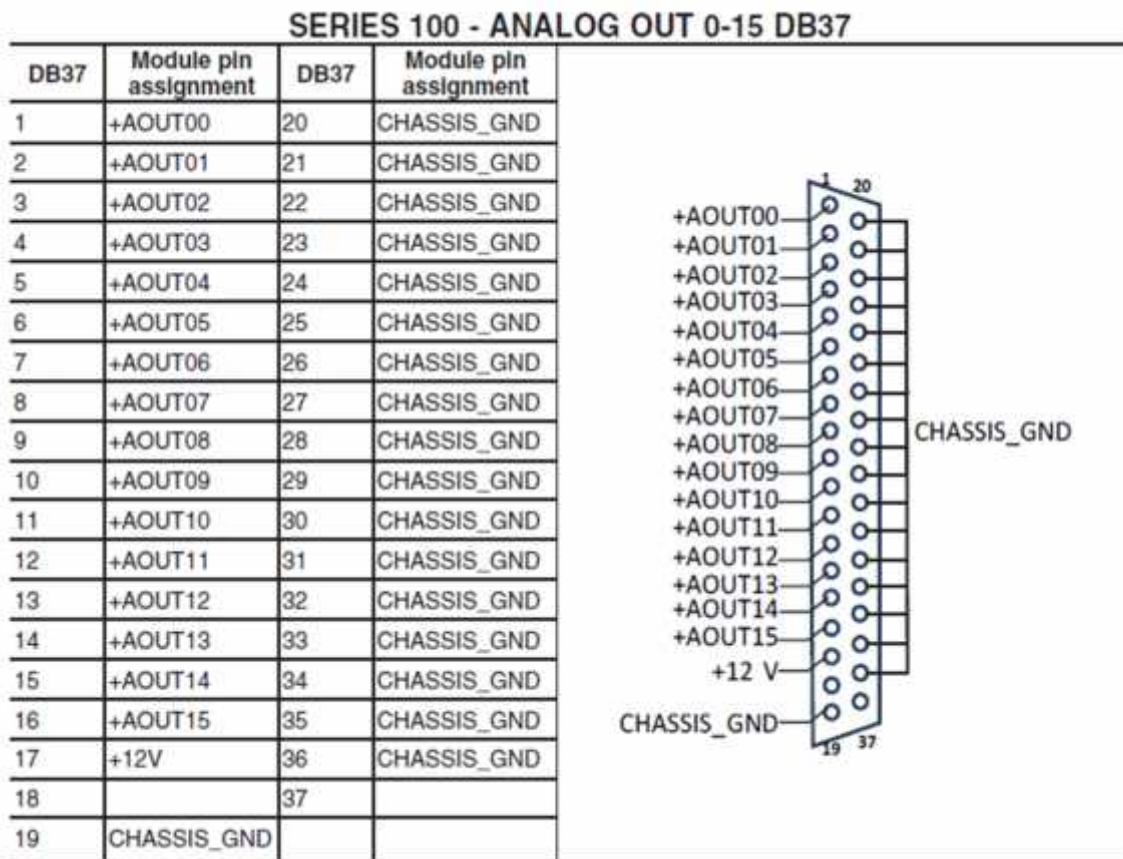
Figure 40. Analog output ports and connection diagrams for Opal Rt OP 4500 series 100

6.4 Simulation and results using OPAL RT OP4500 (on line simulation):

The plant and the controller were designed in Matlab Simulink and was run using OPAL RT OP 4500. This was basically a Software In the Loop (SIL) simulation as both the plant and the controller were simulated in the simulator itself. The following responses were observed:

1. Actual and reference speed
2. Zoomed view of actual and reference speed
3. D axis flux component
4. Electromagnetic torque
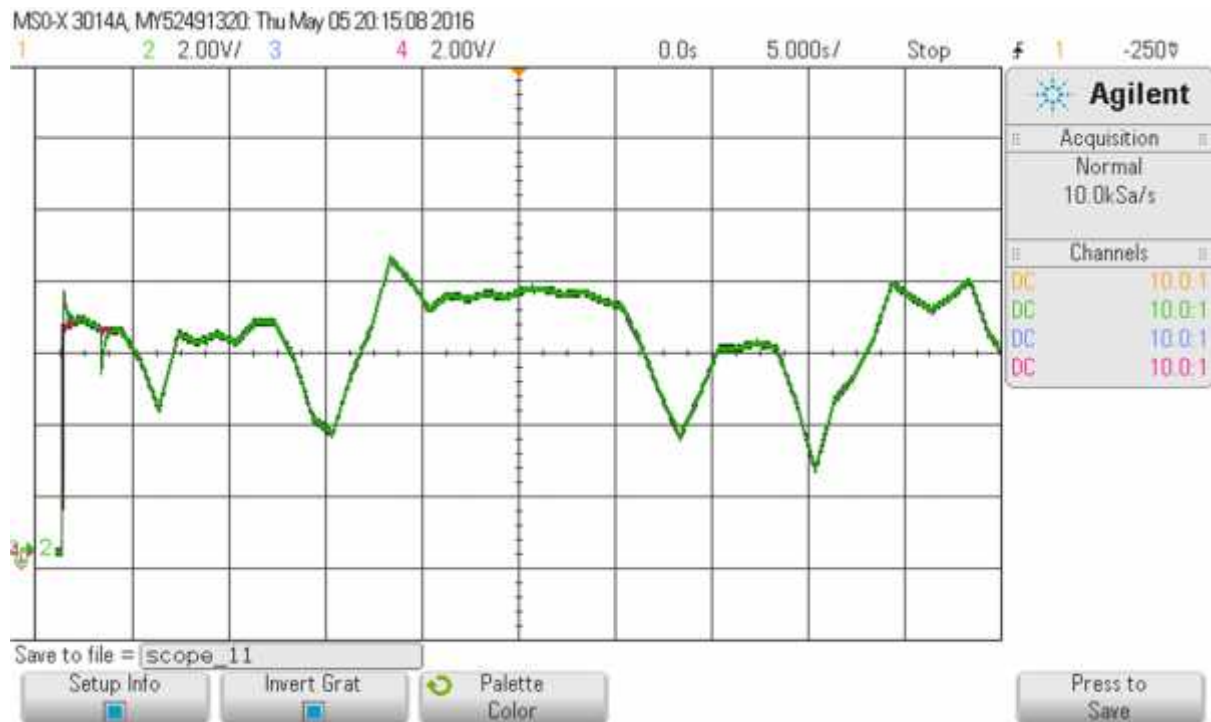
The results obtained are as follows:

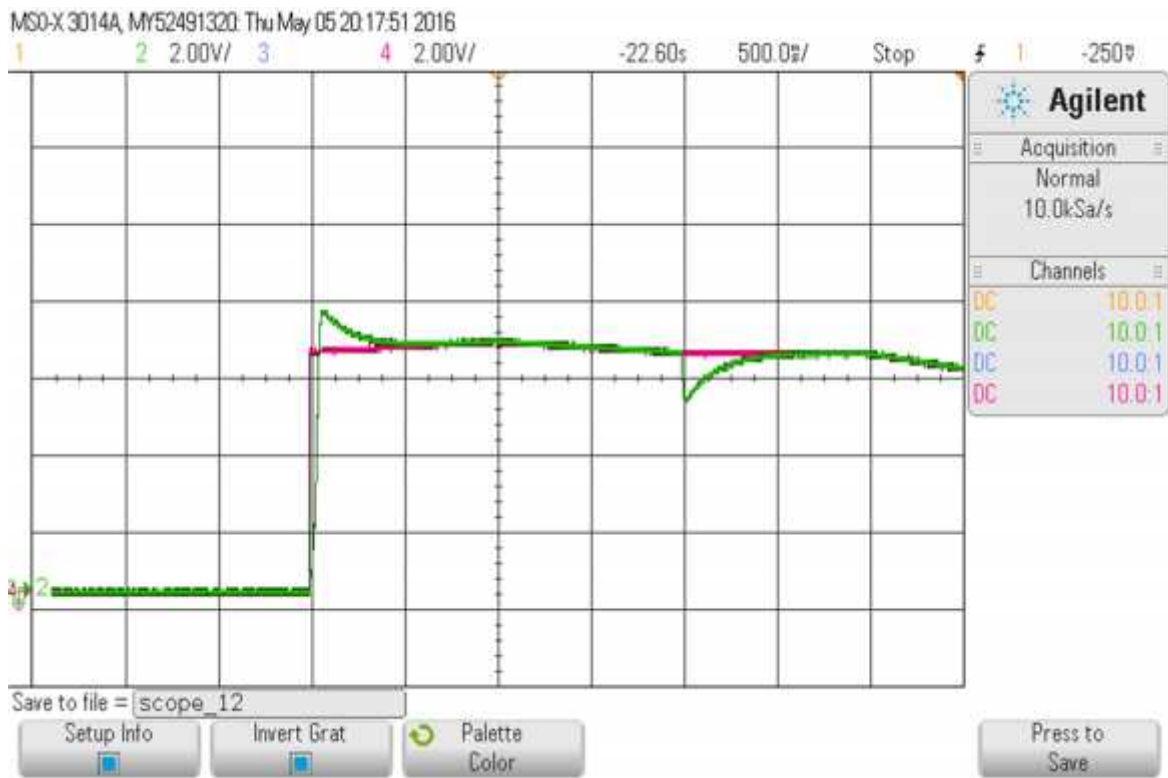**Figure 41. Reference and Actual electrical speeds of the motor**

Figure 42 Zoomed view of the actual and reference electrical speed of the motor

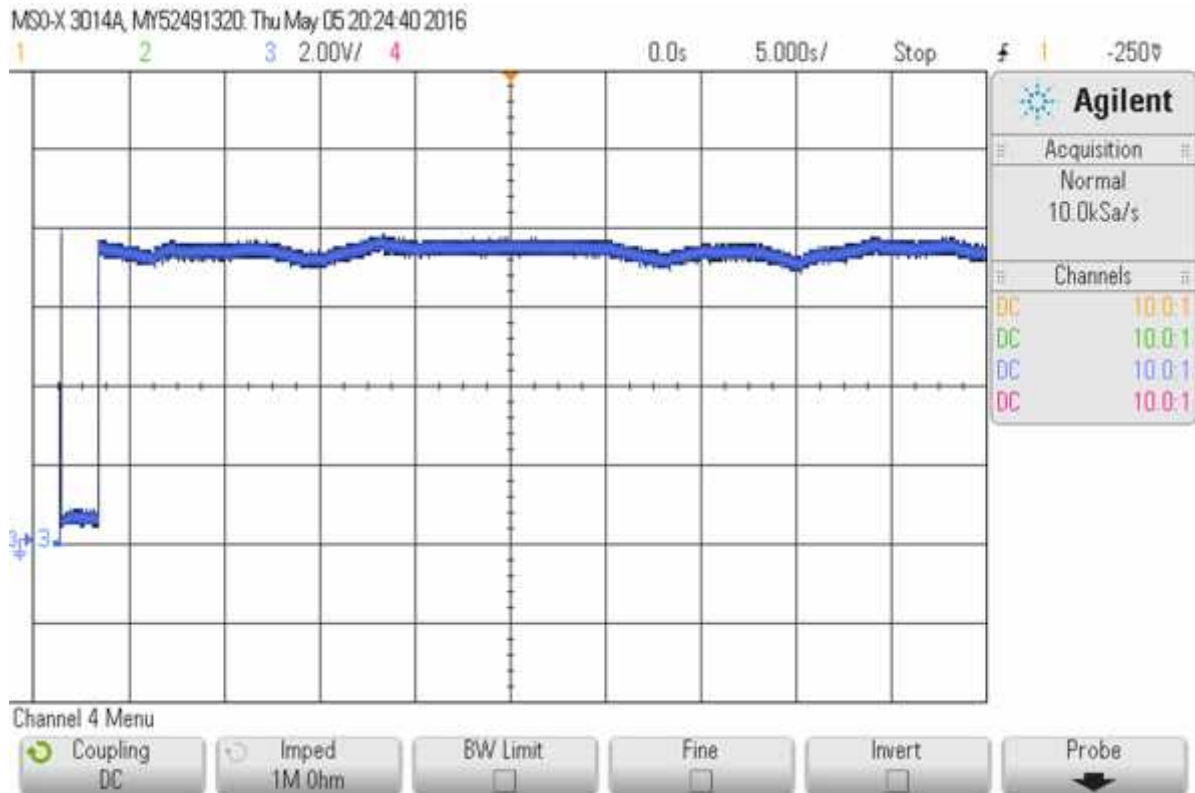**Figure 43. d axis flux of the motor**

Figure 44. Electromagnetic torque of the motor

6.5 Discussion on results:

The figures in the previous section show the performance responses of the Indirect Field Oriented Controlled Induction Motor in terms of tracking a reference speed profile and maintaining a constant d axis field flux(effectively matching the given reference of 0.075Wb). Finally the electromagnetic torque response is also studied.

Case 1- during initial starting:

It is seen that during the initial starting of the motor, the speed increases from zero to meet the given reference speed. A small overshoot is observed which is again minimized by the use of a robust optimal PI controller for the speed control loop of the FOC structure. Initially the motor runs at no load. During this time the torque of the machine should ideally be zero, but

the presence of some friction and windage torque affects the electromagnetic torque such that at no load, it has some minimal value in order to meet the frictional torque

Case 2- Motor Speed and torque response after application of external torque:

After 2 seconds of motor operation, a load torque (applied in the form of a step input of 35Nm) is applied to the motor to study the effects of sudden load torque on stability of the system. It is observed the system is able to maintain stability and after a very short duration of decrease in speed, the actual speed again rises to track the reference speed. This dip in the speed is due to the fact that with the application of load, the electromagnetic torque has to increase in order to meet the new demand. With application of load, the motor now draws more current from the supply. As the electromagnetic torque developed increases, it becomes able to meet the friction torque as well as the externally applied torque, the speed of the motor rises again to meet the reference speed.

Case 3- Steady state operation of the motor:

Even after the electromagnetic torque reaches a steady state and is able to meet the total torque demand, some oscillations are observed in the torque. This is because of the fact that the externally applied reference speed profile that the motor has to track is varying in nature. Thus the electromagnetic torque shows some variations such that the motor efficiently tracks the reference speed. Hence, Indirect Field Oriented Control of an Induction Motor along with a Robust Optimal PI controller designed using LQR method and observed using OPAL RT real time simulator performs satisfactory operation and can handle parametric variations.

.

Chapter 7

Conclusion and Scope of Future Work:

7.0 <u>CONCLUSION:</u>

In the present dissertation, the steady and the transient performance of a three phase squirrel cage induction machine has been studied in offline mode i.e. in Matlab/Simulink and in real-time scenarios i.e. in Opal RT OP4500. For the purpose of independent control of torque and flux, the Field Oriented Control has been adopted. The said control strategy comes with an outer loop speed controller and inner loop coupled current controllers. For the design of outer loop speed controller, the entire control logic is represented is block diagram and is then reduced into a second order transfer function. The second order model is then model order reduced into first order system for the design of PI controllers. Under the various operating conditions, the motor parameters usually vary and hence these bounded parametric uncertainties can be represented as an interval system. Thereafter, a modern optimal control strategy, namely Linear Quadratic Regulator has been used to design a robust speed tracking controller under the circumstances of bounded motor parameter uncertainties. The robust controller accomplishes the task of perfect speed tracking under various operating conditions. The competence of the designed control strategy has been validated both in Matlab/Simulink based offline simulation and Opal Rt based real-time simulation platforms.

7.1 <u>SCOPE OF FUTURE WORK</u>:

This work was carried out in view of applications of induction motor in the automotive industry. Four wheel or two wheel driven vehicles are now much popular which require individual motor for each wheel or a set of wheels. This work can be extended to a four wheel or two wheel driven vehicle where it can be used to drive one wheel or a set of two wheels respectively. Such a scheme would then need proper synchronization between the motors used. For such an application, CAN communication based DSP control techniques

can be adopted that can provide synchronization of the motors. Moreover electric vehicles would need to replace the mechanical differential with electronic differential schemes. Implementation of such a scheme would mean that the mechanical drives can be replaced by electrical drives. This will result in efficient use of energy along with providing a solution to the emerging global challenge of vehicular pollution.

References

1. D.O. Brian, J. B. Anderson, and Moore, "Optimal Control: Linear Quadratic Methods". Englewood Cliffs, NJ, USA: Prentice-Hall,1989.

2. Andrzej M. Trzynadlowski "Field Orientation Principle in Control of Induction Motors",Springer Science+Business Media, LLC. ISBN- 978-1-4615-2730-5

3. R. Krishnan, "Electric motor drives: modelling, analysis and control". Prentice Hall of India Pvt. Ltd. ISBN-81-203-2168-5

4. "Power electronics and variable frequency drives", IEEE Press. ISBN 0-7803-1084-5

5. R. Krishnan, Frank C. Doran, "Study of Parameter Sensitivity in High-Performance Inverter-Fed Induction Motor Drive Systems," IEEE TRANSACTIONS ON INDUSTRY APPLICATIONS, VOL. IA-23, NO. 4, JULY/AUGUST 1987

6. P.S. Bhimbra "Generalized theory of electric machines". Khanna Publications

7. G. Diana, M.W. Pickering, and R.G. Harley, "Design of a speed controller for a squirrel cage induction motor using field oriented control", Electric Power System Research, 18(1990) pages 235-245

8. .L.Umanand, S.R. Bhatt, "Optimal and robust digital current controller synthesis for vectorcontrolled induction motor drive systems", IEE Proc.-Electr. Power Appl., Vol. 143, No. 2, March 1996

9. Jinhwan Jung, Sunkyoung Lim, and Kwanghee Nan "PI Type Decoupling Control Scheme for High Speed Operation of Induction Motor," Power Electronics Specialists Conference, 1997. PESC'97 Record., 28th Annual IEEE (Volume:2) Pages: 1082-1085. ISBN-0-7803-3840-5.

10. Debayan Bose "Analysis and design of inner current control loop for field oriented control of Induction motor", Master's Thesis, Jadavpur University 2014

11. Prasun Mishra "Design and implementation of speed controller with anti-windup scheme for three phase induction motor used in electric vehicle". International Journal of Computer applications (0975-8887), volume 89-No 9, March 2014

12. Noaman M. Noaman "Speed Control for IFOC Induction Machine with Robust Sliding Mode Controller," Asian Journal of Scientific Research 04/2008; 1(4). DOI: 10.3923/ajsr.2008.324.337

13. S.Janardhanan "Model order reduction and Controller design Techniques", web tutorial, IIT delhi.

References

14. Ramon E. Moore, R. Baker Kearfott and Michael J. Cloud, "Introduction to interval analysis". Society of Industrial and Applied Mathematics, Philadelphia. ISBN 978-0-898716-69-6

15. S.M. Rump, "INTLAB - INTerval LABoratory", In Tibor Csendes, editor, Developments in Reliable Computing, pages 77-104. Kluwer Academic Publishers, Dordrecht, 1999

16. Rahul Mittal,"Robust PI and LQR controller design for Active Suspension System with Parametric Uncertainty." 2015 International Conference on Signal Processing, Computing and Control (2015 ISPCC)

17. H. Milan, D. Daney, and E. Tsigaridas. "Bounds on eigenvalues and singular values of interval matrices", SIAM J. Matrix Anal. Applicat., Vol. 31, no. 4, pp 2116-2129, 2010.

18. Shohan Banerjee, Kaushik Halder, Soumya Dasgupta, Siddhartha Mukhopadhyay, Koushik Ghosh and Amitava Gupta. "An Interval approach for robust control of a large PHWR with PID controllers", IEEE transactions on nuclear Science, Vol-62, No.1, February 2015.

19. Jian-Bo He, Qing-Guo Wang, Tong-Heng Lee. "PI/PID controller tuning via LQR approach" Chemical Engineering Science 55 (2000) pages 2429-2439.

20. J. Belanger, P. Venne and J-N. Paquin. "The What, Where an Why of Real time Simulation" PES-GM-Tutorial 04- Real Time Simulation, Oct 2010.

21. P.C. Krause, Oleg Wasynczuk, Scott D. Sudhoff. "Analysis of electric machinery and drive systems," IEEE Press, A John Wiley and Sons, Inc. ISBN: 0-471-14326-X.

22. Aleck W. Leedy."Simulink/MATLAB dynamic Induction Motor Model for use as a Teaching and Research Tool", International Journal of Soft Computing and Engineering (IJSCE), ISSN: 2231-2307, Volume 3, Issue-4, September, 2013.

23. Bimal K. Bose, "Modern Power Electronics and AC Drives," Prentice Hall of India Private Limited ISBN- 81-203-2749-7

24. Analog devices, "Generation of Three-Phase Sine-Wave PWM Patterns on the ADMC401," Application Note: AN401-3

25. Andy Knight , "Variable Speed Drives," University of Caligary, Canada

26. P.S. Bhimbra, "Power Electronics" Khanna Publishers. Fifth edition 2012. ISBN-978-81-7409-279-3
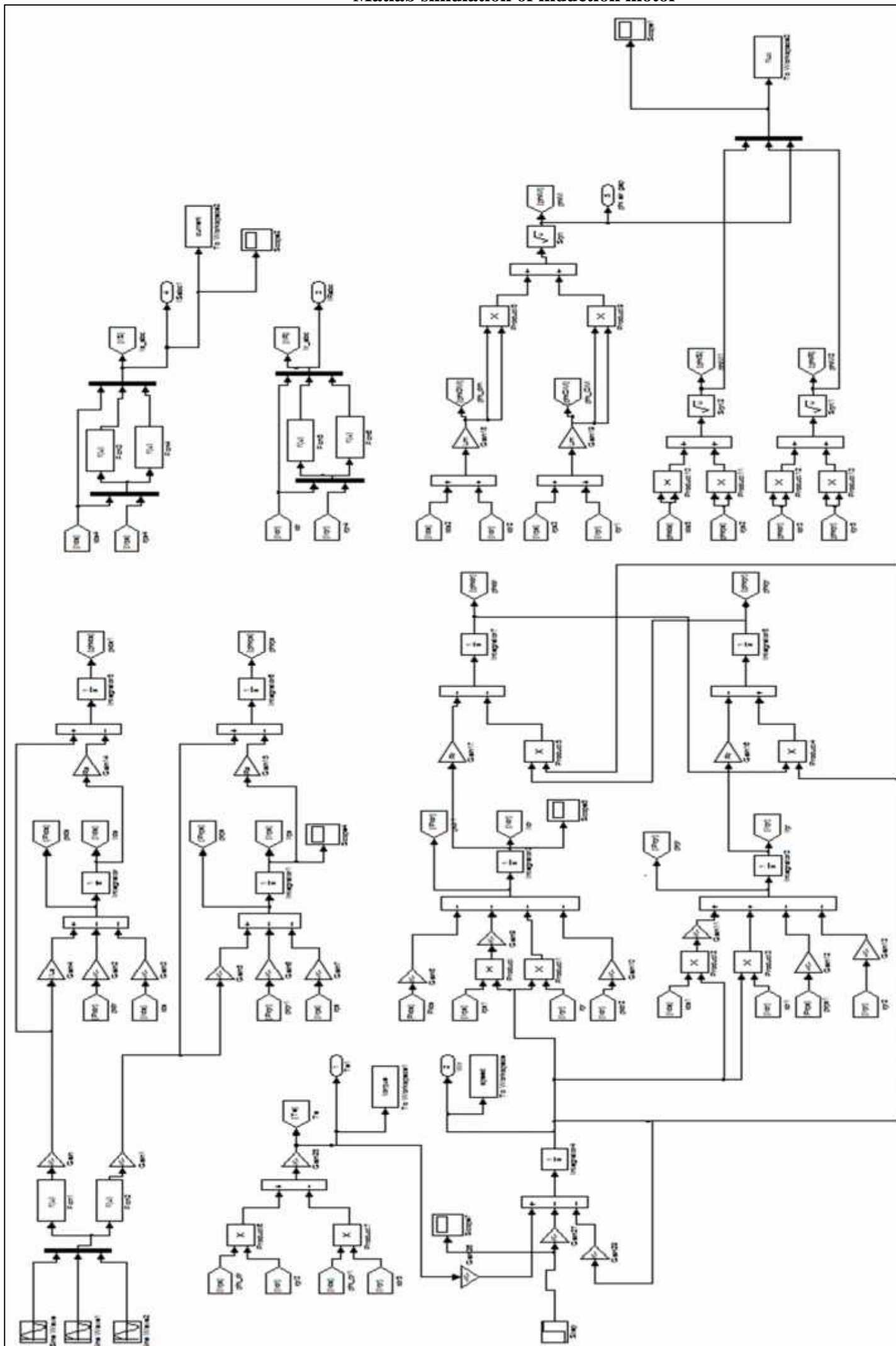
References

27. Sabyasachi Sengupta, N.K. De, D. Prasad, "Power electronics," web tutorial, IIT kharagpur, NPTEL

28. Stanislaw H. Zak, "Systems and control", Oxford University Press, Indian Edition. ISBN: 0-19-515011-2

29. G. I. Hargreaves, "Interval Analysis in MATLAB", Numerical Analysis Report No. 416 December 2002. University of Manchester.

30. Opal RT data sheet- OP 4500 simulator, Opal Rt Technologies.

Appendix-1

Matlab simulation of induction motor

Appendix-2

Matlab simulation of IFOC Induction Motor

Matlab simulation of IFOC Induction Motor